APPLICATION OF A DYNAMIC GREENHOUSE CLIMATE MODEL FOR IRRIGATION SCHEDULING IN A GREENHOUSE ROSE CROP IN ZIMBABWE

By

Niclah Nyamutata

A thesis submitted in partial fulfilment of the requirements of a Master of Science Degree in Agricultural Meteorology

Department of Physics

Faculty of Science

University of Zimbabwe

Harare

May 2010

Abstract

An assessment on the potential of the Gembloux Greenhouse Climate Model (GDGCM) as a tool for irrigation scheduling was done on a rose (Rosa Hybrida) crop grown in an Azrom type greenhouse, located in Harare, Zimbabwe. The transpiration sub-model of the GDGCM, consisting of a canopy resistance model within it was mainly considered in this study. The canopy resistance model and the transpiration sub model were calibrated and validated. Field measurements were done for climatic and physiological parameters required for the canopy resistance model and transpiration sub model input parameters. Climatic data was continuously measured inside and outside the greenhouse throughout the research. Historical data for Whole Plant Transpiration (WPT) measured by stem heat balance sap flow gauges obtained from Floraline (Pvt) Ltd for the period December 2007 and January 2008 was used for calibration and validation of the transpiration sub model. The canopy resistance model was fitted to experimental data of canopy resistances and coefficients a, b and c of 788.38 ± 82.51, 85.78 ±16.14 and -0.146 ± 0.080 respectively were determined. The validation results showed a strong fit between the measured and simulated values (R^2=0.91). Several input parameters were determined, including the canopy resistances from the canopy resistance model, to calibrate the transpiration sub model. The transpiration sub-model was fitted to experimental WPT data and the results showed a good fit between the simulated and measured values (R^2=0.64). Simulations of crop transpiration were carried out for a whole year: winter (May to August 2007) and summer (September 2007 to April 2008). The GDGCM uses outside weather data to simulate the internal greenhouse microclimate, as well as crop transpiration rates. The crop water requirements (CWR) were calculated as the amount of water requirement to replenish the water lost by transpiration. The results showed that the rose crop transpired more in summer than in winter, as expected; and there was also transpiration at night but it was very small. Daily and seasonal CWR were determined. Daily CWR fluctuated everyday depending on the weather conditions, and seasonal CWR showed that the CWR was less in winter than in summer. June and July had the lowest CWR in winter; while December and January had the least CWR in summer. September and October had the highest CWR for that year. The CWR of the rose crop for the whole year was compared with the actual amount of water that was supplied by the existing irrigation system. The existing irrigation system was automated, applying water for 4 minutes whenever the cumulative solar radiation outside the greenhouse reached 1600 kJ/m^2. The results showed that the CWR was lower than the actual water applied by the irrigation system throughout the year. The total CWR for the year was 1.45 Ml/year and the actual water applied was 2.74 Ml hence the existing irrigation system was over-irrigating by almost half the CWR by the crop.

Dedication

To my son

(Kudakwashe Ashley Gonah)

Acknowledgements

First and foremost, I would like to thank the Almighty God for taking me thus far; being my pillar of strength and giving me the courage to go on when I had lost hope throughout this research project.

My utmost appreciation goes to my supervisor, Mr E Mashonjowa for his invaluable effort in the shaping of this research project. Many thanks to all the Physics Department staff, with special mention of Mr Chipindu and Dr Mhizha, and the Floraline team for their assistance. To my colleagues, thank you for the friendship and contribution to making this research project a success in one way or the other. I am greatly indebted to the DAAD and the University of Zimbabwe for the financial assistance they rendered during the entire research period.

My profound gratitude goes to my family, my husband, Naume, Peter, for their patience, encouragement and understanding during my candidature. My heartfelt appreciation goes to my mother for the tireless effort helping me take care of my son during the research study period. You are a cut above the rest.

TABLE OF CONTENTS

LIST OF FIGURES

LIST OF TABLES

LIST OF ACRONYMS AND SYMBOLS

GDGCM	Gembloux Dynamic Greenhouse Climate Model
CWR	Crop Water Requirement
WPT	Whole plant Transpiration
RH	Relative Humidity
DOY	Day of year
LAI_g	Leaf Area Index
VPD	Vapour Pressure Deficit
VPD_m	vapour pressure deficit of the air at which the resistance is minimal
SE	Standard Error Estimate
R^2	Correlation Coefficient
AWS	Automatic Weather Station
MDS	Maximum daily shrinkage
SHB	Stem heat balance
WUE	Water use efficiency
ET	Evapotranspiration
ET_0	Reference evapotranspiration
ANN	Artificial neural network
PET	Potential Evapotranspiration
PAR	Photosynthetically Active Radiation
UV	Ultraviolet
TR	transpiration rate
BFS	Beam fraction sensor
R_n	radiation absorbed by the canopy

RG_0	outside global radiation
D	molecular diffusion coefficient of water vapour in air
d	characteristic dimension
N	number of data points.
t	time
T	temperature
V	greenhouse volume
ρCp	volumetric heat capacity of air
g_a	aerodynamic resistance of the canopy to water vapour transfer.
g_s	stomatal resistance of the canopy to water vapour transfer.
P_{in}	power input to the stem
q_r	radial heat conducted through the gauge to the ambient
q_v	vertical or axial heat conduction through the stem.
q_f	heat carried by sap stream
C_p	heat capacity
dT	temperature rise of the sap
I_0	incident light
I	transmitted light
T_v	canopy temperature
$T_r(t)$	greenhouse crop transpiration rate
P_V	fraction of the total greenhouse floor area covered by the crop,
A_g	total greenhouse floor area
$F_s(t)$	stem sap flow
A_L	total leaf area of the plant on which the gauge is installed
r_l	leaf stomatal resistance to water vapour transfer

r_s	Canopy resistance
$Q_{L(vi)}$	transpiration flux density
$x_s(T_v)$	saturation water vapour concentration at temperature of the vegetation
h_{Tr}'	mass transfer coefficient
h_{P1}	phase change heat transfer coefficient for the upper faces of the leaves
h_{P2}	phase change heat transfer coefficient for the lower faces of the leaves
QS_{int}	solar irradiance incident on the crop,
T_a	air temperature
$e_s(T_a)$	Saturation vapour pressure at air temperature
$e_s(T_v)$	Saturation vapour pressure at vegetation temperature
e_a	vapour pressure
y_i	measured output
$\bar{y}$	Average
y_{sim}	model output
g	acceleration due to gravity
u	velocity of air
RH_{cr}	corrected output relative humidity values
RH_{sr}	sensor output relative humidity values
T_{cr}	corrected output temperature values
T_{sr}	sensor output temperature values
A	surface area
c	specific heat capacity
c_c'	Specific heat capacity per unit area of the cover
x_i	water vapour concentration of the greenhouse air
h_{fg}	latent heat of condensation of water

l	thickness of layer
m_v	vegetation mass per unit greenhouse surface area
$Q_{Z(x,y)}$	density of the net heat flux transferred from layer x to layer y in the way described by subscript Z
$Q_{D(x)}$	conductive heat flux density through layer x
$Q_{S(x)}$	density of the solar flux absorbed by layer x
ρ	Density

The subscripts stand for:

V	convective
D	conductive
R	far infrared radiation
L	(phase change) latent heat
c	cover
e	external air
i	internal (greenhouse) air
s	soil surface
v	vegetation
gr	greenhouse
sky	sky (treated as a full radiator or blackbody)
HS	heating system
s1, s2, s3, s4, ss	four soil layers and subsoil
s12, s23, s34, s4s	the four soil layer interfaces

Greek Symbols

ρ	Density
v	coefficient of kinematic viscosity air
β	thermal expansion coefficient of air
Δ	slope of the water vapour saturation curve at T
λ	latent heat of vaporization
γ	psychrometric constant,

Dimensionless groups

Sh	Sherwood number
Gr	Grashof number
Re	Reynolds number

CHAPTER 1

INTRODUCTION

1.0 Preamble

The amount of fresh water available for agricultural purposes is decreasing in Africa and, since shortages of fresh water are to be expected to intensify due to climate change and the corresponding recurrent droughts and rainfall variability, there is need to improve water use efficiency, either by improving genetic performances and horticultural practices, or by improving irrigation scheduling (Naor, 2004). Water use efficiency includes any measure that reduces the amount used per unit of any given activity, consistent with the maintenance or enhancement of water supply. Water management is very important in irrigated areas since it determines the amount of water used, energy and labor returns.

Horticultural crops are typically grown under drip irrigation systems in greenhouses, where optimal conditions can be achieved for maximum production and to optimize timing of harvest in order to satisfy specific market needs. The greenhouse industry in Zimbabwe is entirely dependent on irrigation water to produce a viable crop. Many irrigation scheduling methods have been developed to assist farmers and irrigators to apply water more efficiently: these may be based on soil water measurement, meteorological data or monitoring plant water use or its response to water stress (Jones, 2004).

The current irrigation control systems in Zimbabwe use timing circuits or weather data such as solar radiation to switch the irrigation. The major problems associated with these control systems are that, when the plant demand increases or declines temporarily under changing environmental conditions and physiological processes, the current control systems do not respond rapidly enough; hence under- or over-irrigation occurs.

An approach to irrigation scheduling with considerable promise is to measure the actual water use of the crop (Van Leeuwen et al., 2001; Jones, 2004; Klein, 2004). This can be achieved through online monitoring of crop transpiration with the use of sap flow gauges to monitor whole plant transpiration rates, which can then be scaled up to the crop transpiration rates (Elings and Voogt, 2008; Ham et al., 1990; Jones, 2004). The quantity of water to be supplied is obtained by integrating the measured sap flow pattern over a specified time. This allows for plant-dependent irrigation control by predicting the optimal timing for irrigation and the exact amount of water required by the plant. Direct crop monitoring can provide many crop management options to greenhouse managers, such as a more efficient use of resources and retrospective analysis of crops' responses to climate control strategies and gives them the ability to detect crop stress in an automated way (Baas, 2003; Ehret et al., 2001).

1.1 Problem statement

The use of the actual crop water consumption, while being the ideal method for irrigation scheduling, is still hampered by the relatively high cost of the monitoring equipment and the low knowledge of the dynamic nature of plant water status. There are also other shortcomings

associated with sap flow measurements. Probably the greatest concern is the fact that they are rather plant intrusive. The sensor itself is attached to the stem, and may restrict growth, and/or diurnal stem diameter changes, cause wounds in the plant and create an entry point for infection. There are also the questions of whether long term use of the sensor might affect the health and performance of the plant being monitored, and the unknown effect of heating of the sap on the condition of the plant (Jones, 2004).

In addition, the instrument must also be periodically adjusted as the plant grows. This results in a period of up to several hours during which no data may be collected as the system stabilizes after an adjustment. These problems hinder the use of sap flow measurements in irrigation control. An alternative method is the use of modeling to simulate the transpiration rates, and hence the water requirements of the crop. In this study transpiration rates of a rose crop in a greenhouse will be simulated using a greenhouse climate model: the Gembloux Dynamic Greenhouse Climate Model (GDGCM), and used for irrigation control in roses. The GDGCM uses basic weather data outside the greenhouse (e.g. air temperature, relative humidity, solar radiation and wind speed) and the greenhouse construction data to predict the greenhouse climatic parameters and crop physiological parameters, including transpiration rates. Use of this model in rose irrigation control systems will improve water management since it determines the amount of water used without involving the high costs of direct crop transpiration monitoring equipment.

1.2 Aim and Objectives

The main aim of this study was to apply the GDGCM for irrigation scheduling in a greenhouse rose crop in Zimbabwe.

Specific objectives were:

1. To calibrate and validate the GDGCM transpiration sub model for roses in a greenhouse.

2. To apply the GDGCM to obtain daily and seasonal crop water requirements for roses in a greenhouse.

3. To assess the potential of the GDGCM as a tool for irrigation scheduling by comparing the crop water requirement against the actual water supplied by an existing irrigation system.

1.3 Expected benefits

The project is expected to benefit horticultural farmers to have efficient water management when growing greenhouse crops, where the crops will not be over or under- irrigated. Economic benefits are expected through a low cost irrigation control system with efficient energy consumption.

1.4 Project Layout

The thesis was made up of five chapters. Chapter 1 introduces the topic and then outlines the problem statement and the objectives of the study. Chapter 2 gives the background theory on the

topic and the literature review relevant to the research methods adopted. Chapter 3 outlines the materials and the methods used in the study. It comprises of a detailed description of the materials and methods used in data collection and analysis to draw conclusions on the objectives of the study. It also gives an overview of the Gembloux Dynamic Greenhouse Climate Model (GDGCM). Chapter 4 lays out the results obtained and the discussions of the findings. The conclusions and recommendations made are presented in chapter 5.

CHAPTER 2

LITERATURE REVIEW

2.0 Introduction

The greenhouse industry has expanded in many parts of the world (Enoch and Enoch, 1999) such that greenhouse production systems are presently among the most sophisticated crop production systems (Challa et al., 1994). The intensive involvement of the grower in the daily production process and the refined control possibilities give rise to a major knowledge requirement in terms of the number of processes and the time-scale of the controls (Challa, 1997). Part of the information requirement of growers could be satisfied by crop growth models. These could provide detailed evaluations of alternatives, support decisions, and improve the performance of control systems by providing on-line estimations of relevant processes (Challa, 2002).

The dominant process in water relation of the whole plant is the absorption of large quantities of water from the soil, its translocation through the plant and eventual loss to the surrounding atmosphere as water vapour. Crop water requirement is the amount of water required to compensate for the water lost from a cropped field. When the crop water requirement is known the right quantity of water has to be supplied at the right time through an appropriate application method to satisfy the crop water requirement (Sharma, 2006).

2.1 Greenhouse Climate

Greenhouses are a means of overcoming climatic diversity using a free energy source, the sun (Hanan, 1998). The microclimate is the complex of environmental variables, including temperature, radiation, humidity and wind, to which the vegetation is, exposed (Jones, 1993). The greenhouse microclimate is affected by several factors, these include: solar heat gain; evapotranspiration; thermal radiation exchange between the greenhouse and its surroundings; conduction through the greenhouse floor and structural cover; ventilation and condensation (Gumbe et al., 2009).

All surfaces inside the greenhouse exchange radiation with their environment. Green plants exchange energy with the environment through heat and mass transfer processes; transpiration, radiation and convection with the air. The leaves are the heat exchanger and are responsible for all the heat and mass transfer processes. Convection (sensible) heat transfer between plants and the air takes place in the boundary layer at both sides of the leaves. Transpiration takes place exclusively through the stomata. The leaves are also responsible for solar radiation absorption and thermal radiation emission (Papadakis et al., 1994).

The greenhouse cover exchanges energy at the inner surface to the greenhouse air and to outside air at the other side. The interaction of the greenhouse cover with the solar radiation determines how much radiation is transmitted and available at crop level (Bakker et al., 1995). The transmittance of the cover varies with the wavelength and incident angle of the radiation reaching it (Hanan, 1998). Heat exchange between the inside and the outside greenhouse is a

complex mechanism involving all processes of the heat exchange: radiation; convection; conduction and latent heat (Baptista et al., 2001). A schematic illustration of energy flows in a greenhouse is shown in fig 2.1.

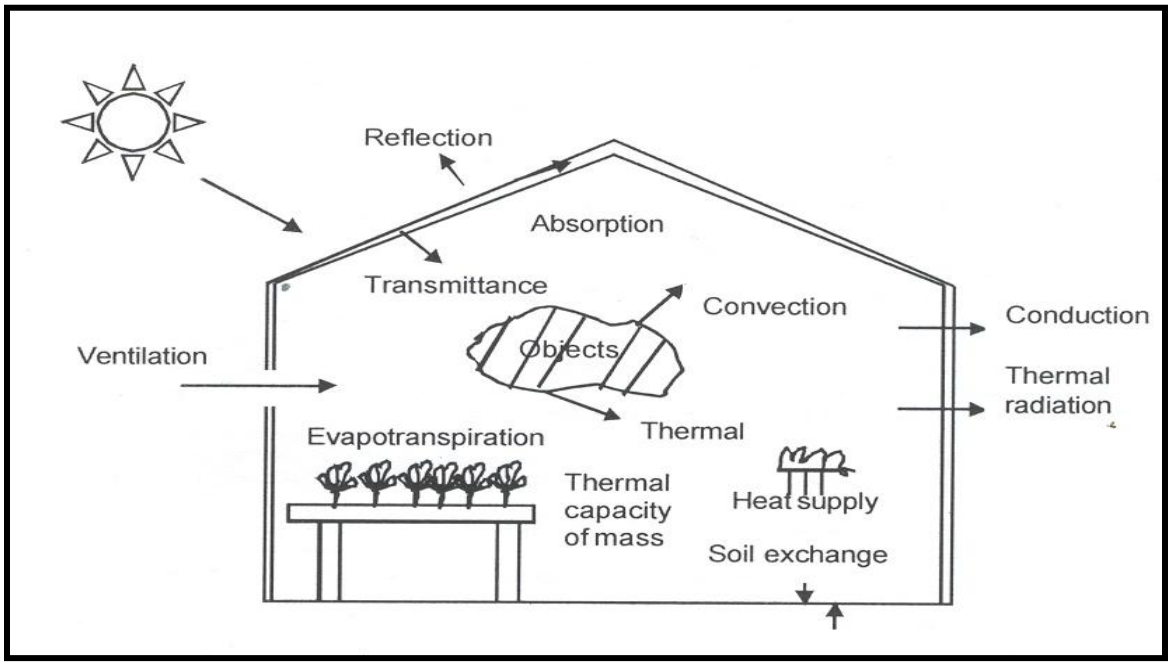

Fig 2.1: Energy flows in a greenhouse. (Adapted from Gumbe et al., 2009).

2.2 The greenhouse water cycle

Evapotranspiration (ET) is the main process that determines the fate of water in the greenhouse and hence the water requirements of crops, which also depend on the nature and stage of growth of the crop and environmental conditions. ET is driven by a constant inflow of energy. The state and content of water in the soil and its vegetation cover is affected by the way the energy fluxes reaching the soil is partitioned and utilized, therefore the water balance is intimately and reciprocally related to the water cycle (Boulard and Baille, 1993). The soil component (or

artificial substrate) and the actual transpiration of a crop are the two components of the greenhouse water cycle that are important to measure and control.

2.3 Transpiration of a greenhouse crop

The transpiration of a greenhouse crop results from prevailing microclimate conditions. It consists of the vaporization of liquid water contained in plant tissues and the water vapor removal to the atmosphere through the stomata (Allen et al., 1998). Stomata are small openings on the plant leaf through which gases and water vapour pass (Fig 2.2). The vaporization occurs within the leaf intercellular spaces and the stomatal aperture control the vapour exchange with the atmosphere. Leaf transpiration can be thought of as a necessary "cost" associated with the opening of the stomata to allow the diffusion of carbon dioxide gas from the air for photosynthesis.

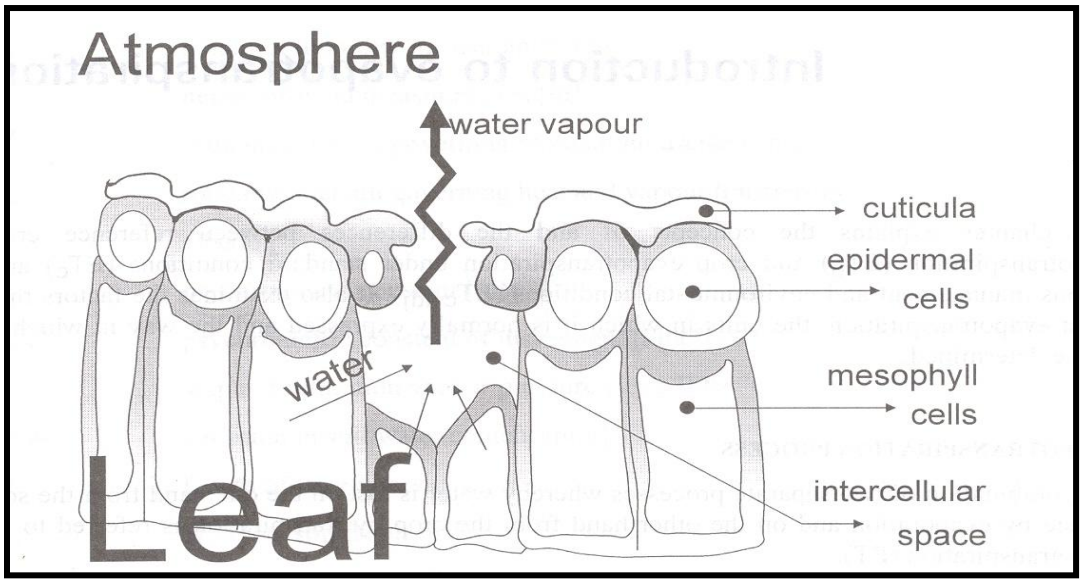

Fig 2.2: Schematic representation of the stoma (adapted from Allen et al., 1998)

The influence of the ambient on the transpiration rate of a greenhouse crop takes place primarily through three variables: radiation, air temperature and humidity (Bakker et al., 1995). The global radiation at crop level contributes to the energy balance of the crop and so affects the crop temperature and transpiration. Transpiration is an active plant response to climatic factors (Yang et al., 1990). It is an energy consuming process which moderates leaf and air temperature changes when subjected to solar radiation or other energy sources (Yang et al., 1990). Plant transpiration is a very important physiological process, which not only serves as the driving force for water uptake and water transport, but also affects the uptake and distribution of nutrients. Only 1% of the available liquid water taken by plants is actually involved in metabolic processes, most of the water taken in through plant roots is vaporized into the air (Rosenberg et al., 1983).

Studies have shown that transpiration rate is directly proportional to plant production and it represents a major mechanism for cooling plant leaves and the environment, through the evaporation process. Maintaining high levels of canopy transpiration rate in greenhouses is one of the most efficient and least costly ways for cooling the greenhouse environment during warm days with high radiation load (Kastoulas et al., 2002). The water lost from a crop canopy is the sum of the water transpired by all individual leaves but there can be differences in the microclimate around individual leaves. Differences arise because there are vertical profiles of radiation, temperature, humidity and wind speed within the canopy. Horizontal variations also exist within the canopy. However, transpiration has a linear response to the mean flux density of available radiation (R_n) and the adiabatic evaporation, and a weak one to temperature and wind speed (Bakker et al., 1995).

Crop transpiration is the most important energy dissipation mechanism determining the thermal environment of protected crops. The crop builds its own climate through transpiration mechanism, which in turn influences the transpiration. Greenhouse crop transpiration is governed by water vapour conductance between the leaves and the bulk of inside air; regulated by physical and physiological processes. (Boulard, 2008).

2.3.1 Factors affecting transpiration

Transpiration depends on the energy supply, wind and vapour pressure gradient; therefore the air temperature, radiation, air humidity and wind are important factors to be considered when assessing the transpiration. The transpiration rate is also determined by the soil water content, water logging and soil salinity. The crop characteristics (e.g. type, development stage and management practices) environmental aspects and cultivation practices are other factors that influence the transpiration rate (Allen et al., 1998). The rate of transpiration is directly related to the degree of stomatal opening, and to the evaporative demand of the atmosphere surrounding the leaf. Transpiration has connections with leaf temperature, if interfered by harsh environments it will make the leaf temperature unstable and abnormal. Plants transpire more rapidly at higher temperatures because water evaporates more rapidly as the temperature rises.

Under high relative humidity and calm condition, the rise of leaf temperature with light increases the VPD in the boundary layer of the leaf, followed by an increase in transpiration rate. As transpiration occurs there is a tendency for a moist layer of air to form next to the leaf surface, particularly in still air. This will decrease the diffusion gradient between the leaf and the

atmosphere and transpiration will consequently decrease. Wind lowers the leaf temperature and decreases vapour pressure deficit (VPD) in the boundary layer of the leaf, causing a decrease in the transpiration rate (Takashini et al., 1997). Air movement carries away a layer of humid air, replacing it with drier air, resulting in an increase in transpiration. The more rapid the air movement the faster the moist air will be carried away and the faster the rate of transpiration.

2.4 Importance of irrigation control in greenhouse crops

The irrigation of greenhouse crops is one of the most critical of all production practices because greenhouse plants entirely depend on irrigation for their water. Proper irrigation management is essential for improving the productivity and quality of crops grown in the greenhouse in which rainfall is obstructed by the cover (Lee and Shin, 1998). Greenhouse crops use large amounts of water continuously, but the rate of use depends on plant species, size, temperature, and other atmospheric conditions. Exact time and amount of irrigation are two deterministic factors for the efficient irrigation management. The timing of irrigation supply influences crop productivity and quality (Shelford et al., 2004) therefore, applications of the right amount of good quality water to greenhouse crops, at the optimum time, is an important factor in production of quality plants. The increasing worldwide shortages of water and costs of irrigation are leading to an emphasis on developing methods of irrigation that minimize water use (maximize the water use efficiency).

2.5 Irrigation systems for greenhouses

The main components of any irrigation system are the water source, pump, and proper sizes of main and lateral lines. These components are frequently undersized for the area to be watered, and serious inefficiencies occur. Proper engineering of a watering system is necessary; hence it is important to carefully determine the area to be irrigated with consideration towards increased capacity (Anonymous, 2010). There are several systems used to apply water to greenhouse crops. The selections depend upon technology, labour and material costs as well as the cultural procedures used in the greenhouses. These methods include hand watering, flood (furrow), sprinkler, capillary (sub-irrigation) and trickle (drip) irrigation. The methods are described as follows:

2.5.1 Drip irrigation

Drip irrigation, also known as trickle irrigation, is widely used for cut-flower and vegetable production in greenhouses and in the field (Hanan, 1998). Water is delivered drop by drop through an emitter to or near the root zone of plants. The principle of drip irrigation is to supply water at very low rates, in the region of maximum root activity. Water is pumped directly to the base of a plant by plastic tubing and bled through an emitter at a slow rate that meets the plant's needs. Drip and sub-irrigation systems do not wet the foliage, thereby significantly reducing disease problems, leading to a considerable savings in water consumption (Harbaugh and Stanley, 1985). If managed properly, this method can be the most water-efficient method of irrigation, resulting in minimised evaporation and runoff; however it is also very expensive and requires diligent maintenance of the hardware to keep the system working as it has a main problem of emitter clogging.

2.5.2 Sprinkler irrigation

Sprinkler irrigation is seldom used for cut-flower production. It is most commonly used for small units on a dense spacing. Water is supplied overhead by spray nozzles (commonly used for bedding plants). Efficiency of overhead sprinklers is influenced by type of spray head, spacing, and wind velocity (Hanan 1998).

2.5.3 Capillary (Sub-irrigation)

Capillary mat systems are commonly used for irrigation of potted plant production on a large scale. However, in areas where soluble salts are a problem, mats do not provide for leaching, thereby increasing the risk of salt injury. In greenhouses, sub-irrigation may also be adapted to any form of bed used, whether raised or solid. In either case the bed should be practically water-tight.

2.5.4 Flood (furrow irrigation)

Water is applied to a medium's surface and is allowed to flow over the surface until reaching the furthest distance from the source. Flooding in greenhouses is usually done where the cultural conditions are primitive, labour is cheap and the structures are unheated.

2.5.5 Hand watering

Hand watering is employed with the planting of a new crop or where it is necessary to establish capillarity in mat watering systems. However, hose watering as a standard procedure is seldom

satisfactory because its success depends upon the skill and care of the laborer. It is generally the cheapest method in terms of equipment but it is labour costly. Hose ends are also very good means to inoculate sterile substrates with pathogens especially since most growers leave hoses lying on the ground.

2.6 Irrigation scheduling techniques for greenhouse crops

Irrigation scheduling is the use of water management strategies to prevent over application of water while minimizing yield loss due to water shortage or drought stress (Evans et al., 1996). It is the process used by the grower to determine the frequency and duration of irrigation (Pardossi and Incrocci, 2008). It determines crop water use efficiency (WUE) and environmental impact. In irrigated agriculture water use efficiency (WUE) is defined as shown in equation (2.1).

$$\text{Water use efficiency (WUE)} = \frac{\text{Yield per unit area}}{\text{Water used to produce yield}} \qquad [2.1]$$

A relatively simple way to make irrigation more efficient is to only irrigate plants when they actually need water, and with the amount of water they need. To avoid over or under irrigation, it is important to know how much water is available to the plant, and how efficiently the crop can use it (Qassim and Tatura, 2006). Irrigation scheduling requires knowledge of the soil, the soil-water status, the crops, the status of crop stress and the potential yield reduction if the crop remains in a stressed condition (Evans et al., 1996).

There are many methods available to measure these factors. They include direct measurements such as plant observation, feel and appearance of the soil, and using soil moisture monitoring devices; or indirect measures which estimate available water from weather data (Qassim and Tatura, 2006). Irrigation should begin when the crop comes under water stress severe enough to reduce crop yield or quality. The level of stress that will cause a reduction in crop yield or quality depends on the kind of crop and its stage of development; the level varies during the growing season as the crop matures. Thus, determining when to irrigate is a scheduling decision that should take into account the crop's sensitivity to stress. Recently, scheduling techniques have been developed that are based on the moisture status or stress condition of the crop. For example, to predict crop stress by infrared thermometry, the temperature of the crop's leaves is related to transpiration rate (Evans et al., 1996).

The choice of irrigation scheduling method depends to a large degree on the objectives of the irrigator and the irrigation system available (Jones, 2004). Practical irrigation scheduling algorithms for greenhouse crops have been developed during the last twenty years. Many of them are based on estimates or measurements of the crop transpiration (Baille, 1996).

2.7 Approaches to irrigation scheduling in greenhouse crops

The approaches to irrigation scheduling in greenhouse crops can be done basing on the plant, soil moisture and the weather. These approaches are as follows:

2.7.1 Weather based

Irrigation scheduling methods based on weather or meteorological data require various climatological and physiological parameters. Some of the parameters are measured directly in weather stations and other parameters are derived from a direct or empirical relationship from measured data.

2.7.1.1 Penman-Monteith equation

During daytime, the greenhouse water balance depends mainly on the crop transpiration and the loss from ventilation. The transpiration rate depends on the amount of radiative energy absorbed by the canopy and the vapour pressure deficit. Transpiration is generally expressed by means of the Penman-Monteith equation (equation 2.2) extended to the whole canopy considered as a ´big leaf`

$$TR = \frac{\Delta}{\Delta+\gamma^*}\frac{R_n}{\lambda} + \frac{\rho Cp}{\lambda}\frac{g_a VPD}{\Delta+\gamma^*} \qquad [2.2]$$

Where:

TR= transpiration rate (kg m^{-2} s^{-1});

R_n = radiation absorbed by the canopy (W m^{-2});

λ = latent heat of vaporization (J kg^{-1});

ρCp = volumetric heat capacity of air (J m^{-3} °C^{-1});

VPD = saturation vapour pressure deficit (kPa) at temperature, T;

Δ = slope of the water vapour saturation curve at T; and

$\gamma^* = \gamma(1+g_a/g_s)$, γ being the psychrometric constant, g_a and g_s (m s^{-1}) respectively are the aerodynamic and stomatal resistance of the canopy to water vapour transfer.

The rapid changes in electronic technology, combined with the world wide research into the Penman equation, (equation 2.2) has enabled the accurate calculation of reference evapotranspiration (ET_0) for real time weather data. The availability of climate sensors in modern greenhouses has allowed the use of the Penman Monteith equation (equation 2.2), with the introduction of crop physiological parameters such as the stomatal conductance. The method is the best adapted to estimate crop water requirements. However, it requires sensors for the measurement of global radiation and vapour pressure, as well as crop parameters such as the aerodynamic and stomatal conductance. The main shortcoming of the method is that it requires leaf area index estimation (Baille, 1996).

2.7.1.2 Solar radiation methods

The main role of solar radiation in determining evapotranspiration showing a strong correlation between daily evapotranspiration and solar irradiance in a greenhouse has been evidenced in numerous works (Morris et al., 1957; Lake et al., 1966; Stanhill and Alberts, 1974). This gave rise to the solar radiation method or solarimeter method. If the outside global radiation, RG_0 and the greenhouse transmission, t were known the method was based on a simple relationship giving the reference evapotranspiration under greenhouse.

$$ET_0 = K\ t\ RG_0/2.5 \qquad [2.3]$$

Where:

K is an empirical coefficient, whose value is 0.6 to 0.7; and

ET_0 in mm/day and RG_0 in $MJ/m^2/day$

When irrigation is operated at daily or weekly intervals, this method generally gives good results. However, the high frequency of water applications implies short estimates of ET for soilless crops; which, in this case, transpiration can be significantly influenced by the saturation deficit inside the greenhouse. When the weather consists of hot and dry periods, inadequate irrigation scheduling can result (Baille, 1996).

2.7.2 Soil moisture based

Irrigation scheduling is conventionally based either on soil water measurement, where the soil moisture status is measured directly to determine the need for irrigation, or on soil water balance calculations, where the soil moisture status is estimated by calculation using a water balance approach in which the change in soil moisture ($\Delta\theta$) over a period is given by the difference between the inputs and the losses (Jones, 2004). Studies have shown that irrigation scheduling using water balance methods can save 15 to 35% of the water normally used without reducing yield. Soil moisture monitoring is used as a basis for irrigation scheduling as it can provide accurate information about the extraction of available water by the crop. Soil moisture can be measured as a suction or volume of water. Soil moisture suction can be used as a measure of plant stress and for that reason it is a handy tool for growers to use in scheduling their irrigations (Qassim and Tatura, 2006).

An irrigation control system based on soil moisture tension was adapted for use on plants growing in ground beds for cut flower production. The irrigation control system consisted of tensiometers, modified with high flow ceramic tips and pressure transducers, an analogue-digital signal converter, a computer, and custom written software. The system continuously monitored the moisture condition of the soil, initiated irrigation when the soil dried to a specific level, and turned off the water when an adequate amount was applied. When the system was installed in a commercial greenhouse of *Rosa hybrida* L. 'Kardinal' plants, water use in the test area was 26% less than the amount applied by the grower. Productivity (stems harvested m^{-2}) was 66% greater in the test area. Flowers harvested from the test plants were not lower in quality than those from the grower irrigated controls. The use of this irrigation control system can reduce both water and fertilizer usage when a liquid feed program is utilized. Increases in productivity and quality can result in significant increases in profitability for commercial producers (Oki et al., 2001).

2.7.3 Plant based

Some plant physiological processes can be used as an effective irrigation indicator. These processes are known to respond sensitively to water deficits in a plant. For plant growing under non-limiting water supply, the use of any plant-based or similar indicator for irrigation scheduling requires the definition of threshold values, beyond which irrigation is necessary. A direct measure of plant water status should be the most rigorous and therefore the most useful indicator of irrigation requirement (Payne and Bruck, 1996). Specific plant based methods include dendrometry, sap flow, leaf turgor pressure, stomata conductance, infrared thermometry

and thermography. The choice of which plant-based measure to use depends on their relative sensitivity to water deficits (Jones, 2004)

2.7.3.1 Sap flow

The transpiration of whole plants is closely approximated by the sap flow rate in the main stem or trunk. This can be measured using heat pulse and energy balance thermal sensors. The changes in transpiration rate indicated by sap flow are largely determined by changes in stomatal aperture but changes in sap flow can occur without changes in stomatal opening since transpiration is also influenced by other environmental conditions such as humidity. The development of reliable heat pulse and energy balance thermal sensors for sap flow measurement has opened up an alternative approach to irrigation scheduling based on measurements of sap flow rates (Jones, 2004). Methods of measuring sap flow include the following methods: the stem heat balance (SHB); thermal dissipation technique; heat pulse and the trunk sector method. In intact plants sap flow measurements can be done using a heat balance method. This method was devised using the specific heat capacity of water for keeping a temperature gradient constant, allowing long term and continuous observations of sap flow in the field.

Thermal dissipation technique

The temperature of a line heat source implanted in the sapwood of a tree can be measured by an improved heat dissipation sensor called a Thermal Dissipation Probe (TDP). The temperature is referenced to the sapwood temperature at a location well below the heated needle. The xylem is

heated with energy supply at one point by a small cylindrical probe containing a resistance wire heater and a thermocouple which is inserted 2 cm into the stem. Approximately 10 cm downstream, a second probe with a thermocouple but no heater measures the temperature (Fig 2.3). The temperature difference between the two probes is strictly influenced by the sap flow density around the heating probe.

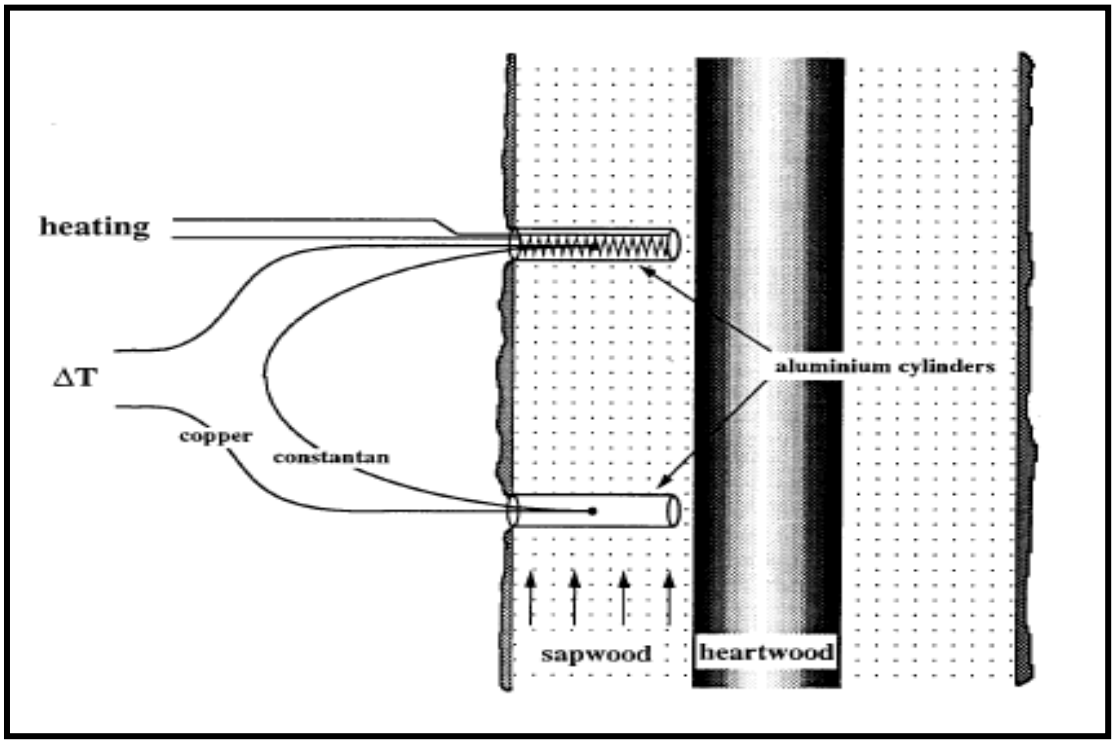

Fig 2.3: The improved Thermal Dissipation Probe (TDP).

Heat pulse Method

The rates of sap flow are measured by determining the velocity of a short pulse of heat carried by the moving sap stream. Short pulses of heat are periodically released from the heater probe and the sensor probes are monitored continuously to measure the velocity of each pulse as it moves with the sap stream. Sap flow velocity, V, can be determined by inserting a heating device at a

measured distance, X on the stem and then measuring the interval, t, between the heat pulse applied by the heating device and the detection of a temperature increase at the temperature sensor

$$V = \frac{X}{t} \qquad [2.4]$$

If the water content of the conducting xylem vessels is known, the mean rate of water transport through the measured section of the stem can then be calculated. The heat pulse method is suitable only for use on woody stems. The velocity of sap ascending a stem is determined by compensation of the measured velocity of a heat pulse for the dissipation of heat by conduction through the matrix of wood fibres, water and gas within the stem, thus the heat-pulse technique is based on the compensation principle.

The stem heat balance (SHB) Method

A SHB sap flow gauge (fig 2.4a) is composed of a heater extended on the stem. The stem is surrounded by a thermopile composed of a thermo-junction on each side of the sheath. The measurement of the temperature differences in the limits of the sampled section of the stem is allowed by thermo-junction pairs. These are installed on two strips, one just above and the other just below the heater. The SHB method requires a steady state and a constant energy input from the heater strip inside the gauge body. Hence the stem section must be insulated from changes in the environment. The gauge time constant is limited from five minutes to an hour, depending on the flow rate and the stem size (Van Bavel, 1994). Sap flow rates are expected to be sensitive to

water deficits and especially to stomatal closure, Ehret et al. (2001) have tested the use of sap flow measurement for irrigation scheduling and control in greenhouse crops.

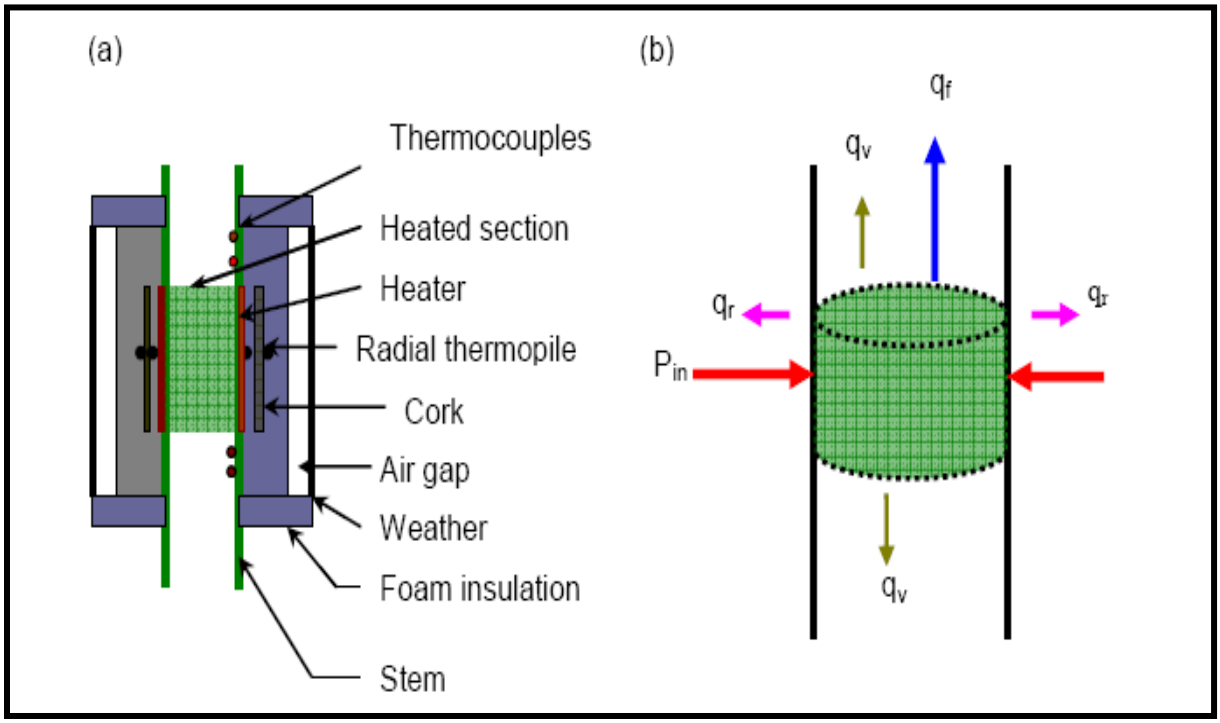

Fig 2.4: Schematic representation of the heat balance sap flow gauge (a) Vertical section through the stem heat balance sap flow gauge. (b) Energy balance components of the heat balance sap flow sensor connected to a plant stem. (Adapted from van Bavel ,1994).

A stem section and the possible components of heat flux, is shown in fig 2.4b. The power input, applied to the insulated section of the stem is divided in the following heat flows (assuming that there is no heat storage):

$$P_{in} = q_r + q_v + q_f \quad [2.5]$$

Where:

P_{in} is the power input to the stem (W);

q_r is the radial heat conducted through the gauge to the ambient (W);

q_v is the vertical or axial heat conduction through the stem. It is made up of 2 components; upward and downward heat conduction (W); and

q_f is the heat carried by sap stream (W).

After solving equation [2.5] for q_f, the mass flow rate, F per unit time is given by the following equation:

$$F = \frac{P_{in} - q_v - q_r}{C_p.dT} \quad [2.6]$$

Where:

C_p is the heat capacity. Plant sap is 99% water hence heat capacity of water (4.18×10^3 J/kg/K) is used as that of the plant sap.

dT is the temperature rise of the sap. All other terms are as defined before.

2.7.3.2 Dendrometry or micromorphometry

Stem and fruit diameters fluctuate diurnally in response to changes in water content. The diurnal dynamics of the changes in diameter, especially fruits, has been used to derive more sensitive indicators for irrigation need. The magnitude of daily shrinkage has been used to indicate water status and at the same time comparisons of diameters on succeeding days gives give a measure of growth rate (Jones, 2004). Promising results for low-frequency irrigation scheduling by use of

maximum daily shrinkage (MDS) have been achieved. Fereres and Goldhammer. (2003) showed that MDS was a more promising approach for automated irrigation scheduling than was the use of stem water potential for almond trees.

2.7.3. Porometry

Stomatal conductances (or resistances) can be measured accurately using a diffusion porometer although the measurements are labour intensive and unsuitable for automation. A diffusion porometer determines stomatal resistance by measuring the rate by which water vapour molecules (or CO_2 molecules) diffuse through the stomatal pores. Changes in stomatal conductance are sensitive to developing water deficits in many plants and therefore potentially provide a good indicator for irrigation need in many species.

2.8 Greenhouse crop models

The first crop growth models were built for field crops and the development of the greenhouse crop models followed several years later. There is little difference between field and greenhouse crop models. The main adaptations that were necessary include: modified radiation conditions due to greenhouse cover (Critten, 1993), the use of supplementary lighting and screens, extreme climate conditions in winter and summer, a more elaborate description of temperature effects on crop performance, Carbon Dioxide (CO_2) concentration effects, and the very important role of maintenance respiration in winter cultivation (Challa and Heuvelink, 1996). Marcelis et al. (1998) reviewed modeling of biomass production and yield of horticultural crops in greenhouse

vegetable production. There are two types of models: descriptive and explanatory. Descriptive models are created with a few parameters and inadequately explain the biological mechanism involved. Explanatory models are based on photosynthesis and are highly effective in studying the crop growth in relation to the environment. Crop modeling is not limited to yield prediction and has been used as part of greenhouse environmental control strategy (Hashimoto, 1993; Carrier et al., 1994).

In greenhouse production, the main application of crop models is the control of the environment, at the operational and tactical levels (Baker et al., 1995). Greenhouses are semi-closed systems, where crop and climate interact. The optimisation of CO_2 concentration, temperature and humidity are based on coupled models of mass and energy balance, and of net photosynthesis and transpiration rates. Models that predict stomata1 conductance against solar radiation, vapour pressure deficit, temperature and CO_2 concentration have been developed and validated for greenhouse crops (Avissar et al., 1985, Boulard et al., 1991). They permit to calculate the maximum crop transpiration rate, as well as the actual transpiration

2.9 Transpiration models

The supply of water is based on simplified forms of transpiration models. Simple transpiration models based on experimentally determined values of the ratio between crop transpiration and solar radiation have been developed for irrigation of greenhouse crops (de Graaf and van den Ende, 1981). The ratio between daily values of ET_o and solar radiation changed throughout the year, depending on the air temperature, in a Mediterranean greenhouse. Stanghellini (1987) developed a model for the relation between the microclimate in a greenhouse and the

transpiration rate of a greenhouse crop. With this model, the desired transpiration rate could successfully be achieved by controlling the humidity and temperature of a greenhouse under a given incoming global radiation. Mechanistic transpiration models, based on the Penman Monteith method (Monteith 1973), have also been developed for estimating greenhouse crop water requirements (Boulard and Wang 2000). However, their use is still quite limited as there is very limited information on the aerodynamic and canopy resistances of cropped surfaces that are required by these models (Fernandez et al, 2010). In greenhouse crops, priority has clearly been given to the modelling of growth, development (Marcelis et al., 1998), and transpiration (Jones and Tardieu, 1998).

2.10 Model Description (GDGCM)

The Gembloux Dynamic Greenhouse Climate Model (GDGCM) is a multiple component semi-one dimensional dynamic greenhouse climate model that describes the energy and mass exchanges between several layers. It was originally developed by the "Centre d'Etude pour la Régulation Climatique des Serres" of the "Faculté des Sciences Agronomiques de Gembloux" in Belgium. Deltour et al. (1985) validated it for a tomato crop in large multi-span and naturally ventilated European glasshouses in Western Europe and then under Mediterranean climatic conditions by Wang and Boulard (2000). The GDGCM was adapted to predict the microclimate in naturally ventilated plastic greenhouses for rose (*Rosa hybrid*) crops in Zimbabwe (Mashonjowa et al., 2007a, 2007b, 2009, 2010a). Detailed descriptions of the equations used in the GDGCM can be found in Pieters and Deltour (1997). In this section, only a short description of the model is given, necessary for understanding of the physical processes and quantities as applied in the model, and with emphasis on the description of the transpiration phenomena.

The GDGCM is made up of eight internal layers upon which it calculates eight heat balances for the greenhouse layers. The layers include the following: cover, air, vegetation, soil surface and four soil layers. It also includes a mass balance for the simulation of the relative humidity of the greenhouse air (Pieters, 1995; Pieters and Deltour, 1997). The greenhouse microclimate is the result of heat and mass exchanges between these layers. The interactions between the layers include heat transfers by conduction, convection, solar and thermal radiation, as well as mass transfers by latent heat. The greenhouse air exchanges heat by convection with the cover, the vegetation, the soil and the heating system (if any) and through exchange with the outside air by advection and ventilation. For the crop the terms of interest are the absorption of solar radiation, radiative exchange with the cover, soil and heating system, convective exchange with the greenhouse air and latent heat linked to evapotranspiration. For the soil, the gains and losses of energy are through the absorption of solar radiation, radiative exchange with the cover, the crop and the heating system, convective exchange with the greenhouse air and conductive exchange with the underlying soil layers. The exchanges of energy and mass between the various greenhouse layers are shown in Fig. 2.5

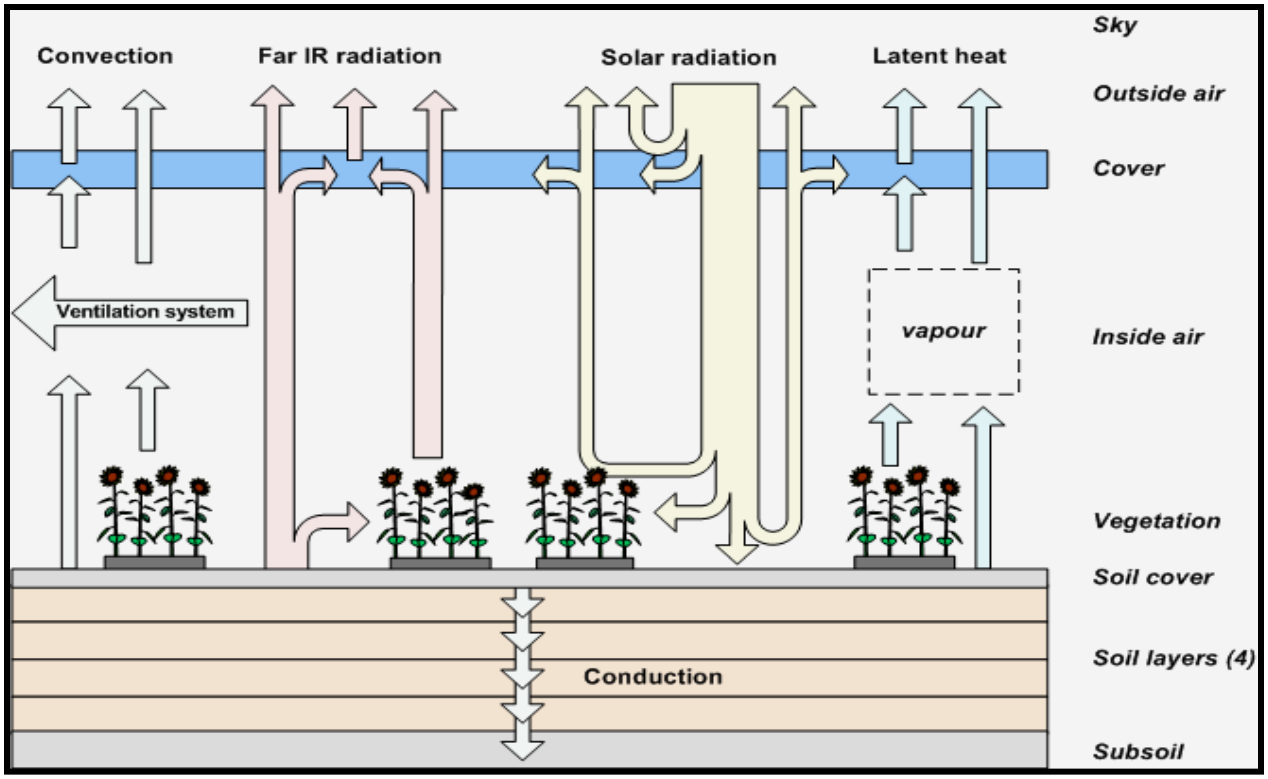

Fig 2.5: The schematic diagram showing the heat and mass exchanges between the greenhouse layers (after Pieters and Deltour, 1997)

The following eight equations describe the heat balance for the cover, inside air, vegetation, soil surface and the four soil layers, respectively and one mass balance equation for the simulation of the humidity of the greenhouse air.

$$c'_c \frac{dT_c}{dt} = \frac{A_{gr}}{A_c} \cdot \left(Q_{V(i,c)} - Q_{V(c,e)} + Q_{L(i,c)} + Q_{R(s,c)} + Q_{R(v,c)} - Q_{R(c,sky)} + Q_{S(c)} \right) \quad [2.7]$$

$$\rho_a \cdot c_i \cdot \frac{V}{A_{gr}} \frac{dT_i}{dt} = Q_{V(s,i)} + Q_{V(v,i)} - Q_{V(i,c)} - Q_{V(i,e)} + Q_{HS} \quad [2.8]$$

$$c_v \cdot m_v \frac{dT_v}{dt} = -Q_{V(v,i)} - Q_{L(v,i)} - Q_{R(v,c)} - Q_{R(v,sky)} + Q_{R(s,v)} + Q_{S(v)} \quad [2.9]$$

$$\rho_s c_s l_s \frac{dT_s}{dt} = -Q_{V(s,i)} - Q_{L(s,i)} - Q_{R(s,c)} - Q_{R(s,sky)} - Q_{R(s,v)} + Q_{S(s)} - Q_{D(s1)} = 0 \quad [2.10]$$

$$\rho_{s12} \cdot c_{s12} \cdot l_{s12} \cdot \frac{dT_{s12}}{dt} = Q_{D(s1)} - Q_{D(s2)} \quad [2.11]$$

$$\rho_{s23} \cdot c_{s23} \cdot l_{s23} \cdot \frac{dT_{s23}}{dt} = Q_{D(s2)} - Q_{D(s3)} \quad [2.12]$$

$$\rho_{s34} \cdot c_{s34} \cdot l_{s34} \cdot \frac{dT_{s34}}{dt} = Q_{D(s3)} - Q_{D(s4)} \quad [2.13]$$

$$\rho_{s4s} \cdot c_{s4s} \cdot l_{s4s} \cdot \frac{dT_{s4s}}{dt} = Q_{D(s4)} - Q_{D(ss)} \quad [2.14]$$

$$h_{fg} \cdot \frac{V}{A_{gr}} \frac{dx_i}{dt} = Q_{L(s,i)} + Q_{L(v,i)} - Q_{L(i,c)} - Q_{L(i,e)} \quad [2.15]$$

Where all fluxes (in W m^{-2}) are expressed per unit horizontally projected greenhouse surface area and with:

A: surface area (m^2)

c: specific heat capacity (J kg^{-1} K^{-1})

c'_c: specific heat capacity per unit area of the cover (J m^{-2} K^{-1})

x_i: water vapour concentration of the greenhouse air (kg m^{-3})

h_{fg}: latent heat of condensation of water (J kg^{-1})

l: thickness of layer (m)

m_v: vegetation mass per unit greenhouse surface area (kg m^{-2})

$Q_{Z(x,y)}$: density of the net heat flux transferred from layer x to layer y in the way described by subscript Z (W m^{-2})

$Q_{D(x)}$: conductive heat flux density through layer x (W m^{-2})

$Q_{S(x)}$: density of the solar flux absorbed by layer x (W m^{-2})

t: time

T: temperature (K or °C)

V: greenhouse volume (m^3)

ρ: density (kg m^{-3})

and where the subscripts stand for:

V: convective

D: conductive

R: far infrared radiation

L: (phase change) latent heat

c: cover

e: external air

i: internal (greenhouse) air

s: soil surface

v: vegetation

gr: greenhouse

sky: sky (treated as a full radiator or blackbody)

HS: heating system

*s*1, *s*2, *s*3, *s*4, *ss*: four soil layers and subsoil

*s*12, *s*23, *s*34, *s*4*s*: the four soil layer interfaces

The energy and mass balance equations are solved for given input parameters and boundary conditions using an iterative procedure to obtain the temperatures of the different layers and humidity of the inside air.

2.10.1 Description of the transpiration sub model

The main component of the greenhouse air water vapour balance is the crop transpiration rate; therefore its estimation is critical for climate control. The transpiration sub-model of the GDGCM was modified by considering the climatic dependence of the rose canopy surface resistance (r_s) and leaf stomatal resistance (r_l) to water vapour transfer. The transpiration flux density, $Q_{L(vi)}$, is given by:

$$Q_{L(vi)} = h_{fg} \cdot h_{Tr}' \cdot (x_s(T_v) - x_i) \qquad [2.16]$$

where h_{fg} is the latent heat of condensation of water (J kg^{-1}), $x_s(T_v)$ is the saturation water vapour concentration at the temperature of the vegetation, T_v (kg m^{-3}), x_i is the water vapour concentration of the surrounding air (kg m^{-3}), and h_{Tr}' is the mass transfer coefficient (m s^{-1}), defined for hypostomatal leaves as (Pieters and Deltour, 1997):

$$h_{Tr}' = \frac{LAI_g}{h_{fg}} \cdot \left(h_{P1} + h_{fg} \cdot \frac{1}{\frac{h_{fg}}{h_{P2}} + r_s} \right) \qquad [2.17]$$

where LAI_g is the leaf area index expressed per unit greenhouse cultivated floor area, obtained as the product of the crop leaf area index, and the cultivated fraction of the greenhouse floor area, r_s

is the canopy resistance to water vapour transfer and h_{P1} and h_{P2} are the phase change heat transfer coefficients for the upper and lower faces of the leaves, respectively, defined as:

$$h_P = h_{fg} \cdot Sh \cdot \frac{D}{d} \qquad [2.18]$$

Where:

Sh is the Sherwood number (a non-dimensional parameter whose value depends on the flow conditions and the properties of the air)

D is the molecular diffusion coefficient of water vapour in air ($m^2\ s^{-1}$)

d is the characteristic dimension (m).

The results of several researchers (Baille et al., 1994a; Baille et al., 1994b; Baille et al., 1994c; Papadakis et al., 1994; Kittas et al., 1999) suggest that the climatic dependence of the crop stomatal resistance on water vapour transfer can be described by a "reduced" Jarvis type model. The leaf stomatal resistance, r_l (s m^{-1}) can thus be predicted as a function of the solar irradiance incident on the crop, QS_{int} (W m^{-2}), the leaf-air vapour pressure deficit, *VPD* (kPa), the air temperature, T_a (°C), and CO_2 concentration:

$$r_l = r_{l\,min} \cdot f_1(QS_{int}) \cdot f_2(VPD) \cdot f_3(T_a) \cdot f_4(CO_2) \qquad [2.19]$$

Where f_1, f_2, f_3 and f_4 represent dimensionless functions, quantifying the relative increase of stomatal resistance whenever one of the parameters is limiting the exchange rate (Jarvis, 1985).

At ambient CO_2, and for well-watered crops, the influence of temperature on r_l may be assumed to be negligible (Pasian and Lieth, 1989), so that r_l can be considered as depending mainly on global radiation above the crop and vapour pressure deficit (Baille et al., 1994a; Baille et al., 1994b; Baille et al., 1994c; Papadakis et al., 1994; Kittas et al., 1999). If we consider that the surface or canopy resistance includes most of the characteristics of the leaf stomatal behaviour, we can normalize equation [2.19] by dividing it by the leaf area index, LAI_g, to obtain the canopy resistance, r_s:

$$r_s = \frac{r_l}{LAI_g} = r_{s,min} \cdot f_1(QS_{int}) \cdot f_2(VPD) \qquad [2.20]$$

Where: $r_{s\min} = \left(\frac{r_{l\min}}{LAI_g} \right)$ is the minimum possible value for r_s in conditions of optimal water supply and environment. For greenhouse roses, the relationship suggested by Baille et al (1994c) was adopted:

$$r_s = \frac{r_{l\,min}}{LAI_g} \left(\frac{a + QS_{int}}{b + QS_{int}} \right) \left[1 + \exp\left(c\,(VPD - VPD_m) \right) \right] \qquad [2.21]$$

Where:

VPD_m is the vapour pressure deficit of the air at which the resistance is minimal. It was taken to be 2.5 kPa. (Baille et al., 1994c; Kittas et al., 1999). The parameters *a*, *b* and *c* have to be derived statistically from experimental data fittings.

CHAPTER 3

MATERIALS AND METHODS

3.0 Introduction

The research project is made up of two main parts: measurements and then modelling. Field measurements were taken at Floraline (Pvt) Ltd, and the modelling part was done at the University of Zimbabwe in the Agricultural Meteorology laboratory. A description of the materials and methods used in the field measurements are outlined first and then a description of the model, its calibration, validation and application follow.

3.1 Site and greenhouse description

The measurement phase of the research project was carried out at Floraline (Pvt) Ltd located within Harare, Zimbabwe (17.8°S, 31.1°E, and altitude 1500 m above mean sea level); between September 2009 and March 2010. The climate of the site is characterised by a dry season from May to October and a rainy season from November–April. The winter season overlaps with the dry season. The summer season overlaps with the rainy season; during this season rain usually comes in the form of afternoon and evening thunderstorms, leaving much of the day clear. Normally October is the hottest month with mean temperatures of 23 °C while June is the coldest month with mean temperatures of 14 °C.

All the experiments were carried out in a 3-span commercial greenhouse, Azrom type (Fig 3.1). Each span was 9.6 m wide and 44 m long with gutter and ridge heights of 4.1 m and 6.5 m respectively (Fig 3.2). The cladding material used for the greenhouse was a 200 µm polyethylene film with terrestrial infrared and ultra violet (UV) absorbing additives (Ganeigar Co., Israel). The greenhouse had ridges that were oriented north-south and had polyethylene sidewall curtains that could be rolled up above the floor from 2.00 m-3.45 m and 2.00 m-3.35 m on the south and north respectively; the openings were covered by plastic (insect-proof) nets.

Fig 3.1: The commercial greenhouse at Floraline (Pvt) Ltd where field measurements were taken.

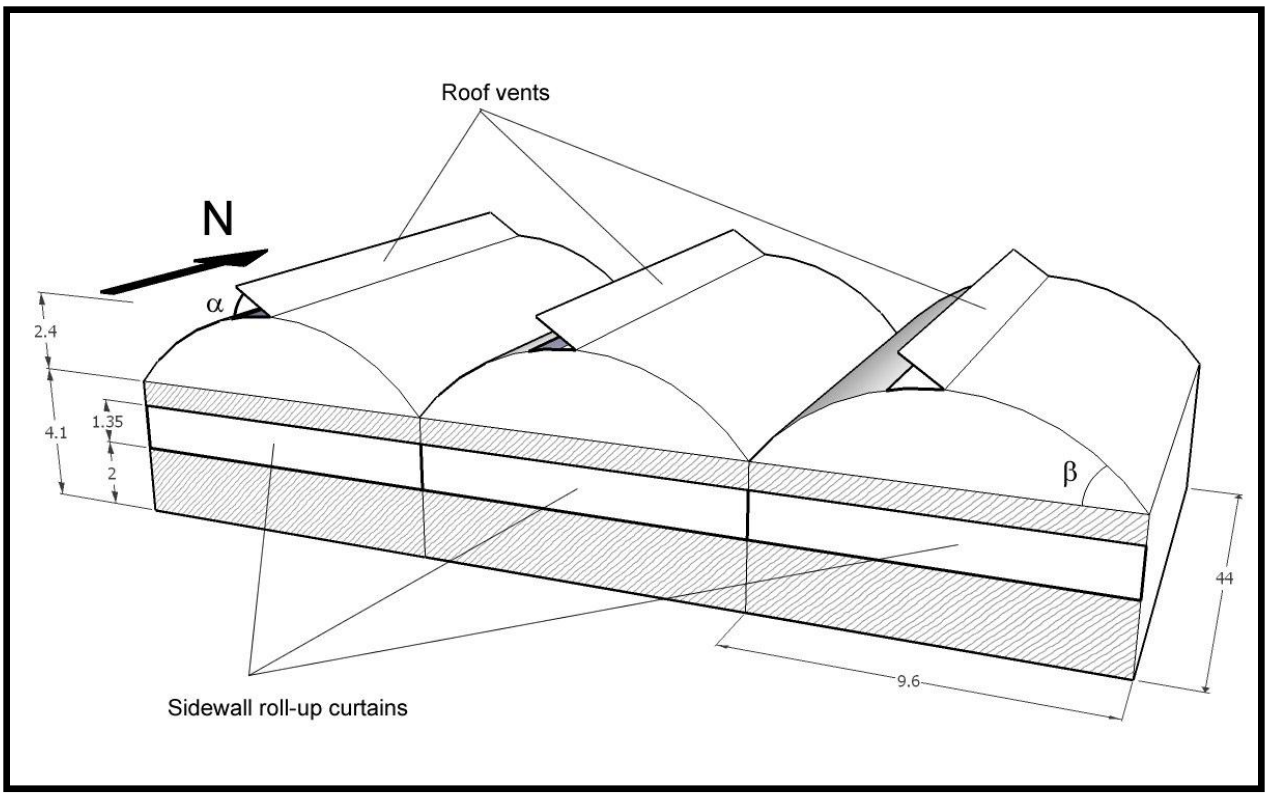

Fig 3.2: The design for the commercial greenhouse at Floraline (Pvt) Ltd where field measurements were taken

3.2 Crop Description

The crop under investigation for this project included several commercial cultivars of roses (*Rosa hybrida*), which were grafted onto Natal briar (*Rosa hybrida* L. 'Natal Briar') rootstocks (Fig 3.3). The cultivars used for measurements included King Arthur, Betsy, N-Tertain, Symponica in Rosso, Upendo, SPE06-2430-10 and SPE05-3904-01. They were cultivated in a soilless media of vermiculite in slightly raised containers with length, width and height of 20 m x 0.45 m x 0.20 m respectively. The crop was fertigated through an automated drip system. The total crop cover represented about 40% of the total greenhouse floor area. In each greenhouse

span the containers were laid in twelve 20 m rows parallel to the gutters. The crop had an average height of 1.20 m, and was watered with an average of 33.30 mm applied per day. The irrigation system was automated and it was triggered to switch on for 4 minutes whenever the outside cumulative solar radiation reached 1600 kJ/m^2. The frequency of watering was divided into about 10 to 14 applications during the day depending on the prevailing climatic conditions measured outside the greenhouse.

Fig 3.3: Several commercial cultivars of roses (*Rosa hybrida*) in a greenhouse where measurements were taken at Floraline (Pvt) Ltd before harvesting.

3.3 Instruments for field measurements

This section describes the instruments that were used for measurements at Floraline.

3.3.1 Air temperature and relative humidity sensors

Air temperature and relative humidity measurements, both inside and outside the greenhouse were taken using two types of air temperature and relative humidity probes. These are outlined as follows:

3.3.1.1 HMP45C temperature and relative humidity probe

The HMP45C temperature and relative humidity probe is designed to measure relative humidity and temperature. It contains a Vaisala HUMICAP® 180 capacitive relative humidity sensor and Platinum Resistance Temperature detector (PRT). The Vaisala HUMICAP® 180 has a relative humidity measurement ranging from 0 to 100 %. At manufacture and at 20 ºC its accuracy is ± 2 % relative humidity in the range (0 to 90 % relative humidity) and ± 3 % (Relative humidity in the range 90 to 100 %). The temperature sensor has a measurement range of -39.2 ºC to +60 ºC and its accuracy at manufacture is greatest (± 0.2 ºC) at 20 ºC and worst (± 0.4 ºC) at -40 ºC. The general operating temperature range for the HMP45C temperature and relative humidity probe is -40 ºC to +60 ºC.

3.3.1.2 RHT2nl temperature and relative humidity probe

The RHT2nl temperature and relative humidity sensors are designed for weather station measurements of relative humidity and air temperature. It contains a relative humidity and air temperature transducer housed in a solar radiation shield. The sensors were equipped with a capacitive relative humidity chip and a platinum resistances thermistor. The RHT2nl gives high temperature precision of ± 0.1 ºC with non-linear thermistor output. The sensor operates at a temperature range of -20 ºC to +80 ºC and relative humidity of 0 to 100 %. It has an accuracy of ± 0.1 ºC over temperatures of 0 ºC to 70 ºC.

3.3.2 Radiation sensors

Several types of radiation sensors were used in the field measurements. Measurements were taken inside the greenhouse and outside the greenhouse. The choice of sensor type to use was mainly dependant on the type of radiation measured and on wether the measurements were taken inside or outside the greenhouse, among other factors. The sensors that were used for taking solar radiation measurements are as follows:

3.3.2.1 TSL Tube solarimeter

A tube solarimeter is designed to measure the average irradiance where the distribution of radiant energy is not uniform, for example in greenhouses and amongst foliage. They are constructed in a tubular way, this provides the necessary spatial averaging and minimises disturbance to the foliage of plants. The sensor element of the tube solarimeter is a black and white painted copper-constantan thermopile and the tube is made of pyrex borosilicate glass. The operating

temperature range is -30 ºC to 60 ºC and its spectral range is 0.4 to 2.2 µm. Its approximate response time for 63 % and 99 % change is 40 seconds and 3 minutes respectively. A tube solarimeter has a directional variation in sensitivity, due to their asymmetric shape. For sun angles greater than 30º this variation in sensitivity is less than ±3 %. Errors due to directional sensitivity are minimised by orienting the tubes North-South and by making comparative measurements with parallel tubes.

3.3.2.2 Q-7.1 Net radiometer

The Q-7.1 net radiometer is a high output thermopile sensor. It was designed to measure the algebraic sum of incoming and outgoing all-wave radiation (the shortwave and long wave components respectively). Outgoing radiation consists of reflected solar radiation and the terrestrial long-wave component while the incoming radiation consists of direct and diffuse solar radiation plus long-wave irradiance from the sky. It contains a high output 60-junction thermopile with low electrical resistance (4 ohms nominal) and linear calibration. It has a spectral response of 0.25 to 60 µm. The thermopile is mounted in a glass reinforced plastic frame with a built-in level. The sensor surfaces (top and bottom) are painted black to reduce internal reflections within the instrument and are protected from convective cooling by hemispherical heavy duty polyethylene windshields which are 0.25 mm thick. Polyethylene is used for the windshield material because it is transparent to both long and shortwave energy.

The operating temperature range for the Q-7.1 net radiometer is 0 to 500 °C and its spectral response ranges from 8 to14 µm. it has a field of view diameter from 1mm and a response time

from 50 ms to 10 s. The effect of wind on the Q-7.1 net radiometer during positive net flux conditions is reduction in the calculated net radiation as wind speeds increase. This reduction increases asymptotically from 0 % at wind speed of 0 m/s to approximately 5.9 % at wind speed of 7 m/s. during negative net flux conditions, wind speed below approximately 1.7 m/s can increase the calculated net radiation from 0 % at 0 and 1.7 m/s to approximately 0.5 % between 0.5 and 0.9 m/s. wind speeds above 1.7 m/s reduce the calculated net radiation from 0 % at 1.7 m/s to approximately 1 % at 7 m/s.

3.3.2.3 CM3 Pyranometer

The pyranometer measures irradiance on a plane surface which results from the direct solar radiation and from the diffuse radiation incident from the hemisphere above. It consists of a thermopile sensor which is coated with a black absorbent coating. The paint absorbs the radiation and converts it to heat; the resultant energy flow is converted to a current by the thermopile. It can be used for measuring diffuse radiation but the direct solar component should be shielded semi-automatically from the pyranometer by a shadow ring. The response time for the sensor for 95% response is 18 seconds. It works at a temperature range of -40°C to +80°C and has a spectral range of 305-2800nm.

3.3.2.4 PAR LITE Sensor

The PAR LITE is a sensor used for agrometeorological and horticulture applications for the measurement of Photosynthetically Active Radiation (PAR). It consists of a Silicon photodiode, filters, a diffuser, housing and a cable. The diffuser ensures a field of view of 180 º. The sensor

operates at a temperature and humidity range of -30 ºC to +70 ºC and 0-100 % respectively. The response time of the sensor is less than 0.1 second and its spectral range is 400-700 nm. The temperature dependence of sensitivity of the PAR LITE is within ±0.2 % per ºC.

3.3.3 Leaf temperature sensors

Fine thermocouples of type K: chromel-alumel, with a diameter of 200 µm were used for measuring leaf temperatures inside the greenhouse. They were connected to a Campbell scientific Data logger and their sensitivity curves were pre-recorded in the logger for the thermocouple outputs to be displayed in ºC. Thermocouple thermometers are precise to about 0.2 ºC. A radiation thermometer (Model MS 35, Heitronics Infrarot., Wiesbaden, Germany) was also used to check on the reliability of the fine thermocouples.

3.3.4 Air movement sensors

A cup anemometer (Model A100L2, Delta T Devices, Cambridge, UK) with a measurement range of 0 to 300ms^{-1} was used to measure wind speed and a wind vane (model WD1, Delta T Devices, Cambridge, UK) was used to measure the wind direction outside the greenhouse at Floraline. The wind vane had an accuracy of ± 2 ° obtainable in steady winds over 5 m/s and a resolution of 0.2 °. The wind vane and the anemometer were connected to a Delta T data logger.

3.4 Instrument Calibration

Calibration is the process of configuring an instrument to provide a result for a sample within an acceptable range. Instrument calibration is one of the primary processes used to maintain instrument accuracy. It is necessary to calibrate an instrument before taking measurements; this ensures that there will not be any bias on data collected from new sensors out of calibration or from failure of older sensors. Calibration of sensors is usually done against an in-house standard; this can keep deviations from the standard within the accuracy limits advertised by the sensor manufacturers. Calibration of sensors was done in from mid- August to September 2009.

3.4.1 Temperature and relative humidity probes

Two types of temperature and relative humidity probes (Model HMP45C, Vaisala Inc., Boston, USA and Model RHT2nl, Delta T Devices, Cambridge, UK) were calibrated against the standard WALZ in-house sensor (Model TS-2 Dew point system, Mess-unit and GegelTechnik). A dew point mirror measuring system was used for this process. It is regarded as one of the most reliable methods for measuring absolute humidity of a gas. The temperature and relative humidity probes were tied together with a platinum resistance thermometer and the WALZ instrument probes and were immersed into the flow chamber of the system. The temperature of the flow chamber was controlled by setting the GRANT LTD 9G at a constant temperature and the relative humidity in the chamber was controlled using a portable dew point generator (Model L1-610). The ambient temperature was presumed to be similar to the water bath temperatures if there were no energy losses. Fixed temperatures were set on the dew point generator but it always had to be less than that of the water bath by 5° C.

All the measurements were recorded automatically by data loggers (Model DL2e, Delta T Devices, Cambridge, UK and Campbell Scientific Ltd., Shepshed, UK) every 5 seconds and these values were averaged every minute. The WALZ was connected to a data logger (Model CR23X, Campbell Scientific Ltd., Shepshed, UK). The outputs for HMP45C temperature and humidity probes should be connected to a Campbell Scientific Data logger and the outputs for the RHT2nl temperature and humidity probes should be connected to a DL2e Delta T Data logger, two separate experiments had to be done for the calibration of the HMP45C and the RHT2nl sensors because there were not enough data loggers to do the experiment at once. The two experiments were carried out on a period from 7 September to 18 September 2009 (DOY 250 to DOY 261). Regressions of the outputs of the tested sensors against the standard sensor were plotted and were used to obtain the calibration factors of the sensors.

3.4.2 Radiation sensors

Calibration of radiation sensors was done at the University of Zimbabwe on the roof top of the Department of Physics (New wing). A pyranometer (Type CM11, serial number 997082, Kipp and Zonen, Delft, Netherlands) was used as the in-house standard. The radiation sensors that were calibrated were tube solarimeters, and CM3 pyranometers. They were tested against the CM11 pyranometer. The tube solarimeters were oriented in the North-South direction. PAR sensors (Model, PAR LITE, Kipp and Zonen, Delft, Netherlands) had no in-house standard; they were compared against each other: one to be used inside the greenhouse and the other one outside the greenhouse. The apparatus was set up away from obstructions, leveled and checked for dryness before they were left to run. The sensors were connected to a data logger (Model CR23X, Campbell Scientific Ltd., Shepshed, UK) and the sensors were left to run from 20-24

August 2009 (DOY 232 to 236). The test sensor output (mV) was plotted against the standard output (Wm^{-2}) and the gradient of that graph was taken to be the calibration constant of each sensor.

3.5 Measurements of climatic parameters

The climatic parameters that were measured inside and outside the greenhouse are described in this section. Two meteorological stations were set up for the measurement of climatic data, one outside and one inside the greenhouse.

3.5.1 Climatic parameters measured inside the greenhouse

An Automatic Weather Station (AWS) mounted at 1.5m height was set up inside the greenhouse (Fig 3.4). As the experiment was running the climatic parameters that were measured continuously in the greenhouse were as follows:

- Global solar radiation above the canopy
- Photosynthetically Active radiation (PAR) above the canopy
- Net all-wave radiation above the canopy
- Air temperature
- Relative humidity

Fig 3.4: The inside automatic weather station at Floraline (Pvt) Ltd

The incoming solar radiation above the canopy was measured using a tube solarimeter (Model TSL, Serial number 058231, Delta T Devices, Cambridge, UK). Net all-wave radiation was measured with a net radiometer (Model Q-7.1, serial number Q03194, Radiation and Energy Balance Systems, Inc). PAR was measured by a PAR sensor (Model PAR LITE, serial number 639-050494, Kipp and Zonen, Delft, Netherlands). Air temperature and relative humidity were measured at 1.5m above the soil height with temperature and relative humidity probes (Model RHT2nl, serial number 900, Delta T Devices, Cambridge, UK). In order to keep track of possible vertical gradients within the greenhouse air, the air temperature and relative humidity were also measured at three other heights of 0.4 m, 0.8 m and 2 m above ground level at the same position as the automatic weather station using three temperature and relative humidity

probes (Model CS500, serial number V3410166 Vaisala Inc., Boston, USA; Model HMP45C, serial number A0130010 Vaisala Inc., Boston, USA and model HMP45C, serial number A0130014, Vaisala Inc., Boston, USA).

Mixing of the greenhouse air was also tested on selected days by measuring the air temperature and relative humidity (at the same height) at four other positions in the greenhouse (fig 3.5). The greenhouse air temperature and relative humidity were taken as the average of the sensor readings at the five positions.

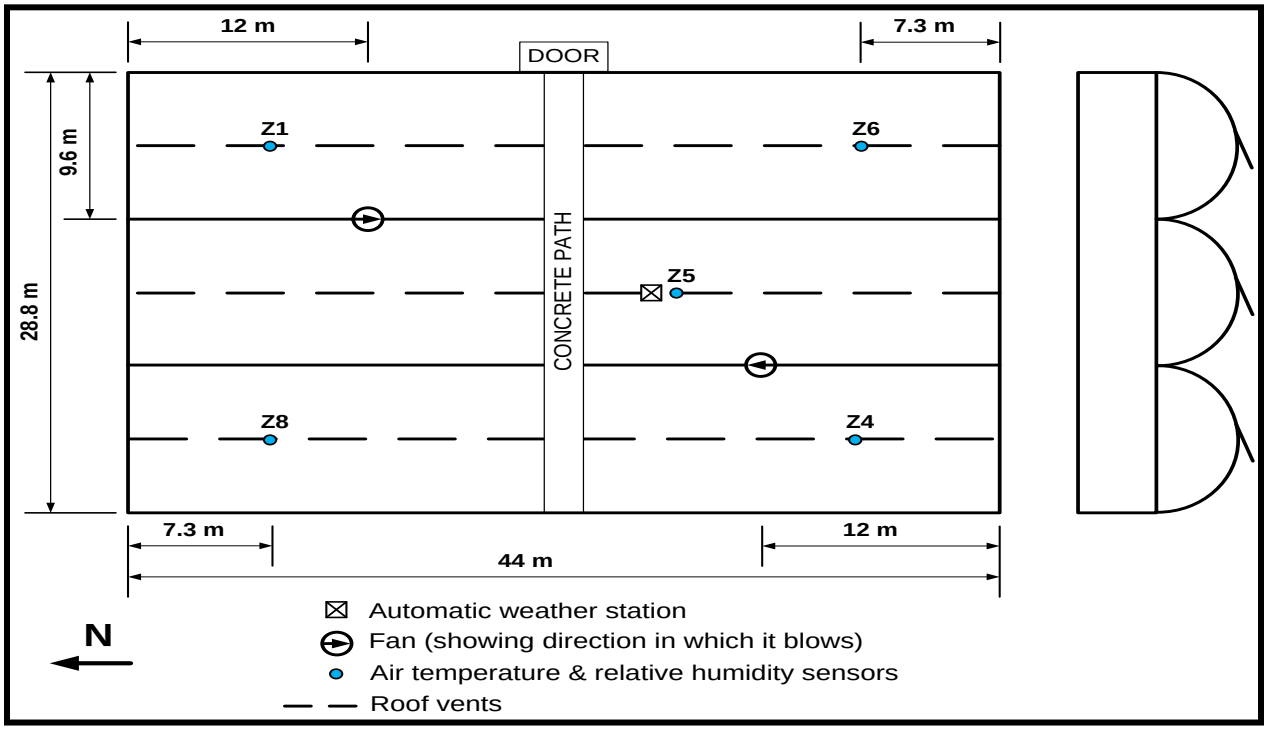

Fig 3.5: The placement of air temperature and relative humidity sensors within the greenhouse for the investigation of greenhouse air mixing

Climatic data were measured every 5 seconds and these values were averaged every 30 minutes and stored in 2 data loggers (Model DL2e, Delta T Devices, Cambridge, UK and Model CR23X, Campbell Scientific Ltd., Shepshed, UK). Several sensors were connected to the DL2e data logger, these were: the tube solarimeter (Model TSL, Serial number 058231, Delta T Devices, Cambridge, UK), the net radiometer (Model Q-7.1, serial number Q03194, Radiation and Energy Balance Systems, Inc), the PAR sensor (Model, PAR LITE label number 639, Kipp and Zonen, Delft, Netherlands) and a temperature and relative humidity probe (Model RHT2nl, serial number 900 Delta T Devices, Cambridge, UK).

3.5.2 Climatic parameters measured outside the greenhouse

Another AWS of similar characteristics were placed near the greenhouse on bare land under open field conditions, well clear of buildings and other obstacles (Fig 3.6). The parameters that were measured continuously outside the greenhouse were as follows:

- Wind velocity
- Air temperature and humidity
- Global solar radiation
- Diffuse radiation
- PAR

Fig 3.6: The outside Automatic Weather Station (AWS) at Floraline (Pvt) Ltd, mounted with all sensors and the shade ring for measurement of diffuse radiation.

The external ambient air temperature and humidity were continuously measured at 1.5 m above the ground. Radiation, and wind speed and direction were also measured continuously at 2 m above the ground. Wind speed was measured using a cup anemometer (model A100L2, Delta T Devices, Cambridge, UK) and wind direction with a windvane (model WD1, serial number 7879, Delta T Devices, Cambridge, UK). Air temperature and relative humidity were measured by a temperature and relative humidity probe with a capacitive relative humidity chip and a platinum resistance thermistor (Model RHT2nl, serial number 453, Delta T Devices, Cambridge, UK). The incoming solar radiation was measured using a pyranometer (Model CM3, serial number 637-058231, Kipp and Zonen, Delft, Netherlands). Diffuse radiation was measured using a pyranometer (Model CM3, serial number 638-058232, Kipp and Zonen, Delft,

Netherlands) mounted onto a shade ring. PAR was measured with a PAR sensor (Model PAR LITE, serial number 380-010281, Kipp and Zonen, Delft, Netherlands). All the measurements were recorded automatically by a data logger (Model DL2e, Delta T Devices, Cambridge, UK) every 5 seconds and these values were averaged every 30 minutes.

3.6 Measurements of physiological parameters

3.6.1 Stomatal Resistance measurements

Stomatal resistances were measured on selected days with a clear sky. Measurements were taken on seven rose cultivars: King Arthur, Betsy, N-Tertain, Symponica in Rosso, Upendo, SPE06-2430-10 and SPE05-3904-0. The leaves were selected from above and within the canopy, where there were two fully expanded, mature and healthy leaves. Stomatal resistances were measured with a dynamic diffusion porometer (Model AP4, Delta T Devices, Cambridge, UK) in continuous cycles (Fig 3.7).

The diffusion porometer was calibrated frequently in order to account for temperature effects that arise when the cup to leaf temperature differences approached ±2ºC and when the set relative humidity differences approached ±5%. Each leaf was measured at least every 30minutes. Stomatal resistance data was to be used for calibration and validation of the stomatal resistance model.

Fig 3.7: Measurement of leaf stomatal resistance with an AP4 diffusion porometer

3.6.1.1 Up scaling to canopy resistance

The stomatal resistances that were measured from the selected leaves were up-scaled to canopy resistance. To get the canopy resistance (r_s) , the average of all the readings taken was divided by the Leaf Area Index (LAI_g). LAI is the ratio of the total upper leaf surface of vegetation divided by the surface area of the land on which vegetation grows.

3.6.2 Determination of LAI_g

A sunscan canopy anaylsis system (Model SS1-TM, Delta T Devices, Cambridge, UK) was used to estimate LAI_g (Fig 3.8).

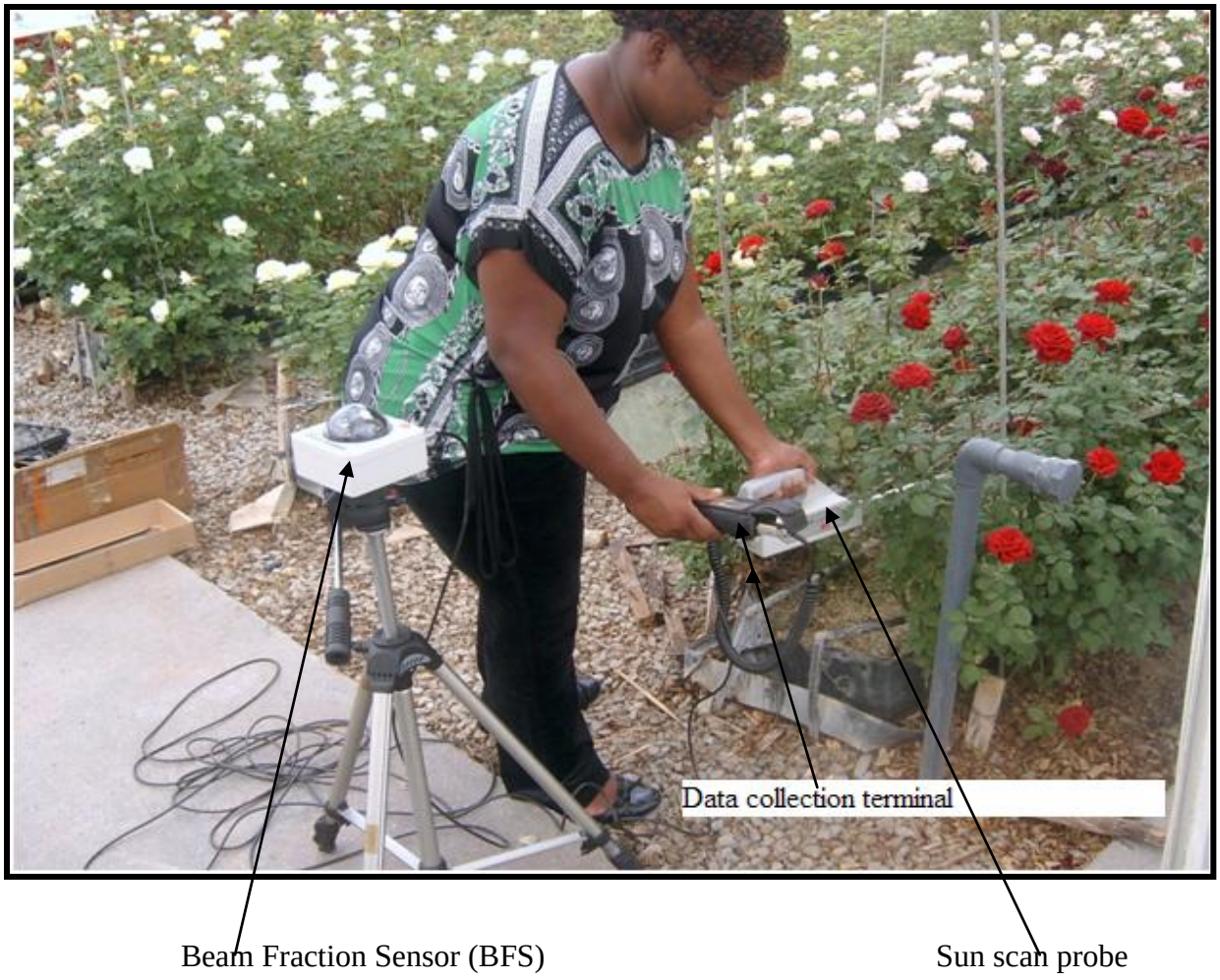

Fig 3.8: Estimation of the Leaf Area Index (LAI) using a sunscan canopy analysis system

Measurements were taken on a clear day at mid-day and replicated 10 times on different rows. A sunscan canopy anaylsis system is a portable instrument for measuring the light levels of PAR in plant canopies. It measures the interception of solar radiation by the canopy, enabling estimates of canopy LAI_g. LAI_g is calculated using Beer's Law from measurements of the incident light (I_0) and transmitted light (I) which gives the following relationship with LAI_g:

$$I = I_0 \cdot e^{-kLAI} \qquad [3.1]$$

Where: k = an extinction coefficient depending on the leaf angle distribution and the direction of the beam. (k =1 for entirely horizontal leaves). This method is non-destructive, and measurements were done once a week during the measurement period.

The sunscan canopy analysis system comprises of a sunscan probe, a beam fraction sensor (BFS) and a data collection terminal (the Psion Workabout). The sunscan probe measures the light transmitted through the canopy beam fraction sensor and the BFS measures the light incident on the canopy. The measurements are observed and stored on the data collection terminal.

3.6.3 Leaf temperature measurements

Leaf temperature measurements inside the greenhouse were done using fine thermocouples. The thermocouples were attached to the lower side of the leaf by plastic clips (Fig 3.9) and measurements were done randomly on the cultivars studied. The leaf temperature was measured at different locations within the canopy.

Four thermocouples were attached to the leaves of the flower stem and two thermocouples were attached to the leaves of the bent shoots on the lower part of the canopy. The canopy temperature (T_v) was then calculated as the average of the six leaf temperatures. The thermocouples were connected to a datalogger (Model CR23X, Campbell Scientific Ltd., Shepshed, UK) and measurements were automatically recorded every 5 seconds and averaged every 30 minutes. The canopy temperature data were used in the calibration and validation of the vegetation model.

Fig 3.9: A rose leaf with a thermocouple attached on its underside by a plastic paper clip

To check on the reliability of the leaf temperature readings from the thermocouples; a radiation thermometer (Model MS 35, Heitronics Infrarot., Wiesbaden, Germany) was also used in the greenhouse to measure leaf temperatures as shown in Fig 3.10.

Fig 3.10: Leaf temperature measurement taken by a radiation thermometer

3.6.4 Crop transpiration rate determination.

This section describes how crop transpiration rates that were available as historical data were collected. Historical data was obtained from Floraline (Pvt) Ltd from several varieties of a rose crop for the period December 2007 and January 2008. SHB sap flow gauges (model SG10WS, Dynamax, Inc., Houston, USA) were used to measure crop transpiration rates. They were installed on the main stems of two rose plants to monitor whole-plant transpiration (WPT) continuously following Rose and Rose, 1998; Baker and van Bavel, 1987; Baker and Nieber, 1989. The sap flow gauges were checked weekly for sap accumulation and gauge contact with the stem. The heaters were loosened when necessary to allow for rapid plant growth. If the stems became too big for the gauges or if the plants showed signs of stress; the gauges were changed to

other stems. After the sap flow was measured, water use by sampled plants was extrapolated to the entire stand or greenhouse. The mass or volume flow rates for individual plants were converted to estimates of transpiration per unit area of ground.

The total leaf area, A_L, of the plant where the gauge was installed was determined destructively by means a WinDIAS colour image analysis system (Delta T Devices, Cambridge, UK) connected to a personal computer and thermocouples were inserted into the stem of the rose plants to measure the stem temperature. Scaling up to crop transpiration was done by assuming that the stem sap flow was uniform throughout the crop. This upscaling assumes that the stem sap flow was uniform throughout the crop (Ham et al, 1990). The crop transpiration rate can be written as:

$$T_r(t) = \frac{1}{1000 \times 3600} \times P_V \times A_g \times \frac{F_s(t)}{A_L} \times LAI \qquad [3.2]$$

Where:

$T_r(t)$ is the greenhouse crop transpiration rate (kg s^{-1})

P_V is the fraction of the total greenhouse floor area covered by the crop,

A_g is the total greenhouse floor area (m^2)

$F_s(t)$ is the stem sap flow (g h^{-1})

A_L is the total leaf area of the plant on which the gauge is installed (m^2)

LAI_g is the crop leaf area index (expressed per unit cultivated greenhouse floor area).

Errors in whole plant transpiration rates in the mornings and late afternoon due to temperature gradients between the soil and air were corrected for using the method proposed by Steppe et al (2005).

3.7 Calibration and validation of the transpiration sub model of the GDGCM

The transpiration sub-model of the GDGCM described in §2.10.1 was calibrated and validated using climatic and physiological data that had been collected from the field and historical data on transpiration rates obtained from sap flow measurements. The historical data was obtained from Floraline (Pvt) Ltd from several varieties of a rose crop for the period December 2007 and January 2008. The model had two parts that were calibrated and validated separately. The canopy resistance model (Equation 2.21) of the transpiration sub-model was calibrated and validated first and then the transpiration model (Equation 2.16) was then calibrated and validated using rose canopy surface resistance (r_s) output values from the canopy resistance model, (Equation 2.21). The climatic and physiological data used for calibration and validation of the canopy resistance model, (Equation 2.21) were collected on selected days in January 2010 to March 2010. Due to shortages of sap flow gauges, it was not possible to physically measure transpiration rates during the period this research study was undertaken. Instead the calibration and validation of the transpiration sub-model of the GDGCM (Equation 2.16) were carried out using historical data of transpiration rates obtained from measurements using sap flow gauges, climatic and other physiological parameters. The historical data was obtained from Floraline (Pvt) Ltd from several varieties of a rose crop for the period December 2007 and January 2008.

3.7.1 Canopy resistance model calibration

The canopy resistance model [Equation 2.21] was calibrated to obtain the coefficients a, b and c. Calibration was done using data collected on 27 and 28January 2010 and 11 and 12 February 2010 (DOY 27,28, 42 and 43 respectively). The input parameters $r_{s,}$ LAI_g and leaf or vegetation temperature (T_v), were obtained from field measurements as discussed in §3.6.1, §3.6.2 and §3.6.3 respectively. The solar irradiance incident on the crop, QS_{int} was obtained from the climatic data that was automatically recorded on the inside weather station by data loggers. The vapor pressure deficit of the air at which resistance is minimal, VPD_m was taken to be 2.5kPa (Baille et al., 1994c; Kittas et al., 1999) and $r_{l,\min}$ was taken as 100 s m^{-1} (Baille et al., 1994a; Baille et al., 1994c; Kittas et al., 1999). VPD was obtained mathematically as described in §3.7.1.1. After inputting all parameters of the canopy resistance model (equation 2.21) a regression wizard tool in a statistical package; Sigma plot 2001(Systat Software Inc., San Jose CA, USA) was used to evaluate the coefficients a, b and c from experimental data fitting.

3.7.1.1 Determination of Vapor pressure deficit

The vapor pressure deficit, VPD (kPa) was obtained mathematically from the climatic data recorded inside the greenhouse. It is the difference between the vapour pressure and the saturation vapour pressure. The following equations were used to obtain VPD.

$$e_s(T_v) = 0.6108 \times EXP\left(\frac{17.3T_v}{T_v+237.3}\right) \quad [3.3]$$

$$e_a = \frac{RH \times e_{s(T_a)}}{100} \quad [3.4]$$

Where: $e_s(T_a)$ and $e_s(T_v)$ are the saturation vapour pressure at the air and vegetation temperature respectively (kPa), T_v and T_a are the vegetation and air temperature (°C) respectively, e_a is the vapour pressure (kPa) and RH is the relative humidity, (%). The difference of [3.3] and [3.4] gave VPD as shown:

$$VPD = e_s(T_v) - e_a \qquad [3.5]$$

(Monteith and Unsworth, 1990)

3.7.2 Canopy resistance model validation

Validation of the canopy resistance model, (Equation 2.21) was done using climatic and physiological data taken on 16 March 2010 (DOY 107). r_s values were simulated using another set of input parameters (LAI_g, QS_{int} and VPD), and the coefficients a, b and c that were obtained from the calibration process and the same values of VPD_m and $r_{l,\min}$ of 2.5kPa and 100 s m^{-1} respectively. To validate the model, the simulated r_s were compared to r_s measured by means of a dynamic diffusion porometer (model AP4, Delta T Devices, Cambridge, UK). To assess how well the canopy resistance model predicted r_s, a regression of simulated and observed r_s values was done and statistical parameters were used to analyse the validation. The statistical parameters used were the coefficient of determination (R^2) and the standard error estimate (SE) of the model, σ. These are defined by Equations 3.6 and 3.7.

$$R^2 = 1 - \frac{SS_R}{SS_T} = 1 - \frac{\sum_i (y_{sim} - y_i)^2}{\sum_i (y_i - \bar{y})^2} \qquad [3.6]$$

$$\sigma = \sqrt{\frac{\sum_i (y_{sim} - y_i)^2}{N}} \qquad [3.7]$$

Where:

y_i is the measured output

$\bar{y}$ is the average,

y_{sim} is the model output

N is the number of data points.

3.8 Transpiration sub-model calibration

The transpiration sub-model (Equation 2.16) was calibrated by determining several parameters that were used to simulate the transpiration for the rose crop. The simulated transpiration was compared with historical data of whole plant transpiration rates that were obtained from Floraline (Pvt) Ltd from several varieties of a rose crop for the period December 2007 and January 2008.

3.8.1 Determination of phase change heat transfer coefficient (h_P)

The phase change heat transfer coefficients for the upper and lower faces of the leaves, h_{P1} and h_{P2} were assumed to be the same for the upper and lower faces of the leaves. To determine h_P, Equation [2.18]; the latent heat of condensation of water, h_{fg} (J kg^{-1}), Sherwood number, *Sh*, the molecular diffusion coefficient of water vapour in air, D (m^2 s^{-1}) and the characteristic

dimension, *d* (m) had to be determined first. To determine *d* was the characteristic length of the leaves of the roses were measured. Ten rose bushes were selected and on these bushes ten fully developed leaves with 3 leaflets each had their lengths measured. The mean length of the leaves was calculated, and the deviation per leaf noted. *D* was taken to be 24.9 x 10^{-6} m^2 s^{-1} at 25°C (General data booklet, 1999). It was assumed to be constant through out the temperature range. h_{fg} (J kg^{-1}). *Sh*, was determined mathematically using the following equations:

$$h_{fg} = 1000 \times [2501 - (2.361 \times T_a)], \quad [3.8]$$

Where:

T_a is the air temperature, (°C).

The equation for determining *Sh* involved the calculation of the Grashof number (*Gr*), the existing convection and the flow type. *Gr* is the ratio of the buoyancy force times the inertial forces to the square of the viscous forces. For air under normal conditions:

$$Gr = \frac{\beta g d^3 (T_v - T_a)}{v^2} \quad [3.9]$$

(Bakker et al, 1995)

Where: β is the thermal expansion coefficient of air (K^{-1}), g is the acceleration due to gravity (ms^{-2}), d is the characteristic dimension of the leaf (m), ($T_v - T_a$) is the temperature difference between the vegetation , T_v and the surrounding air, T_a (K) and v is the coefficient of kinematic viscosity air, (ms^{-2}). v was considered to be a constant with a value of, 15.5 x 10^{-6} ms^{-2} at 25°C. It was assumed that there were no significant differences in v obtained in the temperature range

existing in the greenhouse. g is a constant = 9.81 ms^{-2}. T_v and T_a were obtained from the climatic and physiological data that were measured. Air was assumed to be an ideal gas and β is the inverse of T_a (K). The convection and flow type existing in the greenhouse was determined according to fig 3.11.

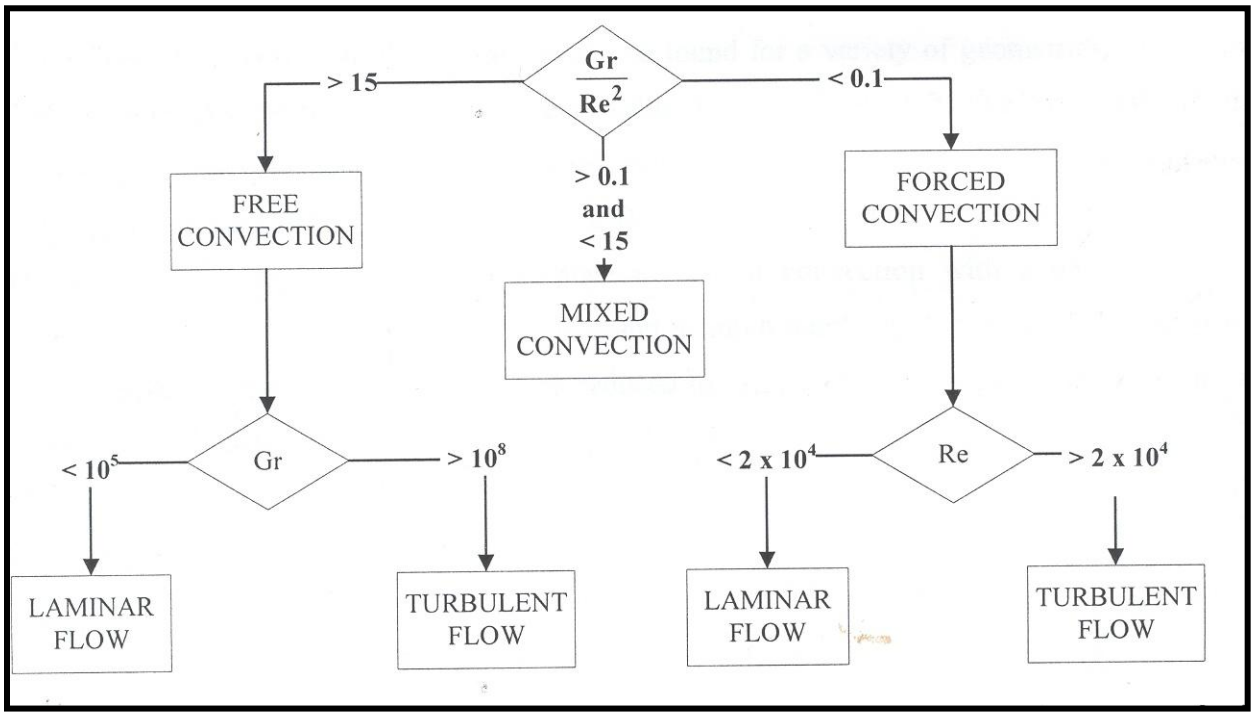

Fig 3.11: A flow chart determining the convection and flow type in heat and mass transfer in the boundary layer (adapted from Monteith and Unsworth, 1990)

Reynolds number (*Re*) is a dimensionless group given by:

$$Re = \frac{ud}{v} \qquad [3.10]$$

(Monteith and Unsworth, 1990)

Where u is the velocity of air (ms^{-1}) and the parameters d and v are as described as before. It was determined that there was free convection and laminar flow and Sh was given by:

$$Sh = 0.47 \times Gr^{0.25} \quad [3.11]$$

(Bakker et al.,1995)

3.8.2 Determination of the mass transfer coefficient (h_{Tr}')

The mass transfer coefficient (h_{Tr}') was given by equation [2.17]. r_s that was input was simulated from the canopy resistance model equation [2.21]. LAI_g was determined as outlined in §3.6.2 and determination of hfg and h_{p1} and h_{p2} was as outlined in §3.9.1

3.8.3 Determination of the transpiration flux density ($Q_{L(vi)}$)

$Q_{L(vi)}$ was given by equation [2.16]. h_{fg} and h_{Tr}'were determined as outlined in §3.8.1 and §3.8.2 respectively. The saturation water vapour concentration at the temperature of the vegetation $x_s(T_v)$ ($kg\ m^{-3}$), was determined following equation [3.12] as shown:

$$x_s(T_v) = \frac{1.323 \times EXP\left(\frac{17.327 \times T_v}{237.3 + T_v}\right)}{T_v + 273.16} \quad [3.12]$$

For the water vapour concentration of the surrounding air x_i ($kg\ m^{-3}$), the saturation water vapour concentration at air temperature, $x_s(T_a)$ was calculated first. This is given by the following equations:

$$x_s(T_a) = \frac{1.323 \times EXP\left(\frac{17.327 \times T_a}{237.3 + T_a}\right)}{T_a + 273.16} \quad [3.13]$$

$$RH\ (\%) = \frac{x_i}{x_s(T_a)} \quad [3.14]$$

$$x_i = \frac{x_s(T_v) \times RH}{100} \quad [3.15]$$

Equations 3.12, 3.13, 3.14 and 3.15 were adapted from Monteith and Unsworth, 1990

3.9.4 Transpiration sub-model validation

To validate the transpiration sub-model, equation [2.16] the simulated transpiration rates were compared to the transpiration rates measured by stem heat balance sap flow gauges (model SG10WS, Dynamax, Inc, Houston, USA). Part of the historical data (January 2008) obtained from Floraline (Pvt) Ltd from several varieties of a rose crop for the period December 2007 and January 2008 data, was used to assess how well the transpiration model predicted $Q_{L\ (vi)}$. A regression of simulated and observed $Q_{L(vi)}$ was done and statistical parameters were used to analyse the validation. The statistical parameters used were R^2, and SE.

3.9.5 Model implementation

The transpiration sub-model (equation 2.16) was considered in this study. In the GDGCM there are 73 subroutines, the transpiration sub model (equation 2.16) is in the subroutine type 64. The simulation of $Q_{L\ (vi)}$ was done by FORTRAN in the subroutine type 64. The GDGCM is within the transient simulation systems (TRNSYS) (fig 3.12) which works out the system of differential equations.

TRNSYS is a computer package developed by the "Solar Energy Laboratory" at the "University of Wisconsin-Madison" for the treatment of solar energy problems; it is described in Klein et al. (1988). With the current version of TRNSYS (version 16) a text file describing the system being simulated is created and then a FOTRAN program is launched to run it. Simulations were carried out for a whole year divided into the winter season (May 2007 to August 2007) and the summer season (September 2007 to April 2008). Table 3.1 shows the values of the parameters that were used in the model.

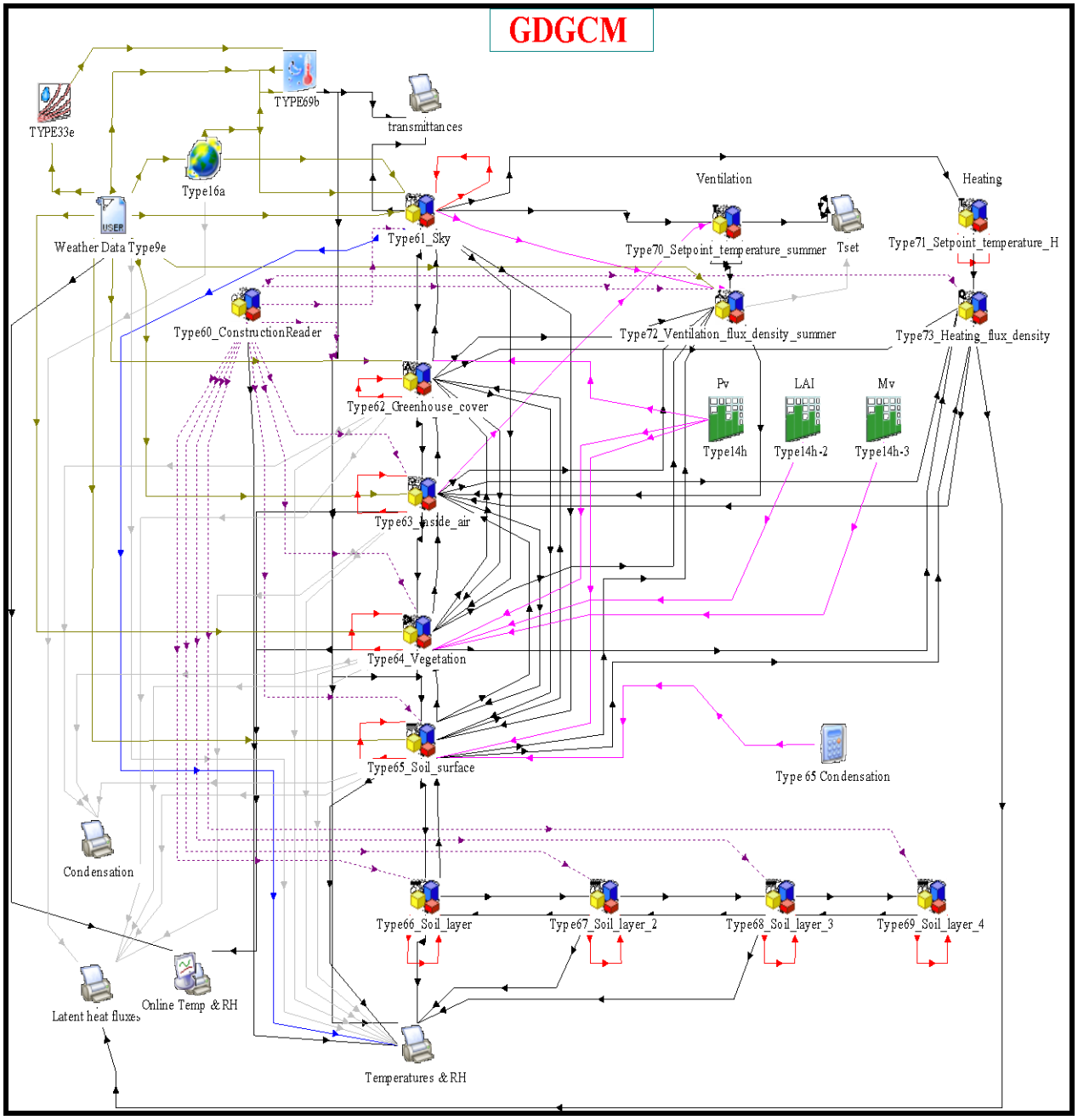

Fig 3.12: The GDGCM within the TRNSYS 16

Table 3.1: Values for the Gembloux Dynamic Greenhouse Climate Model parameters (after Pieters, 1996; Pieters and Deltour, 1997; Pollet and Pieters, 2000)

Soil Characteristics	***First Layer***	***Second Layer***	***Third Layer***	***Fourth layer***	
Thermal conductivity [$Wm^{-1}K^{-1}$]		0.70	1.95	1.9	1.9
Layer thickness [m]		0.05	0.15	0.3	0.7
Density of soil layer [kgm^{-3}]		1300	1450	1600	1650
Heat capacity of soil layer [$kJkg^{-1}K^{-1}$]		1.35	1.25	1.25	1.20
Subsoil temperature [°C]			: 18.5		
Thickness of the subsoil layer			: 8.8		
Floor					
Floor reflectance for solar radiation [-]			: 0.85		
Floor emittance for far infrared radiation [-]			: 0.95		
Characteristic length of greenhouse floor [m]			: 1001		
Cover Characteristics					
Material: 200μm Diffused Polyethylene (DPE)					
Outer cover emittance for far infrared radiation [-]			: 0.79		
Inner cover emittance for far infrared radiation [-]			: 0.79		
Transmittance for far infrared radiation [-]			: 0.18		
Cover absorptance for diffuse radiation [-]			: 0.04		
Dry cover transmittance for diffuse solar radiation [-]			: 0.69		
Wet cover transmittance for diffuse solar radiation [-]			: 0.55		
Frame transmittance for solar radiation [-]			: 0.95		
Dry cover heat capacity per unit area [$kJm^{-2}K^{-1}$]			: 0.725		
Maximum condensation water film thickness [mm]			: 0.12		
Transmittance and reflectances (beam radiation) at 0, 15, 30,45,60,75 and 90° [-]					
Dry cover transmittance:	0.75	0.74	0.72	0.69	0.63	0.46	0.00
Wet cover transmittance:	0.61	0.61	0.59	0.59	0.57	0.46	0.00
Dry cover reflectance:	0.21	0.22	0.25	0.27	0.33	0.50	1.00
Wet cover reflectance:	0.35	0.35	0.37	0.37	0.39	0.50	1.00
Vegetation Characteristics							
Reflectance for solar radiation [-]				: 0.16			
Canopy attenuation coefficient [-]				: 0.61			
Characteristic length of the leaves[m]				: 0.06			
Emittance for far infrared radiation [-]				: 0.95			
Specific Heat Capacity [$kJkg^{-1}K^{-1}$]				: 4.18			
Air characteristics							
Humid air density [kgm^{-3}]				: 1.25			
Volumetric Heat Capacity [$kJkg^{-1}K^{-1}$]				: I.256			
Latent heat of condensation of water [$kJkg^{-1}K^{-1}$]				: 2437			
Inside air velocity [ms^{-1}]				: 0.30			
Lewis number [-]				: 0.89			

3.9 Characterisation of the existing irrigation system at Floraline (Pvt) Ltd

Irrigation at Floraline was done through an automated drip irrigation system. The system had 131 emitters per drip line on a row and the emitters had a spacing of 15 cm. Each flower bed (row) had 2 drip lines parallel to each other; hence the whole greenhouse of 36 rows had 9432 emitters. The manufacturer's emitter rate upon installation was 1,33 litres/hour. Irrigation was triggered automatically whenever the accumulative solar radiation outside the greenhouse reached 1600 kJ/m^2 and the installed irrigation system applied water for a fixed period of 4 minutes each time it was done.

3.9.1 Emitter rate determination

An experiment was done to determine the emitter rate of the drip lines that were used at Floraline; this was done to verify the emitter rate that was given by the manufacturer of the drip lines upon installation of the system. The emitter rate given could have changed over time due to various factors, which include clogging from salts and mud. In the experiment ten emitters from the whole greenhouse were chosen randomly and ten labelled catch cans were set below these emitters ensuring that when irrigation was switched on, the water from the emitters would go into the catch cans directly, (fig 3.13). Irrigation was switched for four minutes while water was collecting into the catch cans and they were removed from the field. The volume of water that was collected from each catch can was measured using a measuring cylinder and recorded. The mean volume of the collected water was calculated and the emitter rate was given by dividing the mean by the time.

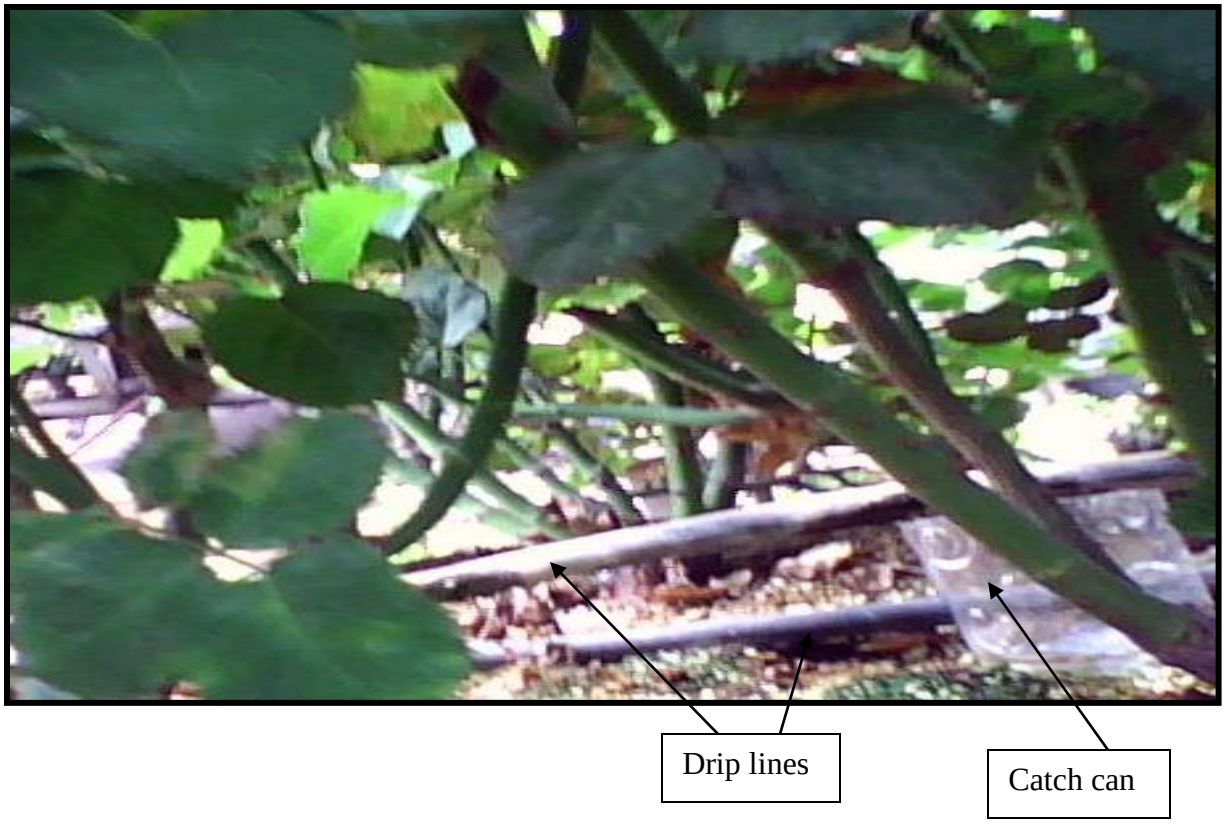

Fig 3.13: A catch can set below an emitter of a drip line in a bed of roses.

3.11 The amount of water required for irrigation

The actual water applied by the existing irrigation system and the CWR simulated by the GDGCM were determined and compared to assess the potential of the GDGCM as a tool for irrigation scheduling for greenhouse crops.

3.11.1 Determination of the water applied by the existing irrigation system

Outside solar radiation data, for May 2007 to April 2008 was used for the calculations of the crop water that was required during the whole year. The data on solar radiation outside the

greenhouse was used to determine the number of irrigation cycles per day. The total solar radiation (kJ/m^2) received per day was divided by 1600 kJ/m^2 to get the irrigation cycles per day. The duration was 4 minutes/cycle and the emitter rate was 0.0167 litres/minute (1 litre/hour). The water used by the system per day was determined as follows:

$$water\ used = irrigation\ cycles\ \times duration/\ cycle\ \times emitter\ rate \qquad [3.16]$$

3.11.2 Determination of CWR using the GDGCM

The water lost by the plant through transpiration is the water that the crop requires to be replenished hence the amount of water needed for irrigation was calculated from the transpiration rates obtained from the model. The daily transpiration was obtained as a summation of the transpiration rates of the whole day and the seasonal transpiration rates were obtained as the summation of the daily transpiration rates per month. The transpiration rates (W/m^2) were converted to litres per day taking into consideration that;

- 1MJ /m^2/day = 0.408mm/day
- 0.1mm/day= 1m^3/ha/day
- 1m^3= 1000 litres

(Allen *et al*,1998)

CHAPTER 4

RESULTS AND DISCUSSIONS

4.1 Introduction

This chapter outlines the results of this research project. The presentation of the results was divided into 3 sections. Instrument calibration results were presented first followed by field measurement results and the model results come at the end. The results that were obtained for the calibration of instruments which was done before field measurements were carried out in this study are presented in this section.

4.1.1 Temperature and relative humidity probes

Table 4.1. shows the corrected and sensor output relative humidity equations (RH_{cr} and RH_{sr} output respectively) and the corrected and sensor output temperature equations (T_{cr} and T_{sr} respectively) of temperature and humidity sensors that were calibrated and used in this study.

Table 4.1: Calibration factors, for temperature and relative humidity probes.

Sensor	Reference number	Correction equation
HMP45C (RH output)	225	$RH_{cr}= (RH_{sr}+ 3.61)/ 0.895$
HMP45C (Temperature output)	225	$T_{cr}= (T_{sr}+ 0.38)/ 0.96$
HMP45C (RH output)	600	$RH_{cr}= (RH_{sr}+ 6.63)/ 0.84$
HMP45C (Temperature output)	600	$T_{cr}= (T_{sr}+ 2.78)/0.85$
RHT2nl (RH output)	900	$RH_{cr}= (RH_{sr} – 0.74)/1.3$
RHT2nl (Temperature output)	900	$T_{cr}= (T_{sr} – 2.5)/1.07$
RHT2nl (RH output)	636	$RH_{cr}= (RH_{sr}+ 0.17)/ 1.16$
RHT2nl (Temperature output)	636	$T_{cr}= (T_{sr} – 2.55)/ 1.09$

4.1.2 Radiation sensors

The gradient obtained when the test sensor output was plotted against the CM11 was taken to be the calibration constant. Table 4.2 shows the calibration equations of the all the radiation sensors that were used for this research project.

Table 4.2: Calibration factors for radiation sensors. R_c and R_s are the corrected and sensor output radiation values respectively.

Sensor	Serial number	Correction equation
Tube solarimeter	058231	$R_c = (R_s - 3.072)/ 0.72$
PAR sensor	639_050494	$R_c = (R_s + 0.982)/0.96$
PAR sensor	380_010281	$R_c = (R_s + 1.236)/1.19$
CM3 pyranometer	638_058232	$R_c = R_s /0.68$
CM3 pyranometer	637_058231	$R_c =(R_s + 5.8)/0.72$

4.2 Field measurements

This section presents the results for the measurements taken at Floraline (Pvt) Ltd. These were used as input parameters for model calibration and validation and also for calculations for the actual water applied at Floraline.

4.2.1 Greenhouse microclimate

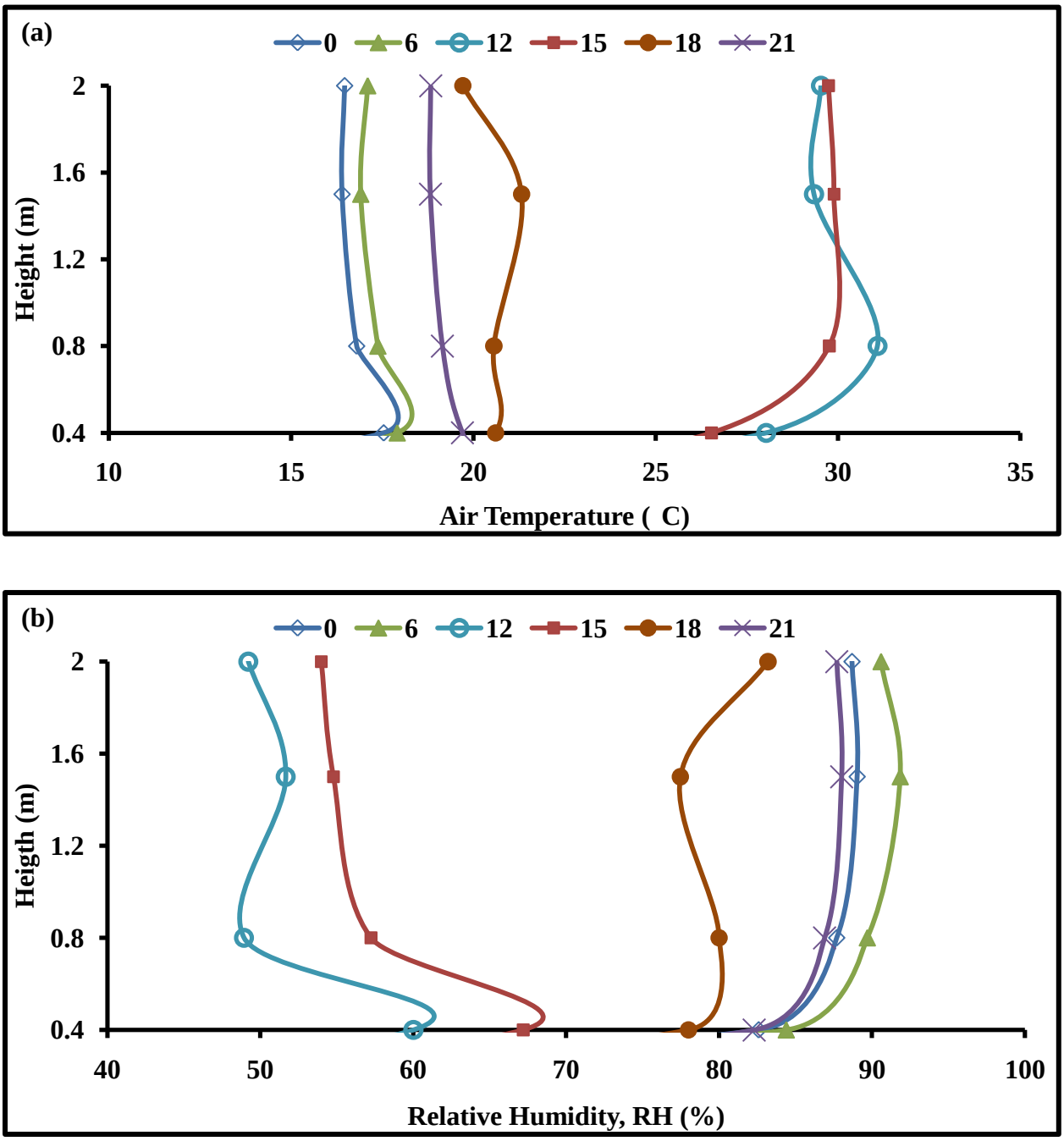

Fig 4.1: The diurnal vertical variation of (a) air temperature and (b) relative humidity in the greenhouse on 28 October 2009. The temperature and relative humidity were measured at heights of 0.4 m, 0.8m, 1.5m (crop height) and 2 m at the position of the internal AWS (see Fig. 3.5).

Although fig 4.1 indicates that there are significant differences between the air temperatures and relative humidity within and above the canopy, the absence of significant vertical variations in the air temperature and relative humidity above the canopy suggests that the greenhouse air was well mixed.

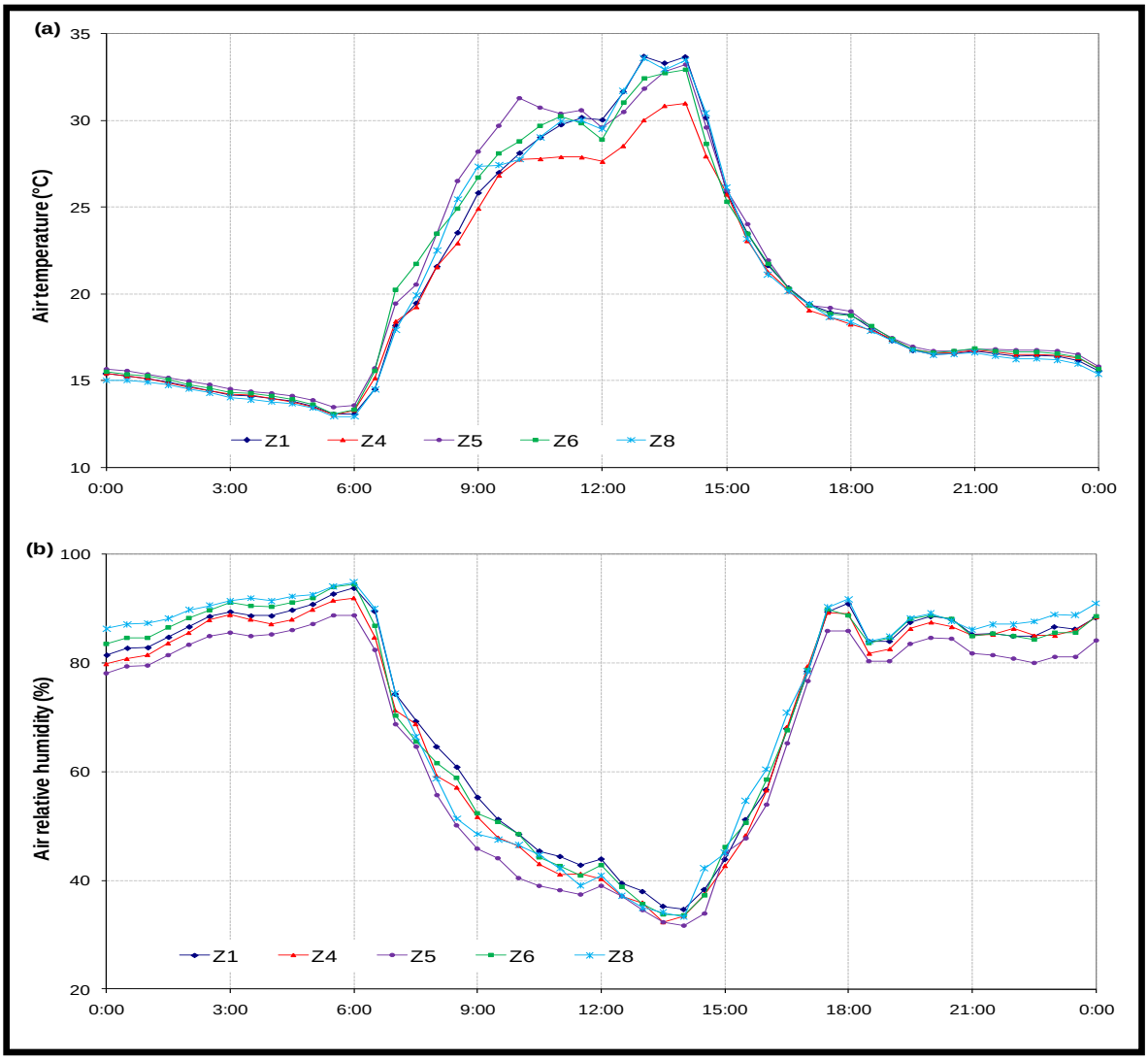

Fig 4.2: Greenhouse air temperature and relative humidity at 5 measuring positions, during a single measuring day (28 Oct 2009).

Fig 4.2 shows the diurnal variations on 28 October 2009 of the air temperature and air humidity measured at the five designated locations in the greenhouse (see fig 3.5) and Table 4.3 gives the 4-day average values of the air temperature and relative humidity.

Table 4.3: Summary of greenhouse air temperature and relative humidity homogeneity test results, measured at five sensor locations, during a 4-day period (27 – 31 Oct 2009).

Sensor	**Z1**	**Z4**	**Z5**	**Z6**	**Z8**
Daytime					
Average temperature (°C)	23.7	22.8	24.1	23.7	23.8
Temperature deviation (°C) from mean value	0.0	-0.8	0.5	0.1	0.2
Average relative humidity (%)	59.6	57.3	54.9	58.9	58.7
Relative humidity deviation (%) from mean value	1.7	-0.6	-3.0	1.0	0.9
Night-time					
Average temperature (°C)	16.0	16.0	16.4	16.0	15.9
Temperature deviation (°C) from mean value	0.0	0.0	0.3	0.0	-0.2
Average relative humidity (%)	78.6	78.0	75.6	80.2	80.0
Relative humidity deviation (%) from mean value	0.1	-0.5	-2.8	1.7	1.4

The results seem to suggest that there are no appreciable gradients in the temperatures and relative humidity in the greenhouse. Sensor Z4 located to the south-west of the greenhouse consistently indicated lower day-time temperatures than the other four sensors. There were no significant differences between the night-time temperatures and the day-time relative humidities measured at the five positions. The night-time humidity measured by sensor Z5 located near the centre of the greenhouse and at the point, at which all climatic measurements were made earlier, was consistently lower than at the other four positions. However, the results seem to confirm the assumption made earlier that because there are no gradients in the greenhouse, the temperature and relative humidity measured at any point in the greenhouse is representative of the whole greenhouse.

The regimes of solar radiation and VPD that were measured on 16 March 2010 (Day Of Year (DOY) 76) are shown in fig 4.3. Solar radiation increased gradually from 0700 Hrs up to 1000 Hrs where it was highest, the increase in solar radiation resulted in an increase in VPD also reaching a maximum at 1000 Hrs when solar radiation was highest. Solar radiation was nearly constant till 1100 Hrs where it decreased gradually until 1700 Hrs. Solar radiation reached its maximum at 1000 Hrs and not around 1200 Hrs as expected because on this day, it was a clear day up to 1000 Hrs then clouds began to gather reducing the solar radiation. When the intensity of solar radiation decreased it resulted in a decrease in air temperature and an increase in RH thus a high VPD. VPD was highest at 1330 Hrs. As more clouds gathered, the sky becoming overcast, solar radiation intensity decreased, VPD decreased reaching a minimum point at 1430 Hrs and it then rained.

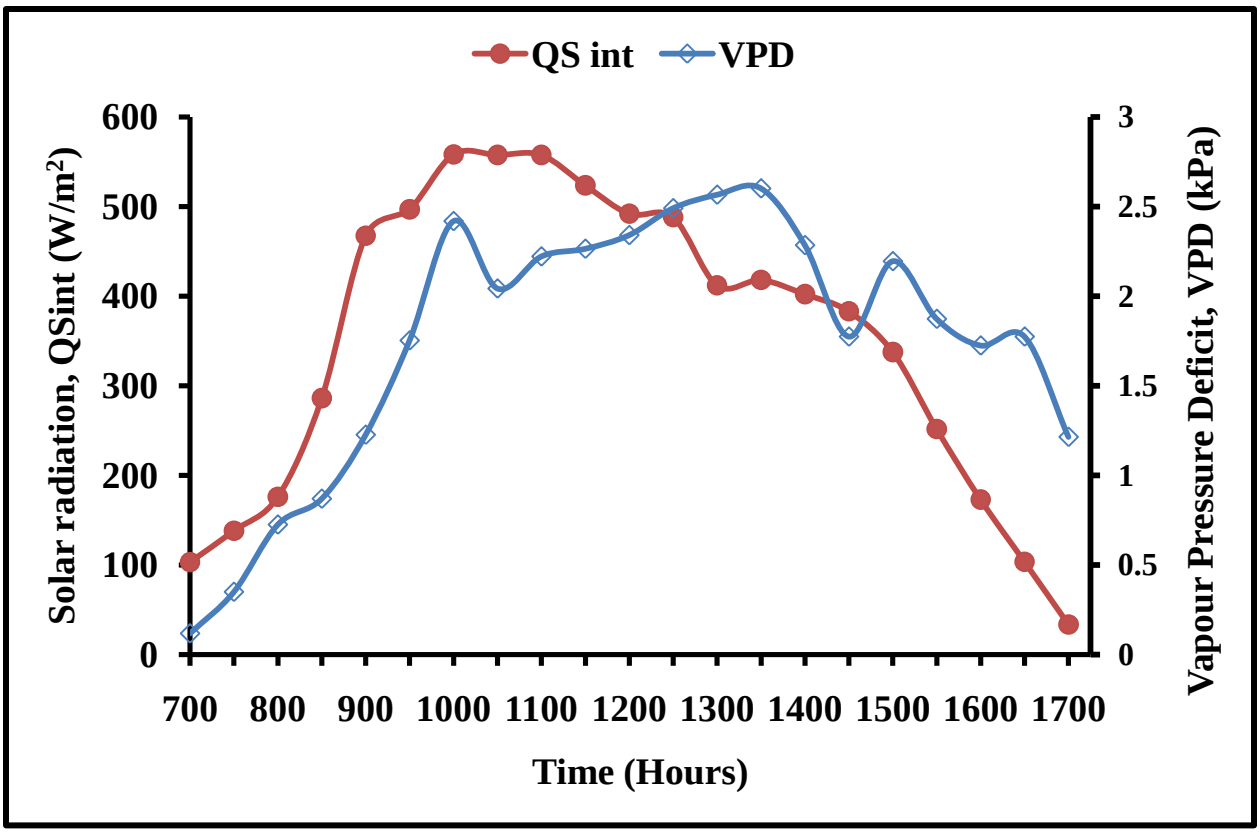

Fig 4.3: Variations of solar radiation received at the top of the canopy QS_{int} and Vapour Pressure Deficit, VPD inside the greenhouse taken on DOY 76 (16 March 2010).

4.2.2 Canopy measurements

Rose surface canopy resistances (r_s) were measured on 16 March 2010 (DOY 76) and on 5 March 2010 (DOY 65), a cloudy and a clear day respectively. (Fig 4.4) showed that canopy resistance was high in the morning at 0700 Hrs reaching to about 700s/m for both days. On the clear day, canopy resistance decreased gradually up to 1000 Hrs where it became constant. On the cloudy day, canopy resistance decreased gradually from 0700 Hrs up to 1000 Hrs where there was a slight increase. From 1000 Hrs up to 1500 Hrs canopy resistance was low but oscillating.

During those oscillations the highest point reached was 400 s/m at 1430 Hrs. Canopy resistance then increased gradually from about 1530 Hrs.

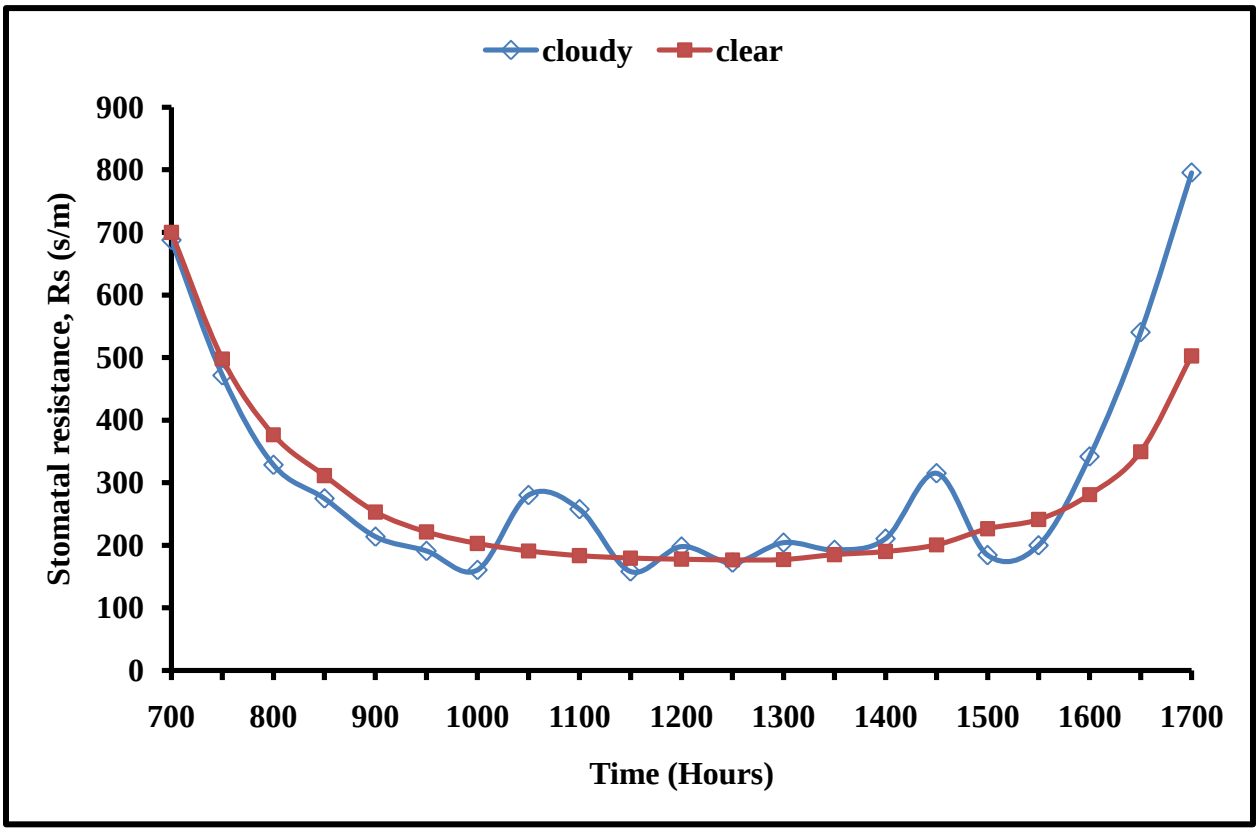

Fig 4.4: Canopy resistance of several cultivars of the greenhouse rose crop on a clear day (5 March 2010) and on a cloudy day (16 March 2010).

Canopy resistance is affected by the prevailing climatic conditions inside the greenhouse. Some of the climatic factors affecting canopy resistance are solar radiation, air temperature and relative humidity and VPD. When solar radiation increases, the air temperature increases because of the heat from the sun and VPD increases which results in a decrease in RH. When such conditions prevail the plant opens its stomatal pores thereby increasing the transpiration rate and reducing

stomatal resistance. DOY 76 was not a clear day throughout, solar radiation normally reaches its peak at midday while canopy resistance reaches its lowest at that point. On this day clouds appeared and reduced the intensity of solar radiation, this resulted in an increase in stomatal resistance. There was a thunder storm at around 1430Hrs which resulted in very high canopy resistances, compared to the clear day. When it rained RH was high and VPD was low. When such conditions prevail the stomata are closed increasing canopy resistance. Fitted logarithmic regressions were done to determine the relationship between canopy resistance and solar radiation; and canopy resistance and VPD; these are shown in figs 4.5 and 4.6 respectively.

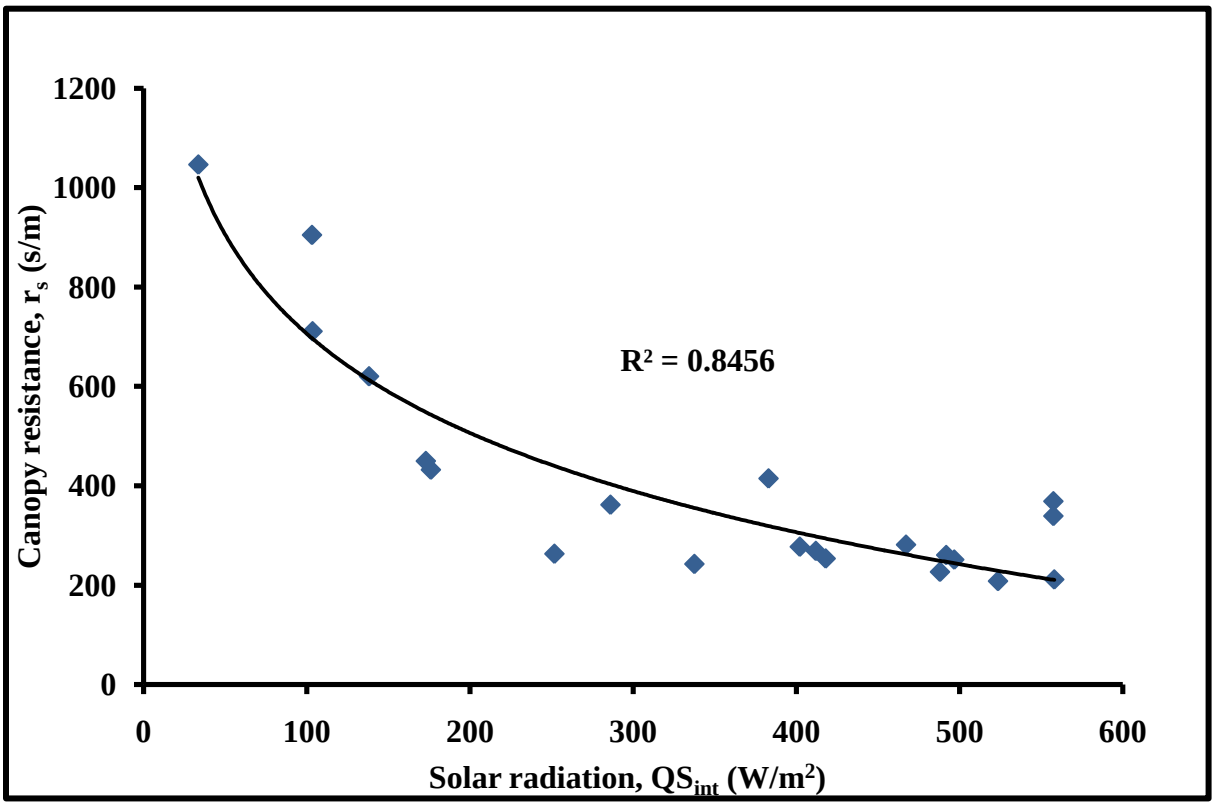

Fig 4.5: Variation of canopy resistance with solar radiation.

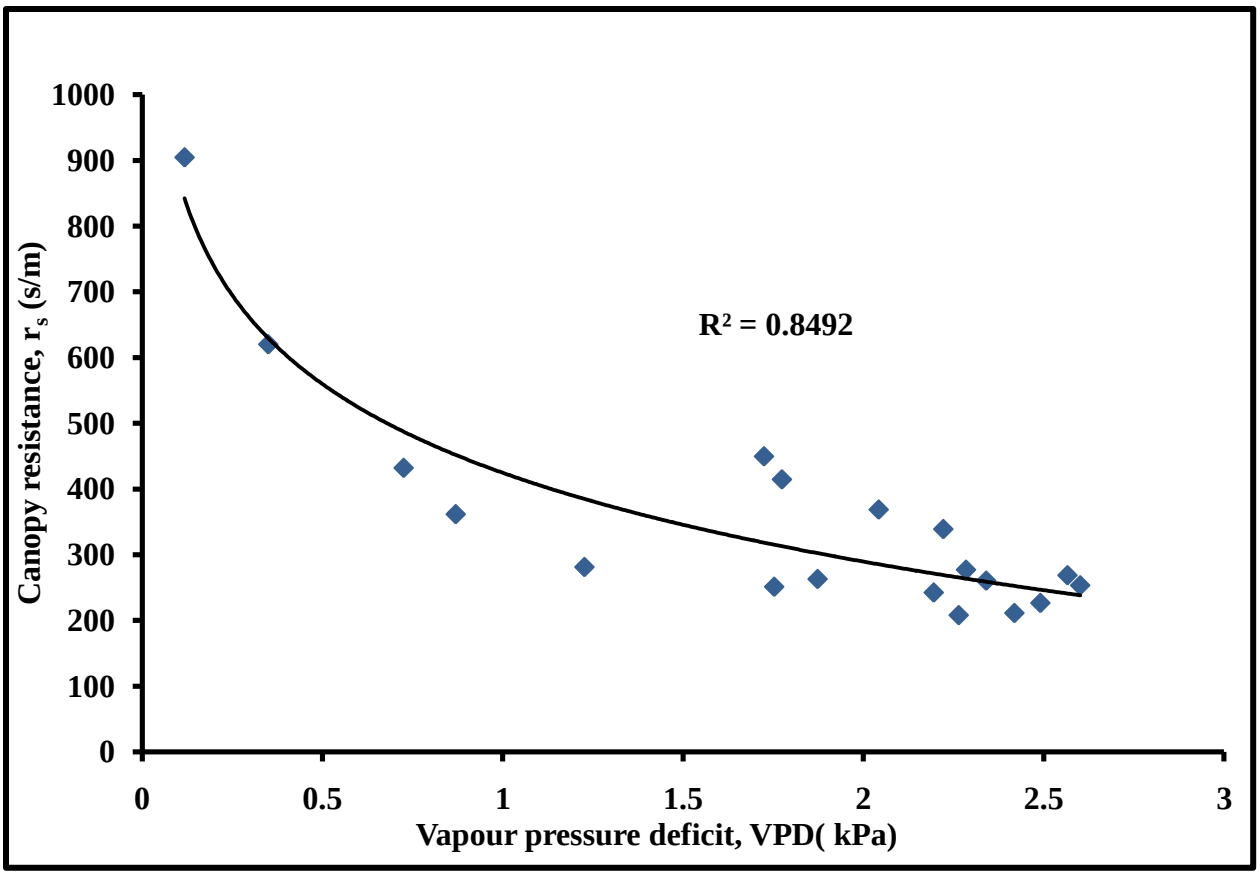

Fig 4.6: Variation of canopy resistance with vapour pressure deficit (VPD).

The results showed that there exists a good fit between canopy resistance and solar radiation as well as canopy resistance and VPD. These variations therefore justify the use of the canopy resistance model (equation 3.17) selected because all the other parameters in the model are constant (not varying with time).

4.2.3 Leaf Area Index (LAI) measurement

Table 4.4 shows the LAI obtained for the greenhouse crop used for the calibration of the canopy resistance model (equation 2.21, §2.10.1). The SunScan canopy analysis system estimated LAI from the mean LAI obtained from the 10 samples where measurements were taken on the same plot.

Table 4.4: LAI of the greenhouse rose crop determined during field measurements at Floraline (Pvt) Ltd on 11 January 2010.

Time	Plot	Sample #	Transmitted	Spread	Incident	Beam Fraction	Zenith Angle	LAI
14:37:43	1	1	527.4	1.11	2497.6	1	49.3	2.2
14:38:08	1	2	752.8	0.21	2497.6	1	49.4	1.7
14:38:39	1	3	620	0.33	2497.6	1	49.5	1.9
14:39:36	1	4	199.2	1.59	2497.6	1	49.7	3.5
14:43:56	1	5	1242.6	0.53	2497.6	1	50.6	1.0
14:44:11	1	6	334.7	0.86	2497.6	1	50.6	2.7
14:44:36	1	7	1341.1	0.55	2497.6	1	50.7	0.8
14:44:46	1	8	298.9	0.54	2497.6	1	50.7	2.9
14:44:57	1	9	572.6	0.82	2497.6	1	50.8	2.0
14:45:54	1	10	732.2	1.11	2497.6	1	51.0	1.7
Average of:	10	readings						
Incident light:		2497.6	**Transmitted fraction:**			0.19	**LAI:**	2.0

4.2.4 Leaf and air temperature measurements

Fig 4.7 shows diurnal leaf and air temperatures measured on 13 December 2009 (DOY347). Leaf and air temperatures were ranging at about 16 °C from midnight up to 0700 Hrs where they increased uniformly but air temperature was higher than leaf temperature from 700 Hrs up to 1100 Hrs, because the leaves gain and lose solar radiation energy at a slower rate than the air.

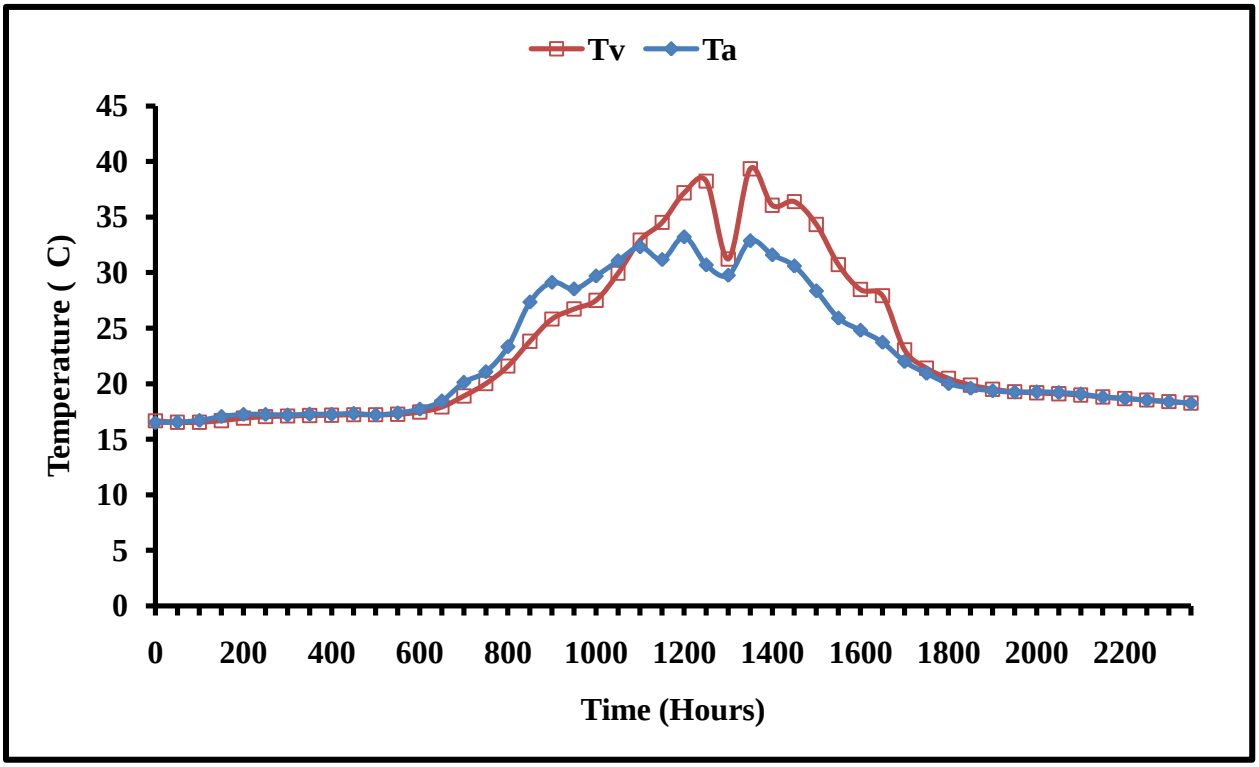

Fig 4.7: Diurnal leaf and air temperature measured on a rose crop on 13 December 2009 (DOY347).

Solar radiation is absorbed by the leaves and it warms the leaves and then leaf temperature rises. At around 1230 Hrs there was an abrupt change in both leaf and air temperatures, normally air and leaf temperature should reach their maximum at that point because solar radiation intensity will be at its maximum. However there might have had been a cloud that blocked the solar

radiation at 1230 Hrs resulting in the change in leaf and air temperatures. Leaf temperature became higher than the air temperature from 1100 Hrs to 1700 Hrs, reaching a maximum of 40 °C at 1330 Hrs. The leaf temperature then decreased gradually, the decrease could have been attributed to sensible heat loss or from evaporative cooling. Sensible heat loss is a process whereby air circulation around the leaf removes heat from the leaf surfaces if temperature of the leaf is higher than that of the air. Evaporative (latent heat) cooling occurs as the leaf transpires; it withdraws latent heat from the leaf and cools it.

4.2.5 Determination of characteristic dimension of the leaves

The characteristic dimension (d) was determined for calibration of the transpiration sub model. Table 4.5 shows the results obtained in determining the characteristic dimension.

Table 4.5: Leaf lengths measured on several varieties of the rose crop, to determine the characteristic dimension (d).

Leaf #	Length 1 (cm)	Length 2 (cm)	Length 3 (cm)	Mean length/ leaf (cm)
1	5.0	5.4	7.2	5.9
2	4.0	4.7	6.8	5.2
3	6.5	7.2	8.4	7.4
4	6.1	6.4	8.5	7.0
5	3.8	4.2	5.3	4.4
6	4.8	5.1	6.8	5.6
7	4.8	5.3	6.5	5.5
8	3.6	3.9	5.4	4.3
9	3.9	4.1	5.2	4.4
10	3.2	3.7	4.8	3.9
Total	45.7	50	64.9	53.5
Mean	4.57	5	6.49	5.35

The results show that the characteristic dimension had a mean of 5.35 cm with a lower and upper limit of 4.57 cm and 6.49 cm respectively. 5.35 cm was used as the characteristic dimension during this research study.

4.2.6 Emitter rate determination

The results of the emitter rate used for determination of the actual water applied by the irrigation system at Floraline (§3.9.1), are given in Table 4.6.

Table 4.6: The volume of water released by each emitter on the onset of irrigation for the greenhouse rose crop, to determine the emitter rate of the drip lines at Floraline.

Emitter #	1	2	3	4	5	6	7	8	9	10	**Total**	**Average**
Volume/4 mins (ml)	65	90	59	60	75	52	63	78	69	57	**668**	**66.8**

$$\text{Emmiter rate} = \frac{60\text{minutes/hour}}{4\text{minutes}} \times \frac{66.8\text{ml}}{1000\text{ml/litre}}$$

$$= 1.002\text{litres/Hour}$$

$$\cong 1\text{litre/hour}$$

The results of the average amount of water released by the emitters showed that the drip lines had an emitter rate of 1litre per hour which was lower than the 1.33 litres per hour emitter rate given by the manufacturer upon installation of the drip irrigation system. The decrease of the

emitter rate may be explained by clogging of the drip lines from salts that accumulate over time. The salts result from fertilizers that are dissolved into the water for fertigation of the rose crop. Clogging of the drip lines can also result from algae developing both on the soilless media (vermiculite) and on the drip line.

4.3 Model Results

Results and discussions of the stomatal resistance model (equation 2.21) and transpiration sub-model (equation 2.16) calibration, validation and the implementation of the GDGCM are presented in this section.

Calibration results using the canopy resistance model (equation 2.21) and the transpiration sub-model (equation 2.16) are outlined to show the effects of changes made on the parameters that were calibrated. The effects of changes are observed on the outputs of the models. A statistical evaluation of the model performance on different data sets is given by the validation results. The model application results show the daily and seasonal CWR modelled for winter and summer seasons of 2007 and 2008 respectively. The comparison results of the modelled CWR against the water applied by the existing irrigation system at Floraline are also shown.

4.3.1 Canopy resistance model calibration

Table 4.7 shows the calculated values of the parameters a, b and c for the canopy resistance model (Equation 2.21) obtained statistically from experimental data fitting, using a statistical package; Sigma plot 2001(Systat Software Inc., San Jose CA, USA).

Table 4.7: Model-specific parameters obtained from the calibration of the canopy resistance model of the GDGCM transpiration sub-model.

Coefficient	**a**	**b**	**c**	**R^2**
Value	788.38 ± 82.51	85.78 ±16.14	-0.146 ± 0.080	0.90

The parameters are generally higher than those found by Mashonjowa et al. (2007a). Differences may be attributed to the different varieties of the rose crop used, differences in the prevailing weather conditions and the different management practices on the rose crop. A part of the greenhouse plastic film was torn and the irrigation was not being done efficiently due to clogging of drip lines on some sections in the greenhouse, this could have been the main reason resulting in the difference in the values of coefficients obtained. The fitted linear regression of the simulated and observed canopy resistance is presented in figure 4.8 and Table 4.8 gives the regression analysis results.

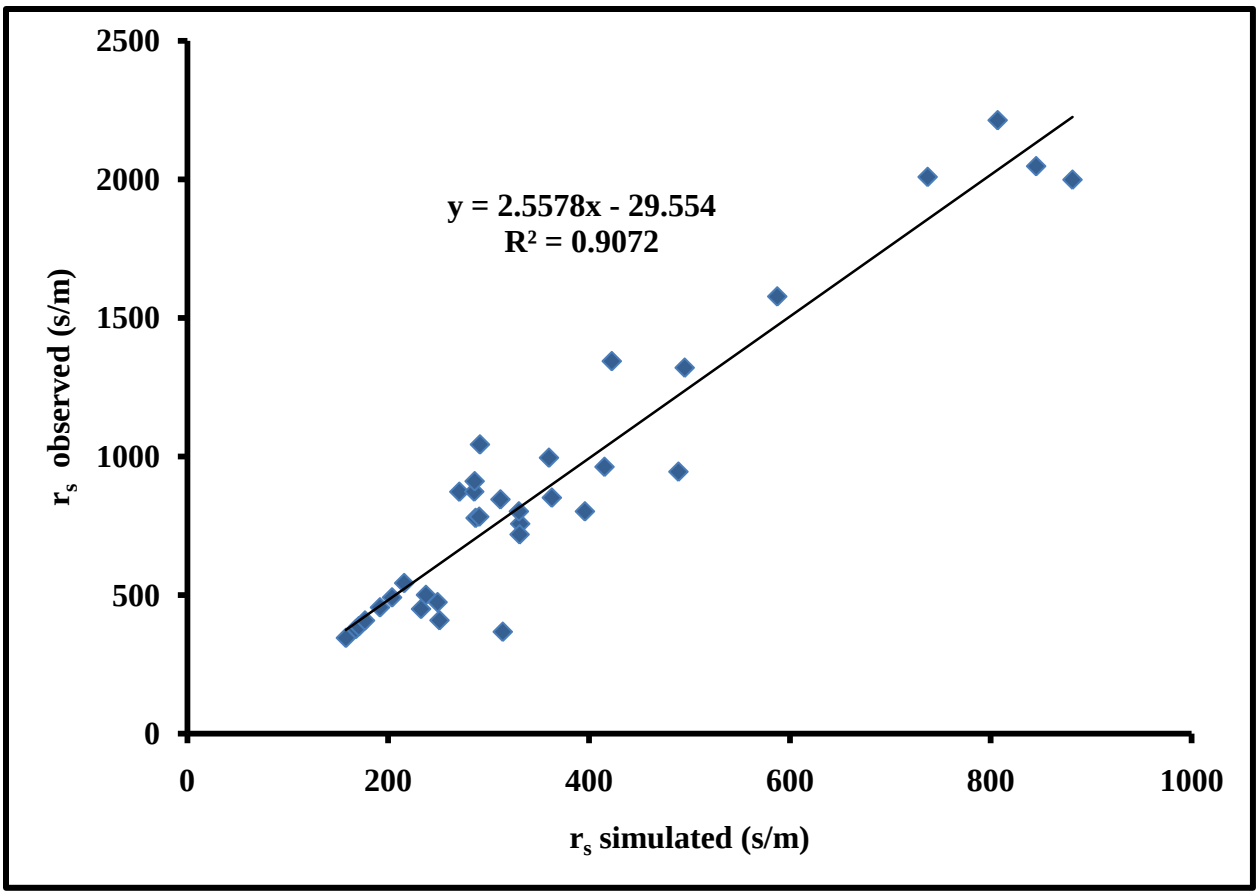

Fig 4.8: Regression between the experimentally observed and the simulated canopy resistances for the canopy resistance model calibration period.

4.3.2: Canopy resistance model validation

Fig 4.9 shows the fitted linear regression of the simulated and observed canopy resistance. A different set of observed canopy resistance data was used. The results show the correlation between the observed and simulated canopy resistances. The coefficient of determination, R^2; and the standard error (SE) between simulated and observed canopy resistances ($r_{s(sim)}$ and $r_{s(obs)}$ respectively) based on the curve fitting equation: $y = mx+c$ are shown in Table 4.8.

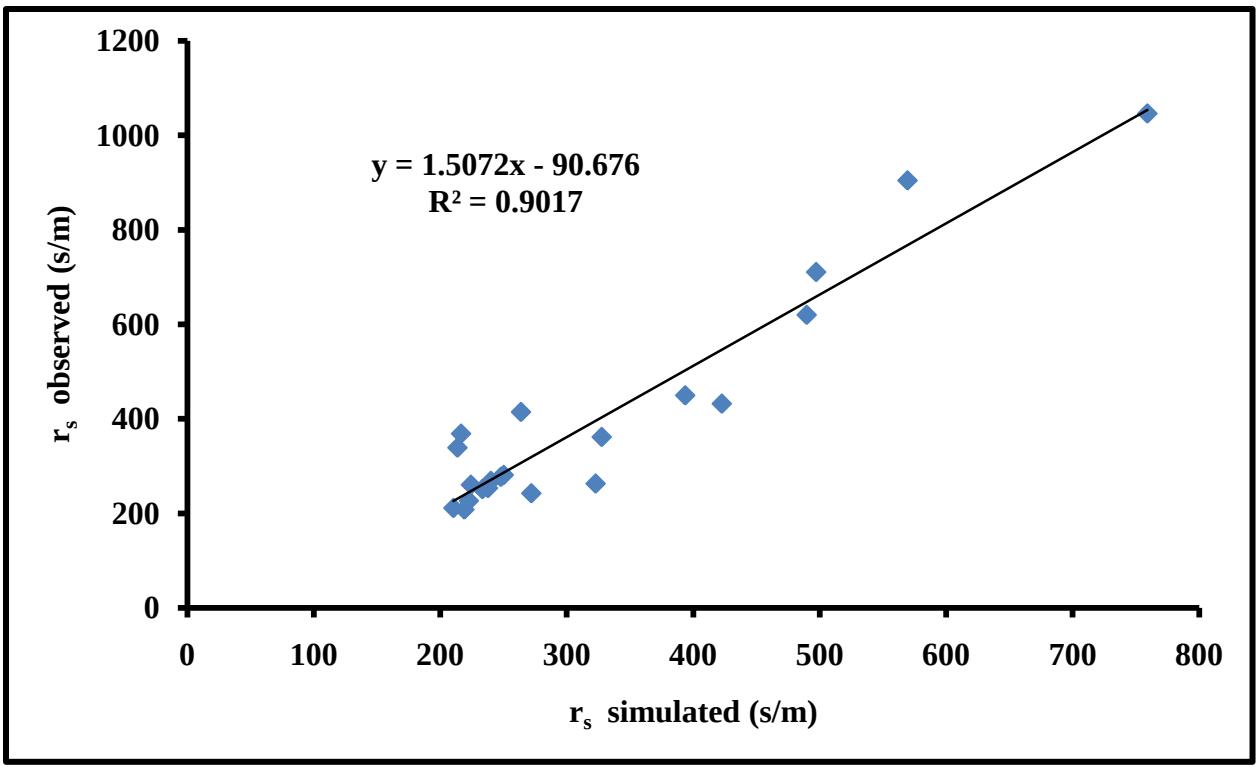

Fig 4.9: Regression between the experimentally observed and the simulated canopy resistances for the canopy resistance model validation period.

Table 4.8: Results for regression analysis between the observed and simulated canopy resistances, including the slope and the 95% Confidence Intervals of the equation;

$r_{s(obs)} = mr_{s\,(sim)} + c$

	Number of observations, N	R^2	Slope *m*	Intercept c	SE	95% confidence interval of slope
Calibration	33	0.901	2.257	-29.554	0.06	[2.35; 2.63]
Validation	21	0.907	1.507	-90.676	0.05	[1.16; 1.37]

4.3.3 Transpiration sub-model calibration

Several parameters of the transpiration sub-model (equation 2.16) were determined as outlined in §3.8.1 and §3.8.2. They were used to simulate transpiration rate. Fig 4.10 shows the data of the simulated and observed transpiration rates fitted to linear regression. Table 4.9 gives the results for the regression analysis. However, there were several outliers. Outliers could have resulted from assumptions made in the determination of model input parameters such as mass transfer coefficient (h'_{Tr}) and heat transfer coefficient (h_P).

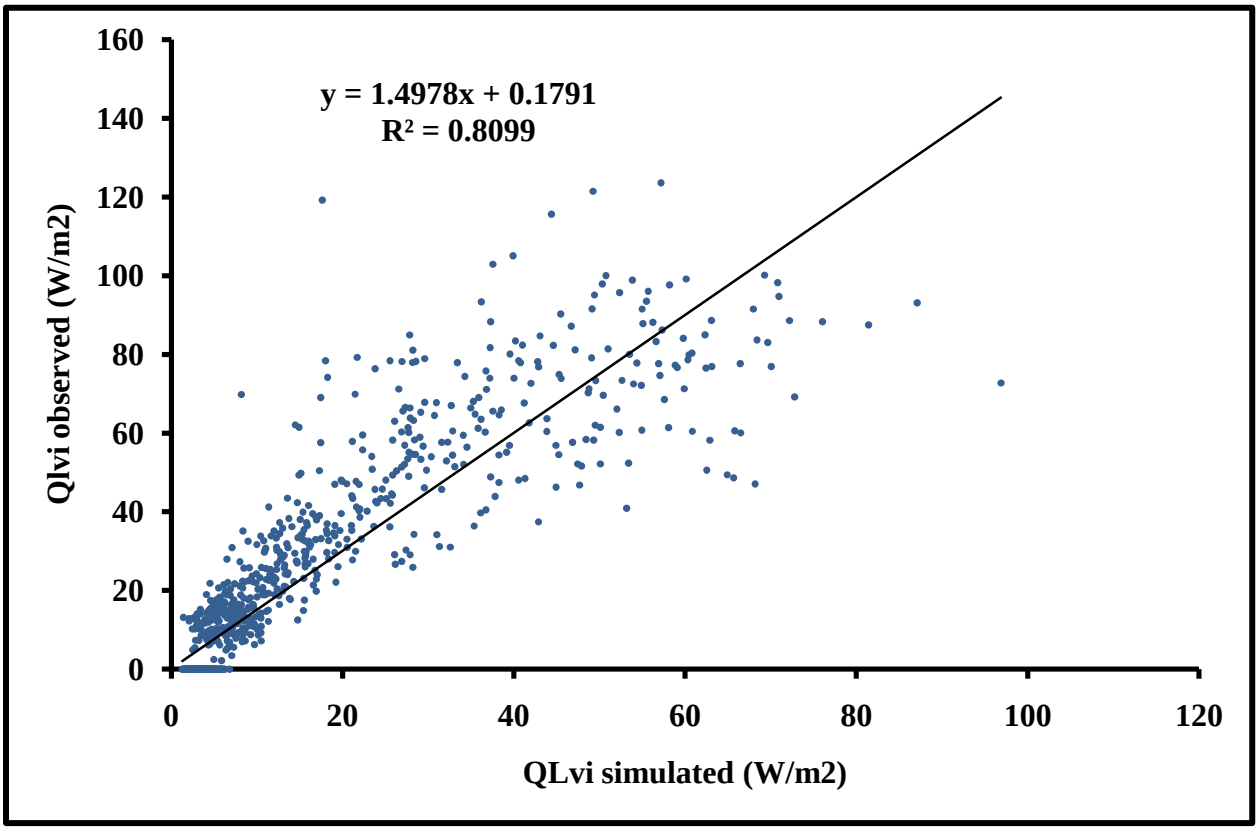

Fig 4.10: Regression between the experimentally observed and the simulated transpiration rates for the transpiration sub-model calibration period.

4.3.4 Transpiration sub-model validation

The transpiration flux density for January 2008 was simulated using the transpiration sub-model (equation 2.16) of the GDGCM. Observed transpiration rates were measured using stem heat balance sap flow gauges. The measured transpiration rates were up-scaled to whole plant transpiration (WPT). Fig 4.11 shows the relationship between the simulated and observed transpiration flux densities **(**$QL_{vi(sim)}$ and $QL_{vi\ (obs)}$ respectively), while Table 4.9 gives the regression analysis results.

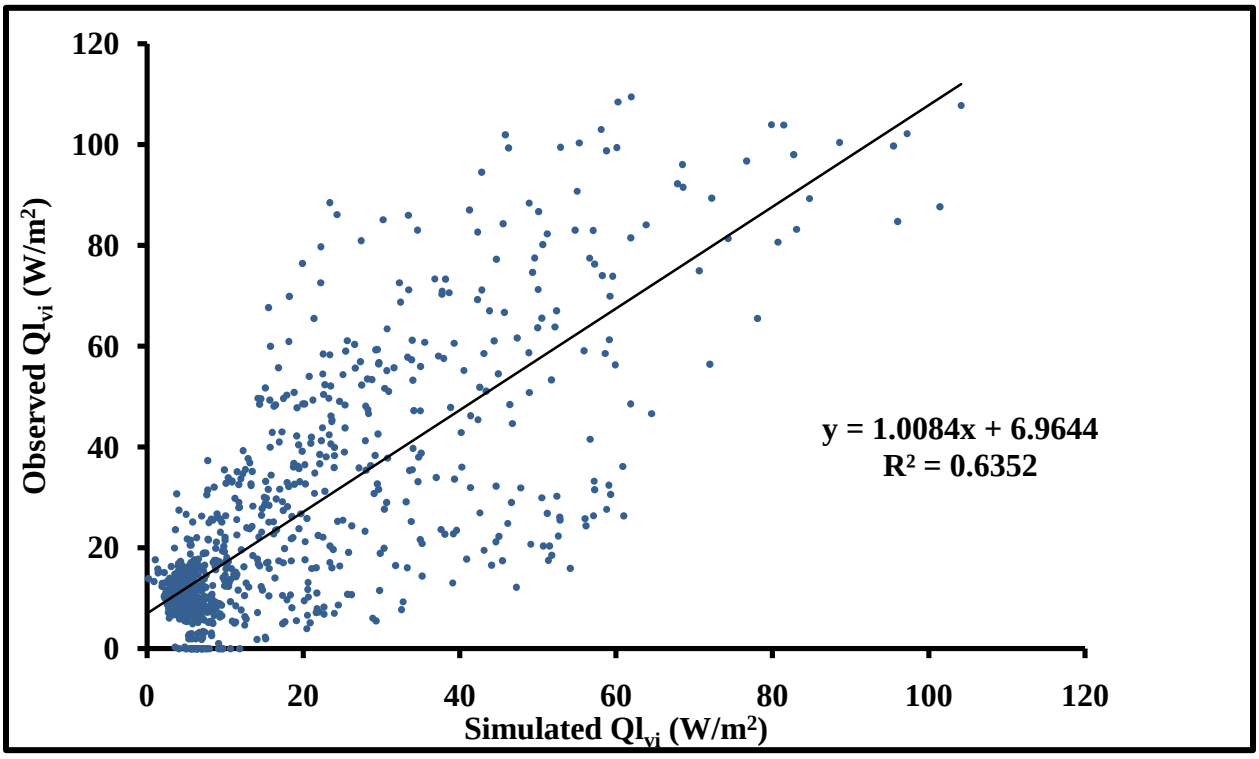

Fig 4.11: Regression between the experimentally observed and the simulated transpiration rates for the transpiration sub model validation period.

Table 4.9: Results for regression analysis between the observed and simulated transpiration flux densities, including the slope and the 95% Confidence Intervals of the equation: $QL_{vi\ (obs)} = mQL_{vi(sim)} + c$

	Number of observations, N	R^2	Slope *m*	Intercept c	SE	95% confidence interval of slope
Calibration	1142	0.80	1.503	0.179	0.0168	[1.47;1.53]
Validation	1118	0.64	1.008	6.964	0.018	[1.17;1.24]

The results show the fit between the experimentally observed and simulated transpiration rates, but there is generally an over-estimation of the observed transpiration rates. Most of the significant differences between the observed and simulated transpiration rates were observed during the early hours of the day. The main source of error of the transpiration measurements may be in the up-scaling of the measured transpiration rates from single to whole canopy transpiration. Errors may also result from the heat balance sap flow gauge error but it is expected to be not more than 10% (Dynamx, 2005). However; Baker and van Bavel (1987), Baker and Nieber (1989) and Grime et al. (1995) have reported that observed over-estimation and under-estimation of whole plant transpiration in the mornings and late afternoons. In the mornings when soil temperatures exceeds air temperature there is a negative temperature gradient in the sensor as warm sap enters a cooler stem, causing a temporary over-estimation of WPT if the sensor is near the soil. In the late afternoon, when the ambient air is at a higher temperature than

the soil, the sensor registers a higher positive temperature gradient in the sensor, resulting in under-estimation of WPT (Mashonjowa et al, 2010b).

4.3.5. Simulations of canopy resistance using the canopy resistance model and the GDGCM

A regression between the canopy resistances simulated using the canopy resistance model (equation 2.21) and that simulated using the GDGCM is shown in fig 4.12. The results show that there is a good correlation between the two simulated canopy resistances.

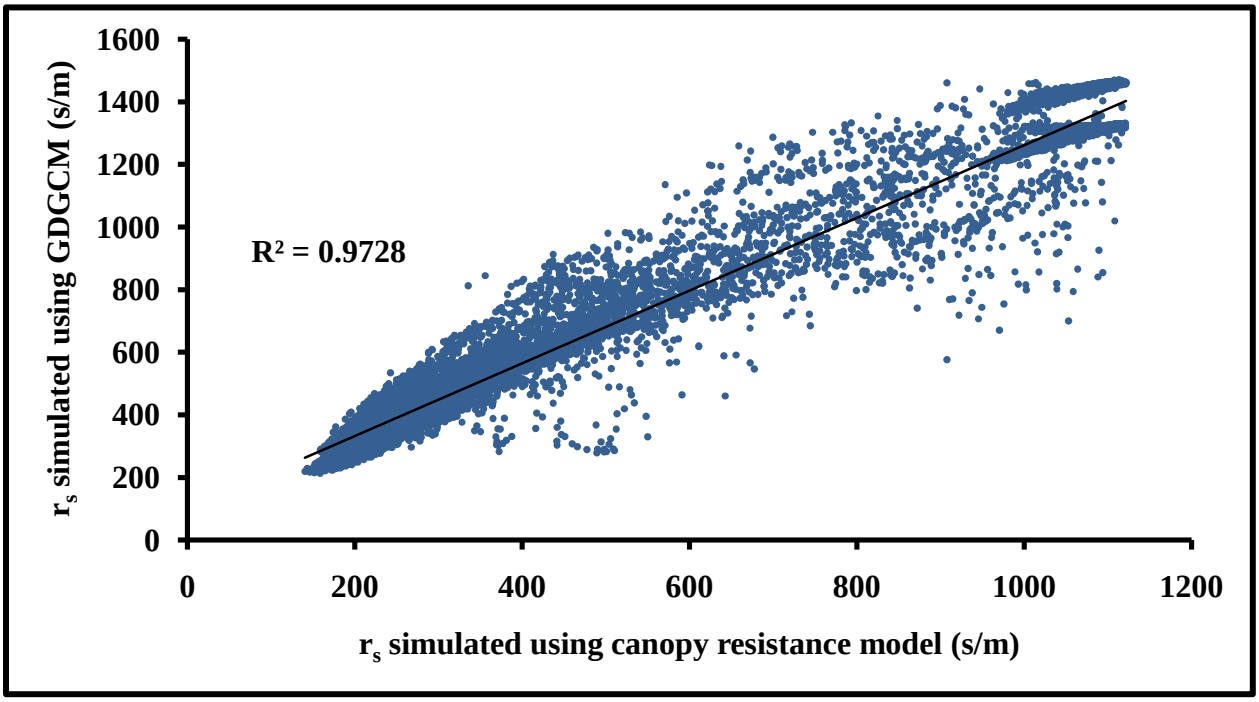

Fig 4.12: Regression line for canopy resistances simulated using the canopy resistance model and canopy resistance simulated using the GDGCM.

4.3.6 Crop transpiration

Crop transpiration for winter and summer seasons (May to August and September to April, respectively) were simulated at 30 minute intervals using the GDGCM. Fig 4.13 shows simulated diurnal transpiration rates for winter (4 June to 8 June 2007) and summer (14 to 18 October 2008).

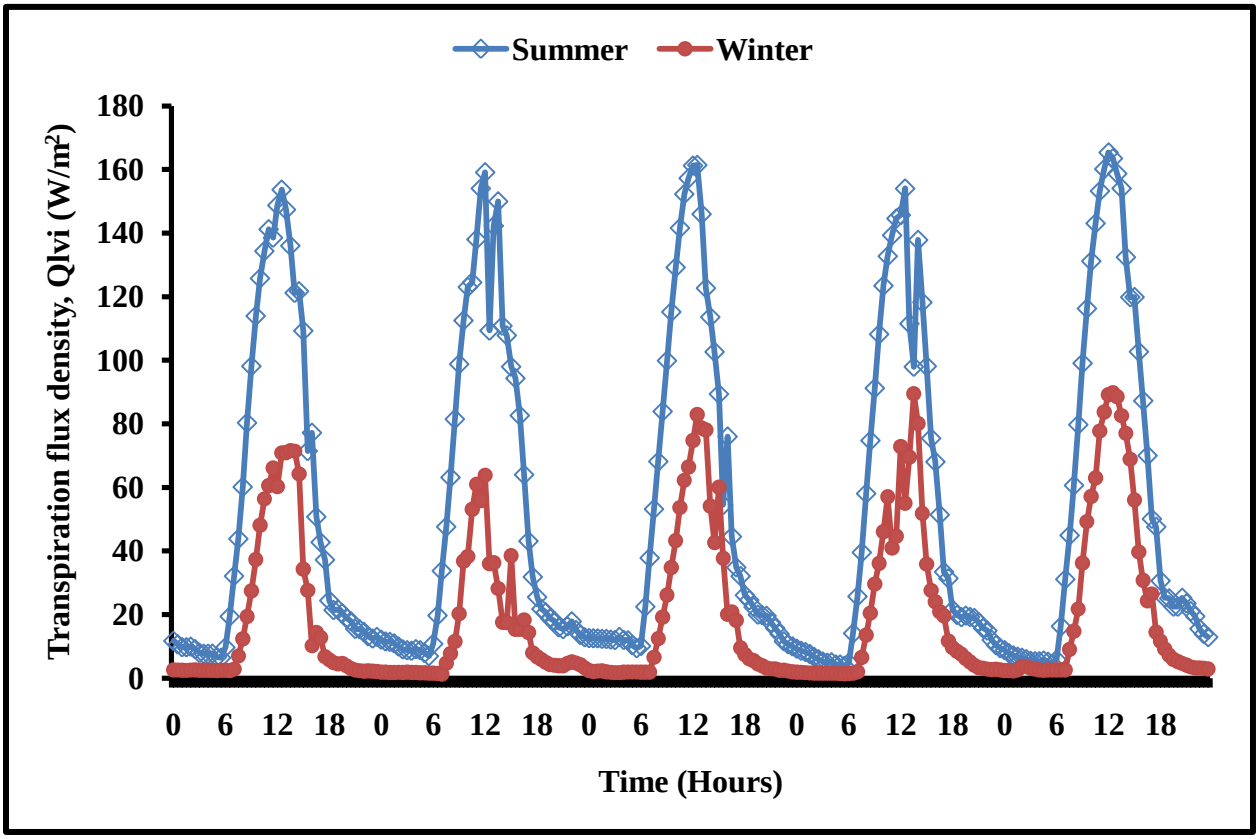

Fig 4.13: Simulated diurnal transpiration rates of a greenhouse crop during winter (4 June to 8 June 2007) and summer (14 October to 18 October) seasons, using the GDGCM.

Transpiration for the 2 seasons shows the same pattern (fig 4.13). Transpiration is low and almost constant before 0600 Hrs. This is because there will be no solar radiation which supplies

energy to the canopy and is, among other factors, the cause of plant transpiration. Transpiration rises from 0600 Hrs reaching its maximum around 1200 Hrs. After 1200 Hrs, transpiration decreases up to around 1800 Hrs where it becomes very low. This pattern shows that the crop loses water in the same way during winter and summer but in different quantities. Fig 4.13 shows that in summer the rose crop transpires to a maximum of $160Wm^{-2}$ while the maximum transpiration for winter is close to 90 W/m^2. The differences in winter and summer crop transpiration are attributed to several climatic factors which include solar radiation, relative humidity, VPD, wind and vegetation temperature. During winter there are low air temperatures, less solar radiation is received resulting in low leaf temperatures. Transpiration rate is decreased because there will be a vapour pressure gradient between the leaf and air temperature. When there are low temperatures and low solar radiation, the canopy resistance increases reducing transpiration rate. In summer there will be high solar radiation intensity resulting in high air and leaf temperatures creating a high vapour pressure gradient between the leaf and air temperature, and low canopy resistance hence increased transpiration rates.

The night-time transpirations for both seasons are low ut the winter transpiration is lower than the summer transpiration. The night-time transpiration is minimal because at night there will be no solar radiation which is the main factor affecting crop transpiration; this shows that solar radiation is not the only factor determining crop transpiration since transpiration takes place at low rates. At night there will be low air and vegetation temperatures, high relative humidities, low VPD and high canopy resistances which result in very low transpiration rates. Fig 4.14 shows the diurnal variations of solar radiation, canopy resistance, transpiration and the vegetation temperature. These were simulated using the GDGCM for 7 May 2007.

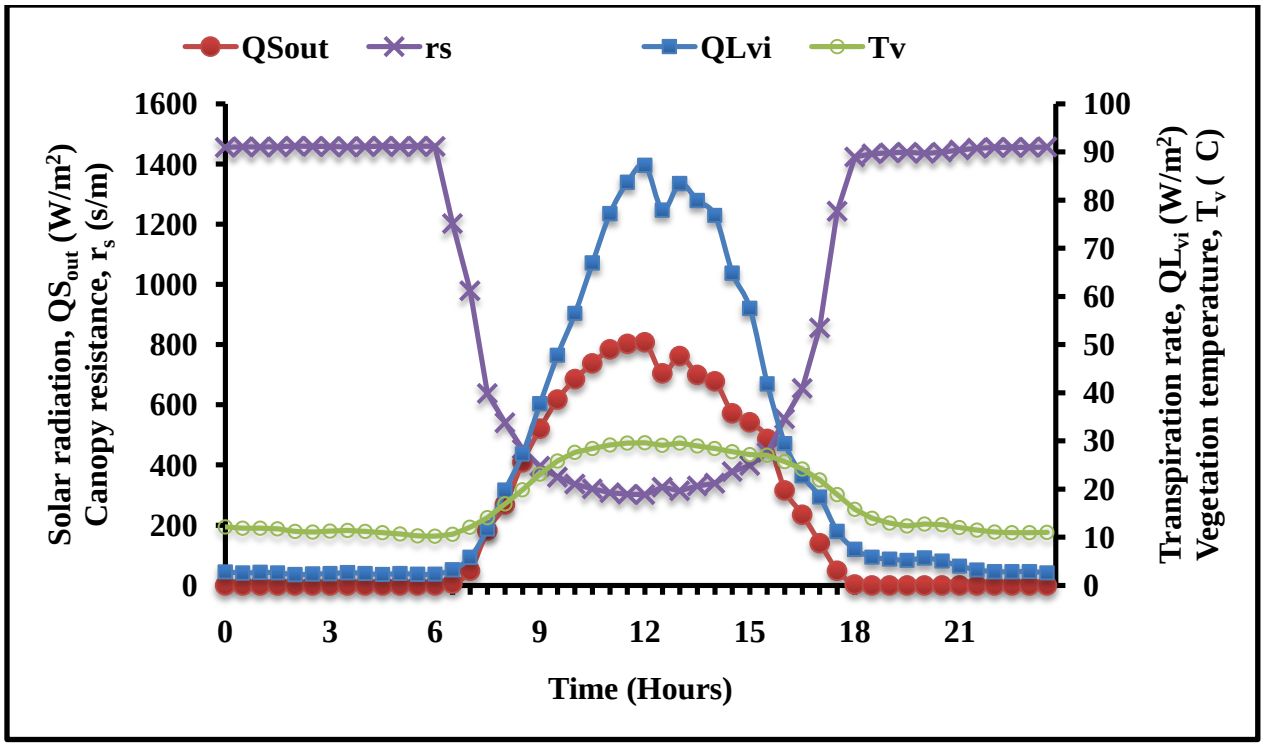

Fig 4.14: Diurnal variations of solar radiation outside the greenhouse, QS_{out}; transpiration flux density, QLvi; vegetation temperature, T_v and canopy resistance, r_s for 7 May 2007, simulated using the GDGCM.

Solar radiation is the main factor affecting crop transpiration as the transpiration follows the pattern of solar radiation (fig 4.14). When the sunrises, solar radiation is expected to increase until it reaches its peak at midday where it decreases until the sun sets. When solar radiation increases it warms up the vegetation increasing the vegetation temperature, the canopy resistance is reduced and transpiration rate increases (fig 4.14). At 1200Hrs there was a slight decrease probably because of a passing cloud, this affected the transpiration rate, vegetation temperature as well as the canopy resistance. When there is no solar radiation transpiration is minimal, and not zero. This shows solar radiation is not the only factor influencing crop transpiration.

4.3.7 Daily CWR

Daily CWR were determined as outlined in §3.10.2. The daily amount of water required by the crop, (summer and winter) were simulated for the whole year (May 2007 to April 2008) by the GDGCM. The CWR were calculated by integrating the GDGCM modelled transpiration rates over time. The daily CWR obtained in winter (fig 4.15) showed that most of the days in May had an average CWR of 3 kL/day to 4 kL/day. Days in June and July had a lower CWR compared to days in May; ranging between 1.5 kL/day to 3 kL/day with a few days requiring close to 3.5 kL of water per day.

Daily CWR for August were generally higher compared to the days of May, June and July. Eight days in June and July had the lowest CWR of just above 1.5 kL/day and 29 August had the highest CWR of close to 5 kL/day. Days in June and July had the lowest CWR because during that period the lowest air temperatures were received as expected. The solar radiation received was low as well as a low VPD resulting in low CWR. The CWR increased as winter went towards the end because air temperatures and solar radiation increased as the days approached the summer season.

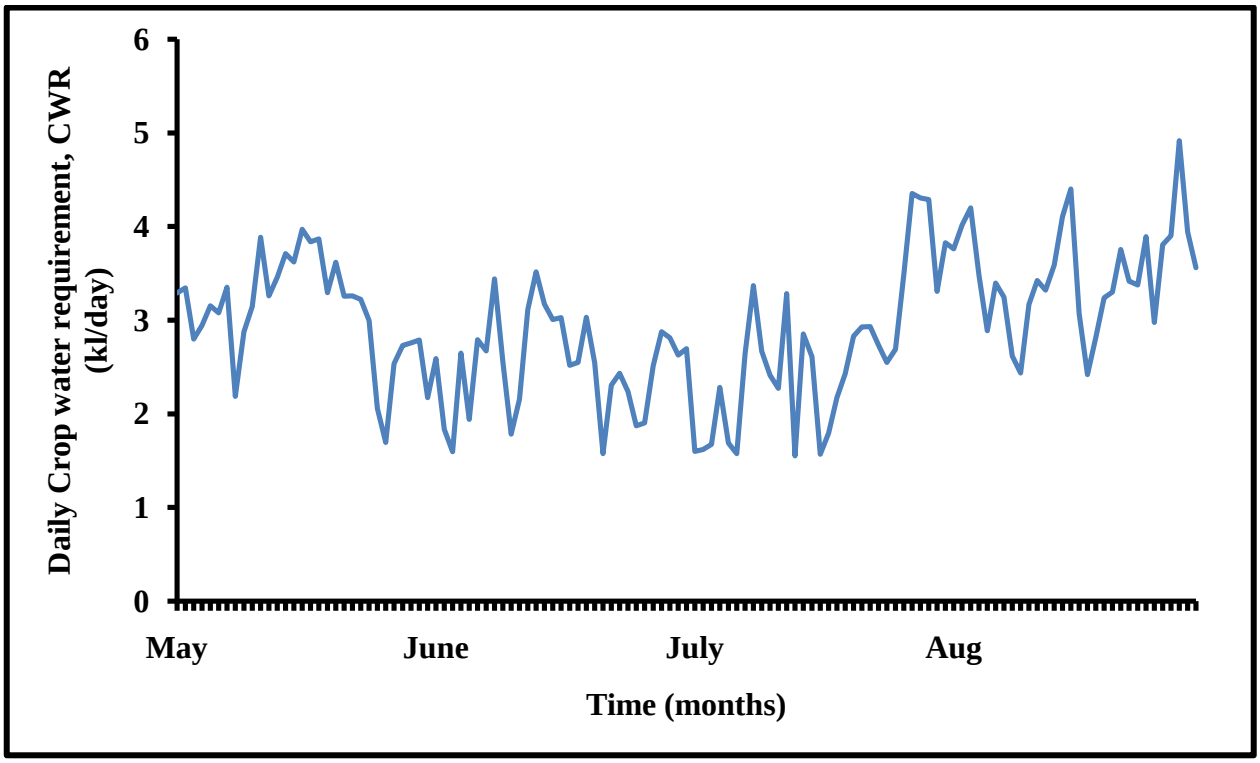

Fig 4.15: Daily Crop water requirements during winter season, for the rose crop at Floraline predicted by the GDGCM.

In the summer season the daily CWR for the days in September and October were generally high as shown in figure 4.16. Days in October had the highest CWR, with an average of 6.6 kL/day, when compared to the other days in summer. Days between December and January had the lowest CWR. Daily CWR increased uniformly from January to February and became constant up to April. The day that had the lowest CWR during summer had 1.1 kL/day on 2 January 2008; and the maximum daily CWR was 8.7 kL/day on 8 October 2007. Normally October receives the highest solar radiation, therefore has the highest CWR resulting from high VPD and vapour pressure gradient between air and leaf temperature. The onset of rainfall starts during October and is highest in December resulting in high RH and low VPD inside the greenhouse resulting in lower CWR. There are almost constant daily CWR for the period

February to April because the days received an average amount of solar radiation, resulting in air and leaf temperatures that were almost constant. VPD was also constant resulting in average CWR of 4.2 kL/day.

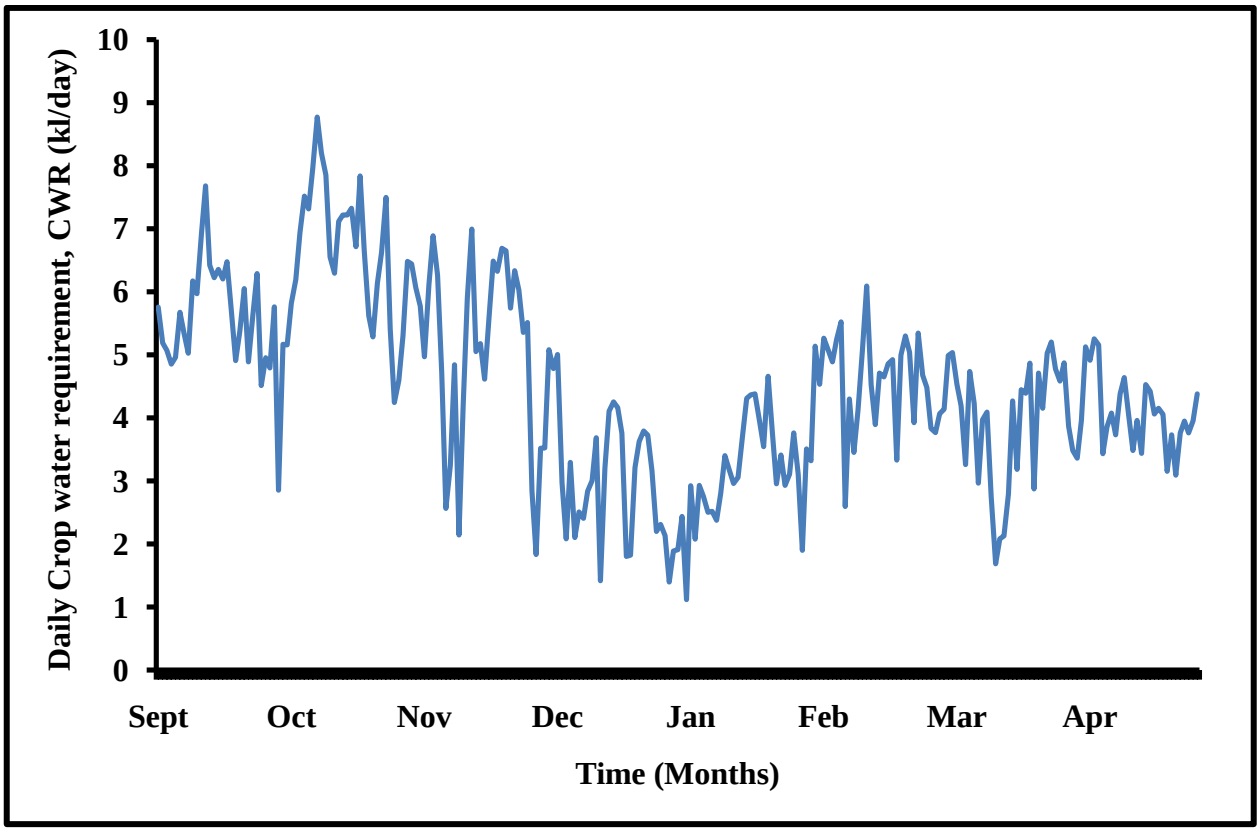

Fig 4.16: Daily Crop water requirements for the rose crop during summer season at Floraline based on the GDGCM.

The daily CWR shown in fig 4.15 and 4.16 were always fluctuating because each day had a different CWR. The CWR for each day differ because it depends on the climatic conditions of each day inside and outside the greenhouse. Some days are clear throughout while others are not such that higher CWR were for clear days while cloudy or overcast days had lower CWR.

4.3.8 Seasonal CWR

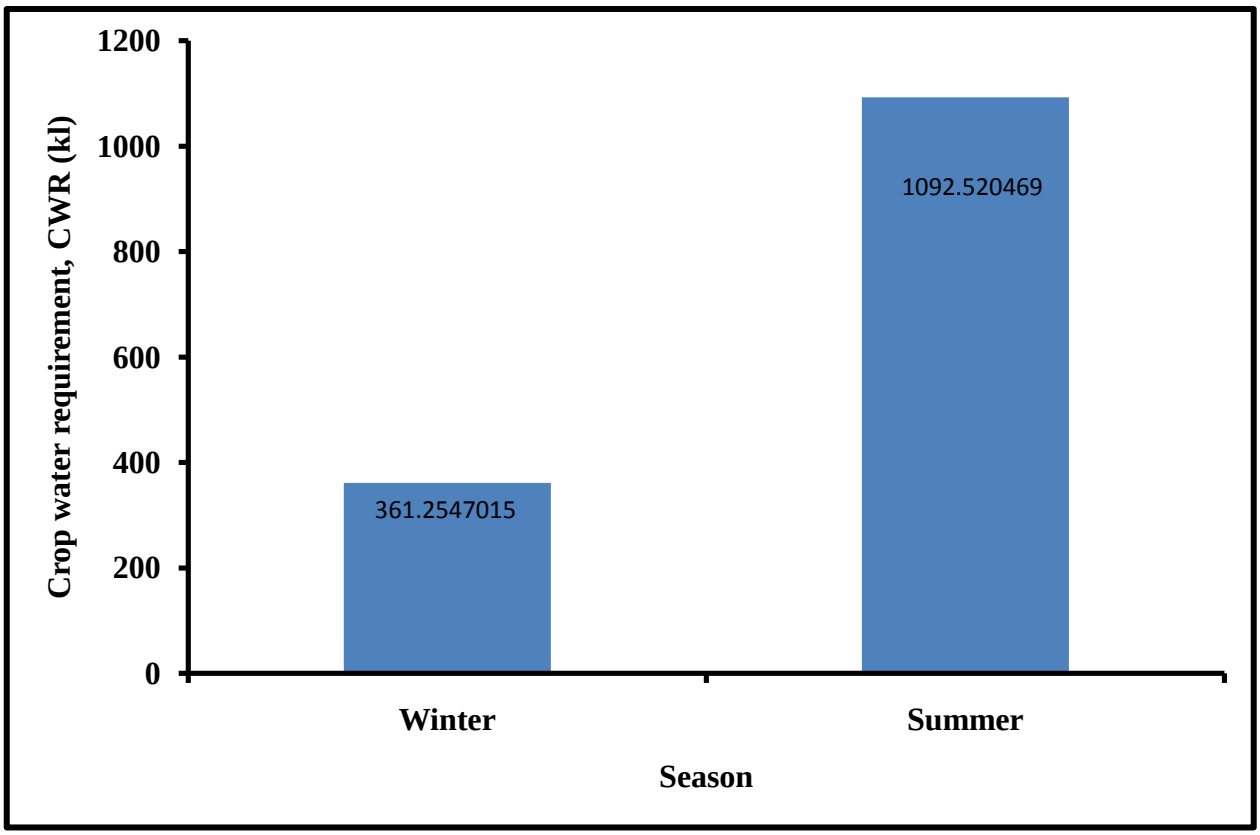

Fig 4.17: Summer and winter season CWR for the rose crop grown at Floraline.

Fig 4.17 shows the crop water required during the summer and winter season. The winter CWR was about 361 kL (translating to 90.31 kL/month) while that of summer was 1.09 Ml (translating to 136.3 kL/month). Winter months generally had lower CWR compared to the summer months as shown in fig 4.18. The CWR for winter and summer show an oscillating pattern throughout. The low points of CWR were from June to July and from December to January with the lowest CWR from June to July. The high peaks were in October and February with October having the highest CWR.

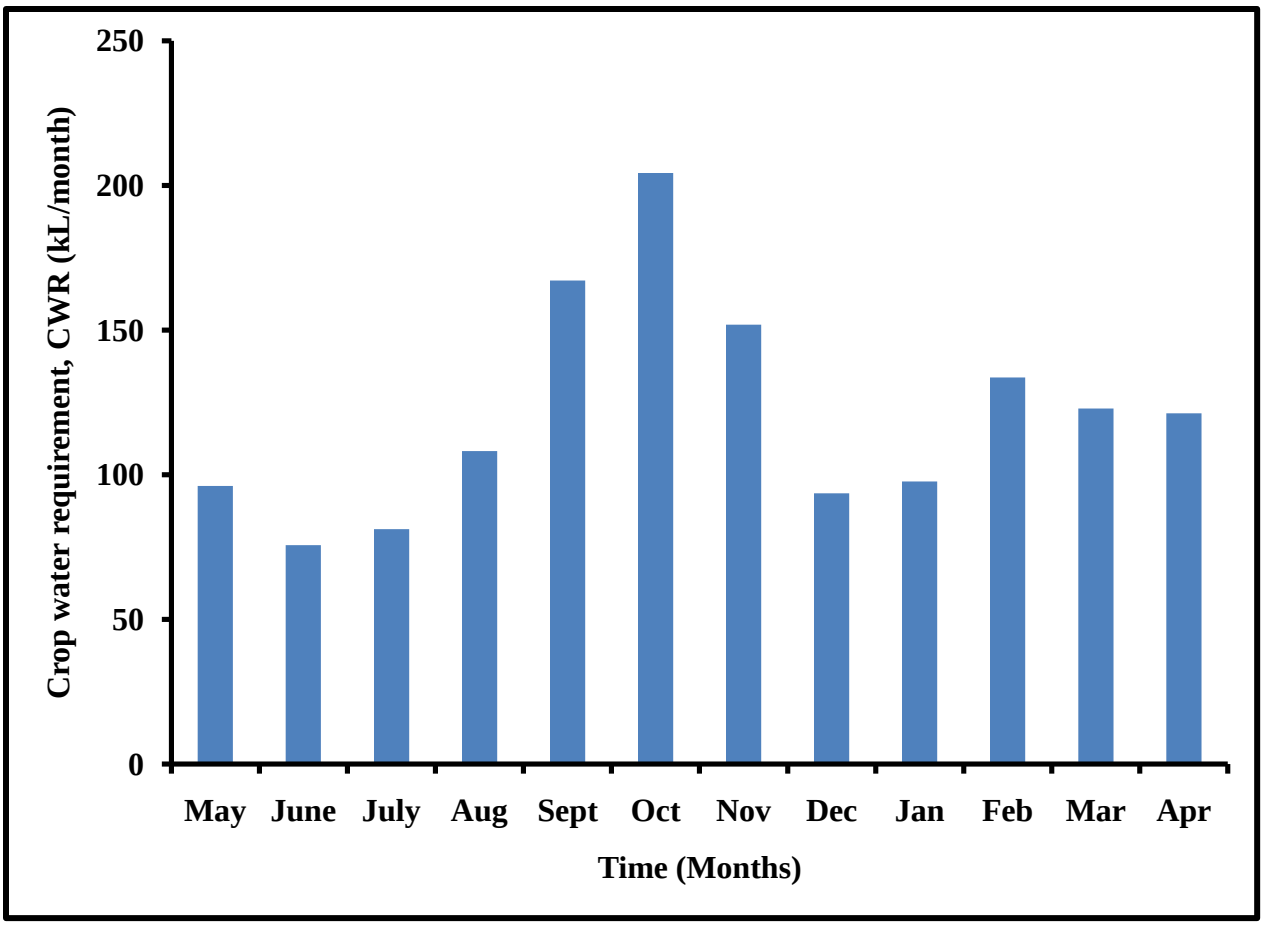

Fig 4.18: Seasonal crop water requirements for the greenhouse rose crop predicted by the GDGCM for both winter and summer seasons (May 2007 – April 2008)

The low CWR in June, July, could have been attributed to low VPD (fig 4.19a), air temperature and solar radiation (fig 4.19b) received inside the greenhouse. Normally in winter the photoperiod has short days and long nights, hence there are less hours of daylight (solar radiation) especially in June and July. Some of the days in winter were overcast also resulting in low solar radiation as it will be blocked by the clouds. When there is low solar radiation and VPD, canopy resistance is increased and the water lost by the plant decreases.

In Zimbabwe rainfall is normally expected during the summer season. Rainfall outside the greenhouse was received starting from October to up to March and the highest amount of rainfall was received in December, as shown in fig 4.19b. December and January had more days of rainfall; when it rains outside the greenhouse, it results in high RH (90%), low VPD and low solar radiation inside the greenhouse (figs 4.19a and 4.19b) thus canopy resistance becomes high reducing the crop transpiration rate and hence decreasing the CWR. The low solar radiation might have been because of heavy rainfall clouds blocking solar radiation. October and February received high solar radiation, February had solar radiation higher than October but October had higher CWR than February. This was because February received higher rainfall and had higher RH and lower VPD inside the greenhouse resulting in lower CWR than in October.

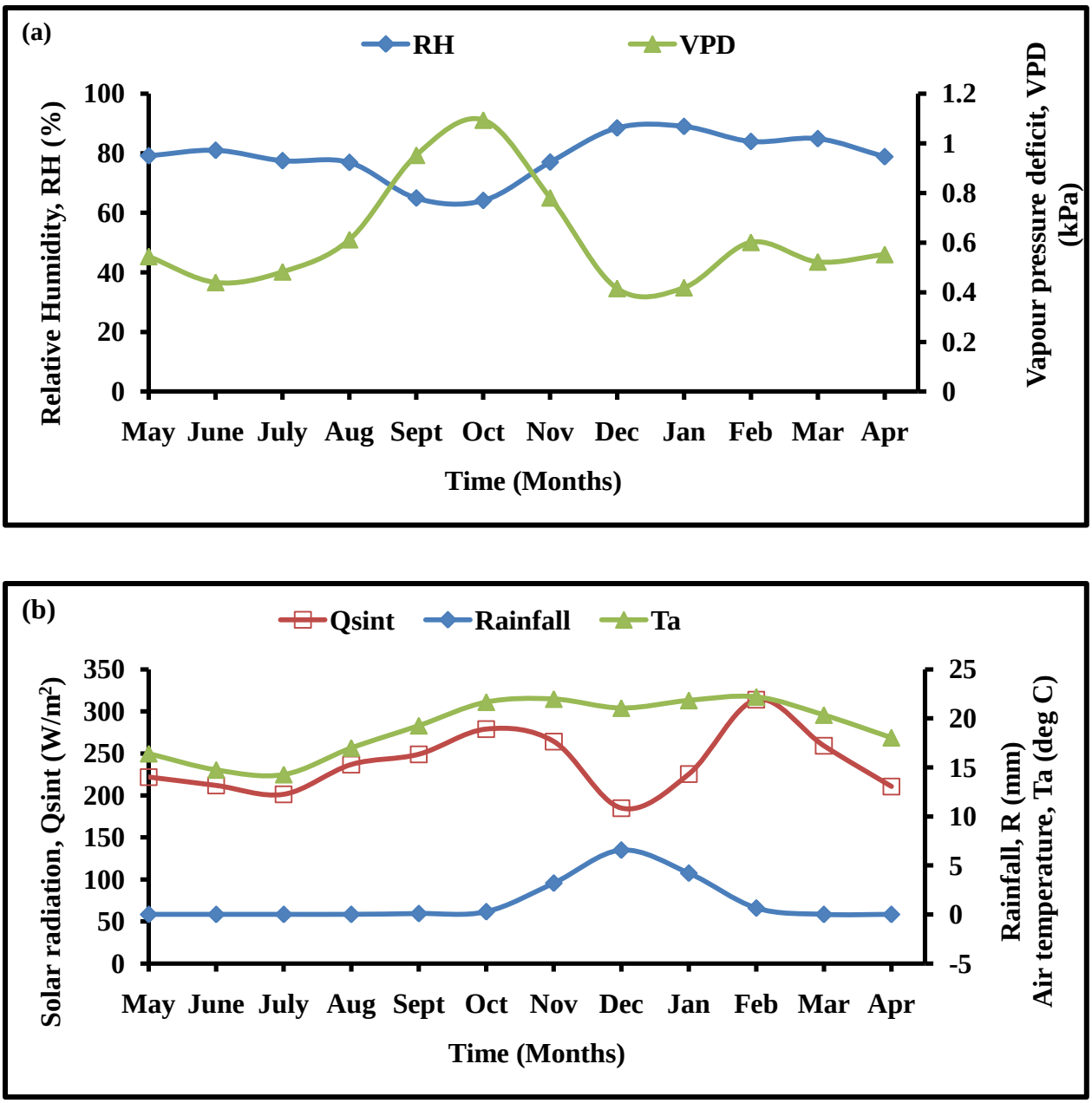

Fig 4.19: Variations of (a) Relative Humidity, RH and Vapour pressure Deficit, VPD over time inside the greenhouse and (b) the total monthly solar radiation and air temperature received inside and the total monthly rainfall received outside the greenhouse during winter and summer seasons; simulated by the GDGCM.

4.3.9 Comparison of CWR against the actual water supplied by an existing irrigation system.

According to the settings of the climate control computer, irrigation was performed whenever the accumulative solar radiation outside the greenhouse reached 1600 kJ m^{-2}. Each emitter supplied water at an average rate of 1 litre per hour and the system applied water for a fixed period of 4 minutes each time. The total number of emitters was 9432 in the sampled greenhouse. The data of solar radiation outside the greenhouse for the period May 2007 – April 2009 was used to determine the number of irrigation cycles per day. The total solar radiation (in kJ m^{-2}) received per day was divided by 1600 kJ m^{-2} to get the irrigation cycles per day. In this way, it was found that the crop was irrigated with an average of 6.85kL (6.85 m^3 or 6.85 $x10^9$ mm) of water per day in winter, divided into an average of 10 applications, and 7.8 kL (7.8 m^3 or 7.8 x 10^9 mm) of water per day in summer, divided into an average of 12 applications.

The CWR for the roses and the actual water applied by the irrigation system followed the same trend (fig 4.20) throughout the summer and winter seasons, except for August to September where the water supplied decreased while the CWR increased.

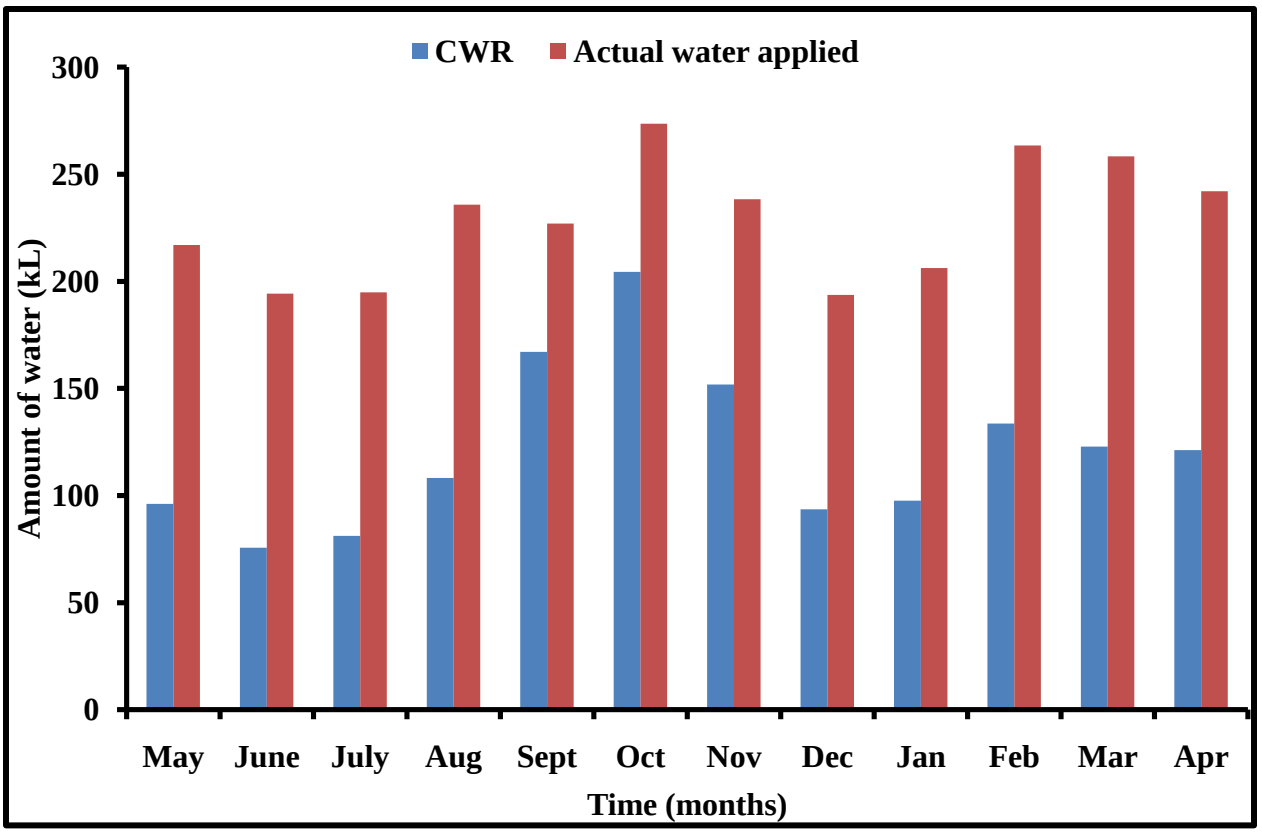

Fig 4.20: The monthly CWR for the rose crop and the actual water applied by the existing irrigation system at Floraline for winter and summer seasons.

The least water was applied by the system for the period June to July in winter and December to January in summer whereas the least CWR simulated by the model was for the period between June and July in winter. This was so because the existing irrigation system was based on cumulative solar radiation outside the greenhouse only and the lowest solar radiation was received in December. Normally it is not expected for December to receive the lowest amount of solar radiation, this could have been because December received the highest amount of rainfall than the other months, and this could imply that there were many cloudy or overcast days resulting in that month receiving the lowest amount of solar radiation. On the other hand the model used all the climatic and physiological parameters that could affect crop water

requirement (solar radiation, air temperature and RH and canopy temperature) to simulate the CWR.

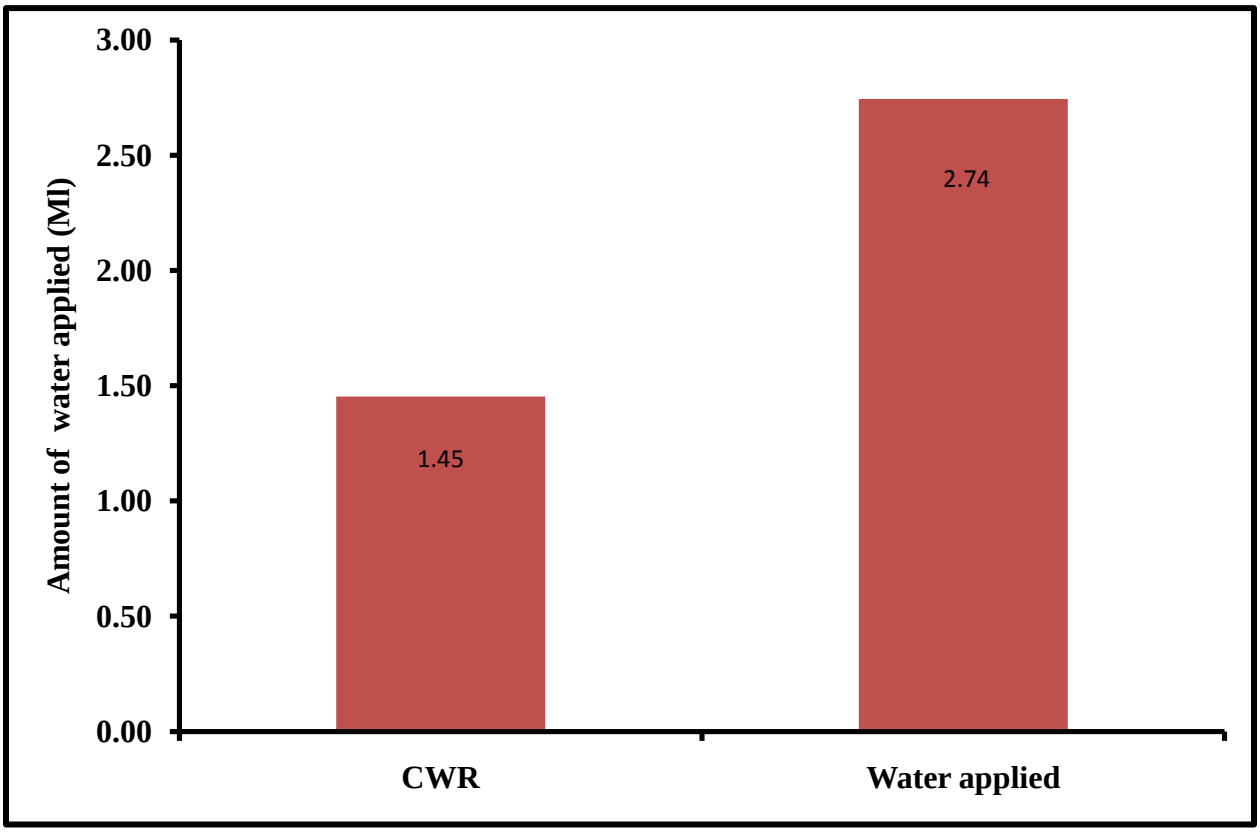

Fig 4.21: Total CWR for the rose crop and the actual water supplied by the existing irrigation system at Floraline (Pvt) Ltd for the whole year (May 2007 to April 2008).

Fig 4.21 shows the total CWR for the rose crop and the total amount of water that was applied by the existing irrigation system for winter (May 2007 to August 2008) and summer (September 2007 to April 2008).

The CWR was less than the actual water applied throughout the whole year (fig 4.20). The margin of the difference between the CWR and the actual water applied was high and almost similar throughout the year except in September and October. During that period there was highest solar radiation, VPD, air temperature and the lowest RH, conditions which result in very high CWR. The water applied by the system in September and October was not very high for that period resulting in the smaller margin between the CWR as compared to the other months, because the system takes into account solar radiation only. The system then can be considered to be inefficient as compared to the model because February had the highest water applied since it received the highest amount of solar radiation but the model showed that even though there were high air temperatures in October and February; the latter did not require that much water applied as there was higher RH, more rainfall received and a lower VPD than the former month.

The irrigation system at Floraline considers transpiration to be zero at night as there will be no solar radiation so irrigation is only done during the day. The total amount of water applied by the existing irrigation system at Floraline was almost twice the CWR that was simulated by the GDGCM for the winter and summer season. The results imply that the existing irrigation system was over-irrigating the crop throughout the whole year. However there could have been errors in the model that resulted to under-estimation of the transpiration rates. Error could arise from the assumption that the model assumes that there is no evapotranspiration from the soil or soilless media in the greenhouse when there actually is a substantial amount of evaporation. Error from the model prediction of transpiration rates may also occur during the night, when RH is very high from instrumental error which should be ±5%.

CHAPTER 5

CONCLUSIONS AND RECOMMENDATIONS

5.1 Conclusions

The Gembloux Dynamic Greenhouse Climate model (GDGCM) transpiration sub-model was calibrated and validated and used to simulate daily and seasonal crop water requirements for a rose crop grown in an Azrom type greenhouse in Zimbabwe. The selected canopy resistance model for greenhouse roses was calibrated to obtain the model parameters using data collected on 27 January 2010, 28 January 2010, 11 February 2010 and 12 February 2010 and validated using data collected on 16 March 2010. The transpiration sub-model was calibrated and validated using historical whole plant transpiration (WPT) data measured using sap flow gauges for the period December 2007 to January 2008.

Simulated canopy resistance and transpiration rates were compared with the measured values. The canopy resistance model and transpiration sub model had correlation coefficients with measured values of 90% and 64%, respectively when they were validated. Possible errors in canopy resistance measurements may have been due to the dynamic diffusion porometer error while errors in transpiration rates may have occurred in the up scaling of the measured transpiration rates from a single plant to whole canopy transpiration.

Daily and seasonal CWR for the rose crop were determined and it was shown that CWR fluctuated with each day as there were different climatic conditions. The rose crop had higher CWR during the summer season compared to the winter season. June and July had the lowest CWR during the year due to low VPD, air temperature and solar radiation received inside the greenhouse, while September and October had the highest CWR there were the highest solar radiation, VPD, air temperature and the lowest RH.

The crop water requirements for the whole year were compared with the actual water applied by the existing irrigation system at Floraline. The total CWR predicted by the GDGCM (1.45 Ml/year) were lower than the water applied throughout the whole year by the system (2.74Ml). The irrigation system at Floraline switched on whenever the cumulative solar radiation outside the greenhouse reached 1600 kJ/m^2, and it applied water for a fixed period of 4 minutes each time. However solar radiation was not the only climatic parameter that was taken into account. The model used all outside weather parameters influencing the microclimate in the greenhouse and results showed that the crop had lower CWR than the water that was applied. The model even found night-time transpiration even though it is very low; the CWR was still lower than the water applied by the irrigation system. The results show that the existing irrigation system was over-irrigating the whole year; besides water being wasted, this may cause many negative effects to the crop which may be indirectly reducing the crop yield, vase life and quality.

5.2 Recommendations

It is recommended to try and adopt the GDGCM into the greenhouse climate control system, and use it as a tool for irrigation scheduling in greenhouse crops. The model should allow estimation of the CWR and improve on water saving. However further investigations should be done to evaluate the practical effect of reduced water application using the GDGCM as the tool for irrigation on yield, length of stems, flower quality and vase life.

To increase reliability and accuracy, the research study should be re-done in other regions in Zimbabwe such that the whole country is represented. The reliability of the GDGCM in decision making for the whole agricultural regions of the country should be investigated. It is also recommended that future research be done to try and estimate CWR for other greenhouse crops using the GDGCM for outside weather data; solar radiation, air temperature, RH, rainfall and wind speed.

REFERENCES

Allen, R.G., Pereira, L.S., Raes, D., Smith, M., 1998. Crop evapotranspiration. FAO Irrigation and Drainage Paper 56. Rome: FAO

American Society of Heating, Refrigeration and Air-Conditioning Engineers (ASHRAE)., 2005. ASHRAE Handbook of Fundamentals, Chapter 27: Ventilation and infiltration. Atlanta, GA.

Anonymous., 2010. Principles of irrigation management. Water management guidelines for nursery or floral producers online at: http://aggie-horticulture.tamu.edu/GREENHOUSE/NURSERY/environ/wmprinc.html. (Accessed: June 2009)

Avissar, R., Avissar, P., Mahrer, Y., Bravdo, B.A., 1985. A model to simulate response of plant stomata to environmental conditions. Agricultural and Forest Meteorology, 34,21-29

Baas, R., 2003. Online monitoring of protected crops and their environment: towards the speaking plant. Proceedings of the International Fert society 532,1-20

Baille, A., 1996. Principles and methods for predicting crop water requirements in greenhouse environments. Cahier Options Mediterraneennes 31,177-187

Baille, M., Baille A., Laury J.C., 1994a. Canopy surface resistances to water vapour transfer for nine greenhouse pot plant crops. Scientia Horticulture 57, 143 – 155

Baille, M., Baille, A., Laury J.C., 1994b. A simplified model for predicting evapotranspiration rate of nine ornamental species vs. climate factors and leaf area. Scientia Horticulture 59, 217 – 232

Baille, M., Baille, A., Delmon, D., 1994c. Microclimate and transpiration of greenhouse rose crops. Agric. For. Meteorol., 71, 83 – 97

Bakker, J.C., Bot, G.P.A., Challa, H., Van de Braak, N.J., (eds.). 1995. Greenhouse climate control, an integrated approach. Wageningen Pers, Wageningen, The Netherlands, pp. 279

Baker, J.M., Nieber, J.L., 1989. An analysis of the steady state heat balance method for measuring sap flow in plants. Agric. For. Meteorol., 48, 93 -109

Baker, J.M., van Bavel, C.H.M., 1987. Measurement of mass flow of water in the stems of herbaceous plants. Plant, Cell and Environment. 10, 777 - 782

Baptista, F.J., Bailey, B.J., Randall, J.M., Menesses, J.F., 2001. Natural ventilation of Greenhouses: Comparison of measured and predicted ventilation rates. Agribuilings 2001, Campinas, SP, Brazil, 136-151

Boulard, T., 2008. Encyclopedia of water science. 2nd Edition. CRC Press, pp.337-342

Boulard, T., Wang, S., 2000. Greenhouse crop transpiration simulation from external climate conditions. Agric For Meteorol 100,25–34

Boulard, T., Baille, A., 1993. A simple greenhouse climate control model incorporating the effects of aeration and evaporative cooling. Agric. For. Meteorology, 145-57

Boulard, T., Baille, A., Mermier, M., Villette, F., 1991. Measurement and modelling of foliar stomatal resistance and transpiration of tomato crop in greenhouse. Agronomie. 11,259-274

Carrier, M., Gosselin, A., Gauthier, L., 1994. Description of a crop growth model for the management of supplemental lighting in greenhouses. HortTech. 4, 383-389

Challa, H., 2002. Crop models for greenhouse production systems. Acta Hort. 593,47-53

Challa, H., 1997. DSS for climate control in greenhouses. In: H.F.M. ten Berge and Stein, A., (eds.), Proc. of the INRA-KCW workshop on decision support systems. Laôn (France) Quant. Appr. In Systems Analysis 15:,3-8

Challa, H., Heuvelink, E., 1996. Photosynthesis driven crop growth models for greenhouse cultivation: advances and bottle-necks. Acta Hort 417, 9-22

Challa,H., Heuvelink, E., Leutscher, K.J., 1994. Modelling in the search for balance between inputs and outputs in greenhouse cultivation. In: Struik, P.C., Vredenberg, W.J., Renkema, J.A., Parlevliet, J.E., (eds.), Plant production on the threshold of a new century. Dordrecht, Kluwer. pp. 187-195

Critten, D., 1993. A review of the light transmission into greenhouse crops. Acta Hort.328, 9-31

Deltour, J., de Halleux, D., Nijskens, J., Coutisse, S., Nisen, A., 1985. Dynamic modelling of heat and mass transfer in greenhouses. Acta Hort. 174,119 - 125

Demrati,H., Boulard, T., Bekkaoui, A., Bouirden, L., 2001. Natural ventilation and microclimatic performance of a large-scale banana greenhouse. J. agric. Engng Res., 80 (3), 261 – 271

de Graaf, R., van den Ende, J., 1981. Transpiration and evapotranspiration of the glasshouse crops. Acta Hort 119,147–158

Dynamax Inc., 2005. Dynagage sap flow sensor user manual. Dynamax Inc., 10808 Fallstone Rd. Houston TX 77099, USA (http://www.dynamax.com)

Ehret, D.L., Lau, A., Bittman, S., Lin, W., Shelford, T., 2001. Automated monitoring of greenhouse crops. Agronomie 21, 403–414

Elings, A., Voogt, W., 2008. Management of greenhouse crop transpiration: the way forward. Acta Hort 801, 1221-1228

Enoch, H.Z., Enoch, Y., 1999. The history and geography of the greenhouse. In: Stanhill, G., Enoch, H.Z., (eds) Greenhouse ecosystems. Ecosystems of the world 20. Amsterdam, pp. 1-15

Evans, R., Sneed, R.E., Cassel, D.K., 1996. Irrigation scheduling to improve water and energy use efficiencies. North Carolina cooperative extension service. Publication number, AG 452-4

Fatnassi, H., Boulard, T. and Bouirden, L., 2003. Simulation of climatic conditions in full-scale greenhouse fitted with insect-proof screens. Agric. For. Meteorol., 118, 97 – 111

Fereres, E., Goldhamer, D.A., 2003. Suitability of stem diameter variations and water potential as indicators for irrigation scheduling of almond trees. Journal of Horticultural Science and Biotechnology 78, 139–144.

Fernandez, M.D., Bonachela, F., Orgaz, F., Thompson, R., Lopez, J.C., Granados, M. R., Gallardo, M., Fereres, E., 2010. Measurement and estimation of plastic reference evapotranspiration in a Mediterrenean climate. Journal of irrigation Science.

Grime, V.L., Morison, J.I.L., Simmonds, L.P., 1995. Including the heat storage term in sap flow measurements with stem heat balance method, Agric. For. Meteorol., 74, 1 - 25

Gumbe, L.O., Agullo, J.O., Brugger, M.F., 2009. Environmental simulation of a greenhouse system in Kenya. AJST 10(2), 108-121

Ham, J., Heilman, J.L., Lascano, R.J., 1990. Determination of soil water evaporation and transpiration from energy balance and stem flow measurements. Agric. For. Meteorol., 52,287-301

Hanan, J.J., 1998. Greenhouses: Advanced technology for protected horticulture. CRC Press LLC, Florida.

Harbaugh, B.K., Stanley, C.D., 1985. Guidelines for the use of capillary mat, spaghetti tube and trickle irrigation systems for floricultural crops. Foliage Digest 8(8),1-4

Hashimoto, Y., 1993. Computer integrated system for the cultivating process in agriculture and horticulture. In: Hashimoto Y., Bot G.P.A., Day W., Tantau H.J., Nonami, H.,(eds). The computerized greenhouse. Academic Press, Inc., San Diego, USA. pp.175-196

Jarvis, P.G., 1985. Coupling of transpiration to the atmosphere of horticultural crops. Acta Hort. 171, 187 - 205

Jones, H.G., 2004. Irrigation scheduling: Advantages and pitfalls of plant-based methods. J Exp Bot 55(407), 2427 – 2436

Jones, H.G., Tardieu, F., 1998. Modelling water relations of horticultural crops. Sci. Hortic., In press.

Jones, M.B., 1993. Plant microclimate. In: Photosynthesis and production in a changing environment: A field laboratory manual. Edited by Hall, D.O., Scurlock, J.M.O., Bolhar-Nordenkampf, H.R., Leegood, R.C. and Long, S.P., 1993. Chapman & Hall, London, pp.47

Kastoulas, N., Baille, A., Kittas, C., 2002. Influence of leaf area index on canopy energy partitioning and greenhouse cooling requirements. Biosystems Engineering 83(3), 349-359

Kittas, C., Boulard, T., Papadakis, G., 1997. Natural ventilation of a greenhouse with ridge and side openings: Sensitivity to temperature and wind effects. Transactions of the ASAE., 40(2), 415 – 425

Kittas, C., Katsoulas, N., Baille, A., 1999. Transpiration and Canopy Resistance of Greenhouse Soilless Roses: Measurements and Modelling. Acta. Hort. 507, 61 – 68

Klein, I., 2004. Scheduling automatic irrigation by threshold-set soil matric potential increases irrigation efficiency while minimising plant stress. Institute of Horticulture, ARO, The Volcani Centre, Israel.

Klein, S.A., Beckman, W.A., Cooper, P.I., Duffie, N.A., Freeman, T.L., Mitchell, J.C., Beekman, D.M., Oonk, R.L., Hughes, P.J., Eberlein, M.E., Karman, V.D., Pawelski, M.J., Utzinger, D.M., Duffie, J.A., Brandemuehl, M.J., Arny, M.D., Theilacker, J.C., Morrison, G.L., Clark, D.A., Braun, J.E., Evans, B.L., Kummer J.P., 1988. TRNSYS: A transient system simulation program. Engineering experiment station report 38-12, Solar Energy Laboratory, University of Wisconsin-Madison, USA.

Lake, J.V., Postlethwaithe J.D., Slack, G., Edwards, R. J., 1966. Seasonal variation in the transpiration of glasshouse plants. Agric. Meteorology, 3,167-196

Lee, B.W., Shin, J.H., 1998. Optimal Irrigation Management System of Greenhouse Tomato based on Stem Diameter and Transpiration Monitoring. Agricultural Information Technology in Asia and Oceania. The Asian Federation for Information Technology in Agriculture, Suwon, Korea, pp.87-90

Marcelis, L.F.M., Heuvelink, E., Goudriaan, J., 1998. Modelling of growth and yield in horticultural crops: a review. Sci. Hortic., in press.

Mashonjowa, E., Ronsse, F., Milford, J.R., Lemeur, R., Pieters, J.G., 2010a. Calibration and validation of a dynamic greenhouse climate model in Zimbabwe. Submitted to Agricultural and Forest Meteorology.

Mashonjowa, E., Ronsse, F., Milford, J.R., Lemeur, R., Pieters, J.G., 2010b. Measurement and simulation of the ventilation rates in a naturally ventilated greenhouse in Zimbabwe. Applied Engineering in Agriculture, in press.

Mashonjowa, E., Ronsse, F., Mhizha, T., Milford J.R., Lemeur, R., Pieters, J.G., 2009. The effects of whitening and dust accumulation on the microclimate and canopy behaviour of rose plants (Rosa hybrida) in a greenhouse in Zimbabwe. Solar Energy, 84(1): 10 – 23

Mashonjowa, E., Milford, J R., Pieters, J.G; Denys, S., Lemeur, R., 2007a. The effect of covering material on the microclimate of rose plants in a greenhouse. Acta Hort.,751, 51 – 59.

Mashonjowa, E., Ronsse, F., Pieters, J.G., Lemeur, R., 2007b . Modelling heat and mass transfer in a naturally ventilated greenhouse in Zimbabwe. Communications in Agricultural and Applied Biological Sciences, 72(1), 239 – 243.

Monteith, J.L., and Unsworth, M.H., 1990. Principles of environmental physics. 2nd Edition. Chapman and Hall Inc. New York.

Monteith, N. J., 1973. Principle of environmental physics. London, Edward Arnold.

Morris, L.G., Neale, F.E., Postlethwaithe, J. D., 1957. The transpiration of glasshouse crops and its relationship to the incoming radiation. J. Agric. Eng. Research, 2:,111-22

Naor, A., 2004. Sources of uncertainty in irrigation scheduling, and practical ways to resolve some of them. Acta Hort. 664,427-433.

Oki, L.R., Lieth, J.H., Tjosvold, S., 2001. Irrigation of rosa hybrida L. 'Kardinal' based on soil moisture tension increases productivity and flower quality. Acta Hort 547,213-219.

Pardossi, A., Incrocci, L., 2008. Traditional and new approaches to irrigation scheduling in vegetable crops. Online at: http://www.flow-aid.wur.nl/UK (Accessed: December 2009)

Papadakis, G., Frangoudakis, A., Kyritsis, S., 1994. Experimental investigation and modelling of heat and mass transfer between a tomato crop and the greenhouse environment. J. Agric. Engng. Res., 57, 217 - 227

Pasian, C.C., Lieth, J.H., 1989. Analysis of the response of net photosynthesis of rose leaves of varying ages to photosynthetic active radiation and temperature. J. Am. Soc. Hortic. Sci. 114(4), 581-586

Payne, W.A., Bruck, H., 1996. Evapotranspiration and other soil water balance terms estimated from neutron and capacitance probe measurements. In: Camp, C.R., Sadler E.J., Yoder, R.E., (Eds). Proceedings of the International Conference on Evapotranspiration and Irrigation Scheduling. American Society of Agricultural Engineering, San Antonio, Texas, pp. 455-462

Pieters, J.G., Deltour, J.M., 1997. Performances of greenhouses with the presence of condensation on cladding. J. Agric. Engng. Res., 68, 125 – 137

Pieters, J.G., 1996. Condensation and PAR transmittance of greenhouses. Plasticulture 112(4), 23 – 31

Pieters, J.G., 1995. Influence of condensation on the heat balance and the light transmission of a greenhouse. Ph.D. thesis, University of Ghent, Faculty of Agricultural and Applied Biological Sciences, Ghent, Belgium, pp.260

Pollet,I.V., Pieters, J.G. 2000. Condensation and radiation transmittance of greenhouse cladding materials, part 3: results for glass plates and plastic films. J. Agric. Engng. Res., 77(4), 419 – 428

Quassim, A., Tatura, B.A., 2006. Irrigation scheduling for vegetable crops. Agriculture notes. State of Victoria, Department of Primary Industries. Publication number: AG0787.

Rose, M.A., Rose, M., 1998. Performance of heat-balance sap-flow gauges on rose. Acta Hort. 421, 201-208

Rosenberg, N.J., Blad, B.L., Verma, S.B., 1983. Microclimate - The Biological Environment. Wiley, New York, NY, 2nd edn., pp.495

Roy, J.C., Boulard, T., Kittas, C., Wang, S., 2002. Convective and ventilation transfers in greenhouses, part 1: the greenhouse considered as a perfectly stirred tank. Biosystems Engineering, 83(1), 1 – 20

Sbita, L., Boulard, T., Baille, A., Annabi, M., 1996. A greenhouse climate model including the effects of ventilation and crop transpiration: Validation for the south Tunisia conditions. Acta Hort., 458, 57 - 64.

Sharma, B.R., 2006. Crop water requirements and water productivity concepts and practices. International water management Institute. New Delhi, India. pp.10

Shelford, T.J., Lau, A.K., Ehret, D.L., Chieng, S.T., 2004. Comparison of a new plant-based irrigation control method with light-based irrigation control for greenhouse tomato production. Canadian Biosystems Engineering 46, 1.1-1.6

Stanhill, G., Albert, J. S., 1974. Solar radiation and water loss from glasshouse roses. J. Amer. Soc. Hort. Sci., 99,107-10

Stanghellini, C., 1987. Transpiration of greenhouse crops: an aid to climate management. Ph.D. Dissertation. Wageningen Agricultural University, The Netherlands.

Steppe, K., Lemeur, R., De Pauw, D.J.W., 2008. A novel methodology for irrigation scheduling using plant-based measurements and mathematical modelling. Acta Hort 792

Steppe, K., Lemeur, R., Dierick, D., 2005. Unravelling the relationship between stem temperature and air temperature to correct for errors in sap-flow calculations using stem heat balance sensors. Functional Plant Biology, 32, 599 – 609.

Takashi, N., Masayuki, O., Hidekazu, S., 1997. Effects of wind and vapour pressure deficit on transpiration of tomato scions. Japanese society for horticultural science 66(1), 105-112

Van Bavel, M.G., 1994. Flow 32^{tm} installation and operation manual version 2.11 software. Houston: Dynamax.

Van Leeuwen, C., Chone, X., Tregoat, O., Gaudillere, J.P., 2001. The use of physiological indicators to assess vine water uptake and to manage vineyard irrigation. The Australian Grape grower and Winemaker. 449, 18-24

Wang, S., Boulard, T., 2000. Predicting the microclimate in a naturally ventilated plastic house in a Mediterranean climate. J. Agric. Engng. Res., 75, 27 – 38

Yang, X., Short, T.H., Fox, R.D., Bauerle, W.L., 1990. Transpiration, leaf temperature and stomatal resistance of a greenhouse cucumber crop. Agric. For. Meteorol., 51, 197-209